H24/3432

MONASH UNIVERSITY
THESIS ACCEPTED IN SATISFACTION OF THE
REQUIREMENTS FOR THE DEGREE OF
DOCTOR OF PHILOSOPHY
ON..... 20 December 2002 .....
.....[redacted].....
Sec. Research Graduate School Committee

Addendum

Chapter 2 page 27: the following few paragraphs should be added to page 27 after the end of the first paragraph

Induced magnetic dipoles as a means of varying inter-particle force

"Consider a bed of iron particles placed between a pair of Helmholtz coils. The magnetic field on the particles can be decomposed into two components

$$B = B_o + B_m = \mu_o(N/l)I + B_m$$

Where B_o is the applied field due to the solenoid and B_m is due to the magnetic dipole fields of the other particles. N is the number of coils of length l in the solenoid, I, is the applied current and μ_o is the permeability of free space. This can be written in terms of the applied field H and the total magnetic moments of the shot as

$$\begin{aligned} B &= \mu_o H + \mu_o M \\ &= \mu_o H + \mu_o \chi_m H \\ &= \mu_o(1 + \chi_m)H = \mu_o K_m H \end{aligned}$$

where K_m is the relative permeability and χ_m is the susceptibility of the material. The susceptibility of the material will depend upon the susceptibility of the iron particles in the bed, which are ferro-magnets. It will be very sensitive to the density of the particles and the nature of the packing of the bed. Further, the relative permeability and susceptibility of ferromagnetic materials vary as a function of applied field H.
The values of the permeabilities are typically very large for a wide range of applied fields and so the magnetic behaviour of the particles will be dominated by the neighbouring dipoles. For ferromagnetic materials it is usual to quote the maximum permeabilty. B typically increases rapidly with H until the ferro-magnet reaches a saturation point. Above this point, increases in field are due only to increases in H. The iron shot used in these experiments consists of a type of low carbon steel which is 98.5 % Fe and has a maximum relative permeability of 2000.

We can model the cohesive forces involved *within* the granular material as follows. The permeability of each particle is much higher than the surrounding air and so the field will pass through the particles. The force between two dipoles is given by

$$F = -\nabla U = -\mathbf{m}\bullet B = -(\mu_o/4\pi)[\mathbf{m}_1\bullet\mathbf{m}_2/r^3 - 3(\mathbf{m}_1\bullet r)(\mathbf{m}_2\bullet r)/r^5]$$

where $\mathbf{m}_1$ and $\mathbf{m}_2$ are the magnetic moments of dipole 1 and 2 respectively. This can be simplified by considering the maximum force between the dipoles that occurs when the dipoles are aligned. This is reasonable since both of the dipoles are induced by the local field and will therefore be aligned with it. Using

$$\mathbf{m}_1 = \mathbf{m}_2 = \mathbf{m} = \langle \mathbf{m} \rangle = \mathbf{M}/N$$

the maximum cohesive force[1] can be estimated as

$$F_{max} = (\mu_o/2\pi)[\mathbf{m}^2/r^3] = (\mu_o/2\pi)[\mathbf{M}^2/r^3]$$

where **M** is the magnetisation and *N* is the number of particles which, in this case, equals 1. Using a mean field approximation, the magnetisation can be written in terms of the local field as

$$M = \mu_o \chi_m(H)\, H_l$$

where $\chi_m(H)$ has been used to emphasise that the susceptibility of the ferromagnetic granular material will vary with the applied field. Following Osanger (Osanger, 1935), we can model the surrounding granular material as a hollow spherical cavity that contains a point dipole of magnitude **m**. The dipole acts to orientate the iron particle and represents the average direction of the *local* field. The local field due to the material can be modeled as the field H_i inside the cavity, not including the dipole field due to the particles. By solving Laplace's equation the internal field can be written in terms of the external or applied field as

$$H_i = H + [(\mu_b - 1)/2\mu_b + 1)]\, H + [2(\mu_b - 1)/(2\mu_b + 1)a^3]\, \mathbf{m}$$

where μ_b is the permeability of the bed and a is the radius of the spherical cavity. The second term in this equation may be written as

$$[4\pi\chi_m(H)/(8\pi\chi_m(H)+3)]\, H$$

The third term is the reaction field to the particle. It is always parallel to the dipole of the particle and unlike the local field does not exert any orientating force and so can be neglected. The local field can therefore be written in terms of the applied field as

$$H_i = [1 + (4\pi\chi_m(H)/(8\pi\chi_m(H)+3))]\, H$$

This equation assumes that the local field and the applied field are perfectly aligned, which is not necessarily true. Mechanical forces within the packed granular material will tend to shift the direction of the local field with respect to the applied field as groups of particles roll, slump and/or rotate during the packing process[2]. In fluidised beds, turbulence and viscous forces within the bed will also alter the direction of local fields within the bed. The local field within the material, can therefore be best thought of as a function of the angle it makes with the applied field, ϕ.

$$H_i(\phi) = [1 + (4\pi\chi_m(H)/(8\pi\chi_m(H)+3))]\, H * f(\phi)$$

where $f(\phi)$ will depend upon the nature of the mechanical or viscous forces acting on the material. The nature of the mechanical forces in packed granular materials is an active

area of research and they are, as yet, poorly understood (Cates, 1999), (da Silva, 2000) as are the nature of viscous forces in fluidised granular matter (Clift, 1993).
Summarising the above arguments, the force on the dipole can be given by

$$F = \mu_o \chi_m(H) H_l = \mu \times [1+(4\pi\chi_m(H)/(8\pi\chi_m(H)+3))] H/\mu_o K_m$$

From this equation it can be seen that the relationship between the cohesive forces between the particles is extremely complex and depends upon the relationship between the mechanical forces and the applied magnetic field and also on the way the susceptibility varies with the applied field.
To avoid these complications, in these experiments, the relationship between cohesive force and applied field was established experimentally."

Footnotes

1. For simplicity, the dipoles in this model have been treated as point dipoles located in the center of the particle.

2. In general, the details of the network of forces in a granular material will be quite complex and large local anisotropies exist, as we pointed out in chapter 1.

The passage beginning from the second paragraph on page 27 should be rewritten as.

"The inter-particle force between the particles will wary in proportion to the square of the applied magnetic field ($F_{mag} \propto B_o^2$). Calculating the field from theory is difficult for reasons mentioned above. To avoid these difficulties, the force will be measured directly, as described below.
The interactions between particles in the magnetic field will, in general, be very complex. Experience with many complex systems has shown that often the detailed nature of the forces within the system is not important in describing large-scale behaviour. Properties emerge which do not depend heavily upon the details of the interactions. There are some recent indications that this holds true for granular systems.
Tan et. al. (Tan and Jones, 1993) have conducted experiments on the induced magnetic force between individual spherical particles and between spherical particles and between spherical particles arranged in regular configurations."

Chapter 3

page 51 the following sentence should be added to the end of the last paragraph of section 3.3 "The results obtained here are remarkable in that the results of the experiments suggest that the detailed nature of the individual forces are not important in determining the voidage. Rather the results indicate that it is the ratio of the inter-particle force to buoyant weight that is the important factor."

Chapter 4

"Within the fluid bed, the drag force, gravity and magnetic field are all aligned in the vertical direction. These forces compete against one another leading to isotropic behaviour within the fluid bed. Increased particle-particle interactions, in the field direction, due to dipolar forces are counteracted by drag forces due to air forced from below the bed. The bubbling fluidisation regimes observed in the magnetic bed closely mirror those observed by other researchers in powders."

The sentence "This effect is due to the packing of particles." 4th line from the bottom line on page 62 will be replaced by .
"The hysteresis effect is due to the formation of inter-particle bonds between neighbouring particles. When the particles are well separated, the effect of the induced inter-particle forces is weak. However, when attempting to increase the fluidisation of a relatively close packed bed, the strong induced inter-particle forces must be overcome. This leads to the observed hysteresis effect. A similar effect is observed in granular powders with strong van der Waals forces."

Chapter 5

The following few paragraphs should be added to page 82 after the end of the last paragraph of chapter 5

"Another effect that needs to be taken into consideration is changes in coefficient of restitution and increased dissipation in the magnetic experiments. The presence of any inter-particle forces will alter the co-efficient of restitution. Liquid bridging forces, Van Der Waals forces and induced magnetic forces will all have an effect on the effective coefficient of restitution since they increase the attraction between particles during collisions.
An additional effect in the magnetic field experiments is an increase in dissipation due to eddy currents induced in the balls. Eddy currents in the balls will oppose the motion of the balls and dissipate energy as heat. The conductivity of the balls (according to information supplied by the manufacture) is approximately $0.2 \times 10^{+7}\ \Omega\text{-m}^{-1}$.
This presents difficulties in studying the detailed mechanisms of pattern formation. In Shinbrot's model, the patterns arise due to competition between dissipative collisions and random motions of the particles and so the amount of dissipation should influence the pattern forming process. Subtle differences in the alteration of dissipation and coefficient of restitution may account for differences in the patterns observed in clay suspensions, granular layers with magnetic or Van der Waals forces. By using and comparing the behaviour of materials with different permativities and conductivities, it may be possible to study these effects in isolation. However this would be beyond the scope of this preliminary research."

Chapter 8

"The use of magnetic induced inter-particle forces has several strengths

- It gives continuous control of the inter-particle forces allowing the effect of inter-particle forces to be studied

- Inter-particle force can be increased and decreased easily.
- The inter-particle force can be varied in isolation from other factors (for example, the inter-particle force can be varied for one species of particles in a binary mixture whilst leaving the other (non magnetic) particle species interactions unchanged.
- Within fluidised granular materials, the drag force, gravity and magnetic field can all be aligned in the vertical direction so that they oppose each other leading to isotropic behaviour within the fluid bed. Increased particle-particle interactions in the field direction due to dipolar forces aligning with the field, are counteracted by drag forces due to air forced from below the bed.

The biggest drawback of using this technique is the tendency for particles to align with the direction of the applied field. In the experiments carried out here this was only evident for close packing of very small particle at very high fields. This led to slightly anisotropic behaviour in the material. The most visible effect of this anisotropy was the formation of chains of particles at the surface of the material at very high fields (approximately 5×10^3 A/m).

Eddy currents may have small effects on the dynamics of the particles under consideration. Related to this is an alteration of the dissipation during collisions.

The induced inter-particle forces alter the coefficient of restitution during collisions. This effect is difficult to quantify but needs to be considered in the pattern formation and axial segregation experiments. It should be noted that the coefficient of restitution is also altered by other inter-particle forces."

Minor changes

Preface	The sentence "In recent years there has been a resurgence of interest in granular matter. This is due in part, to the suggestion by Bak et.al. ...." should be replaced by "Interest in the engineering community in granular physics started with the seminal work of Bagnold \cite{Bagnold}in the 1950's. Interest in granular matter by the physics community began to grow in the physics community began to grow in the early 1980's. This is due in part, to the suggestion by Bak et.al. ...."
Page 3	"... makes granular dynamics very different to other ..." should read "... makes granular dynamics very different from other ..."
Page 3	midpage should read "physicist's
Page 6	should read "If the granular material is shaken (but not fluidised) its, density will increase slowly ..."
Page 10	section 1.4.1 top line "When rigid container ... shaken in a horizontal plane" should read "When a rigid container ... shaken vertically, unexpected ..."
Page 12	The reference suggested by the examiner (PRL, 58, 1038-1042, 1987) will be added before the reference to (Duran, 2000),
Page 18, line 20	The second occurrence of the word "is" should be removed.
Page 19	The sentence which begins "The above summary suggests ..." should be deleted and the following paragraph added before the beginning of the last paragraph on page 19.

"Experience with a wide range of complex systems have shown that while the detailed nature of the forces applied to the particles in a granular system can lead to very different dynamics, there are circumstances where these details are not relevant to the system being examined (Ball 1999b)."

Page 19 The following footnote should be added after the introduction of the term "interparticle forces" on page 19.

\footnote{There are a wide variety of forces which influence the behaviour of powders and granular materials that involve electrostatic interactions. In the following discussions, the terminology of Israelchevilli is used to describe these forces and the term Van der Waals forces will be used to describe all inter-particle forces involving electrostatic forces.}

Page 23 A full discussion of the physics of liquid bridges appears on pages 25 and 26. to make this clearer the following sentence could be added "The surface tension and the concave nature of these bridges draws the particles together." on line 19 after "liquid bridges".

Page 29 mid page. The sentence "The magnetic field axis orientation was in the vertical direction and was measured as a function of current ..." should read "In all experiments conducted in this research, the field was applied along the vertical direction. The field was measured as a function of current..."

Page 36 line 7 "Repulsive due to" should read "Repulsive forces due to ..."

Page 43 (Kepler 1976) refers to a 1976 translation of the manuscript of Kepler's manuscript of 1611. This should be changed to (Kepler 1611)

Page 44 Line 4 "here F_{drag} ..." should be "where F_{drag} is the drag force on a particle, and ..."

Page 46 The sentence "As in the previous experiments the applied field was in the vertical direction." should be inserted after the sentence ending in "...field strengths." in the bottom line on page 46.

Page 48 "Figure 5" should read "Figure 3.2"

Page 60 The sentence "As in previous experiments the applied field was in the vertical direction." should be added to after the last sentence in section 4.2.1 on page 60.

Page 65 The word "of" that appears on this line should be deleted

Page 67 5 lines from bottom should read "In previous experiments..."

Page 68 line 25 Correction "...where the motion of each individual grain is simulated."

Page 79 Figures 5.11 the caption should read "Sequence of high speed images showing pattern development. Frequency ~50Hz, amplitude ~3, 125 frames per second. Particle size 350 um. Sequence is from left to right and down."

Figure 5.12 should end with ".....(Sequence is from left to right then down)"

Page 72	should read "Shinbrot's"
Page 78	The sentences "The container was placed in the Helmholtz coils. As in previous experiments the applied field was in the vertical direction." should be inserted after the second sentence in section 5.3.3 on page 78.
Page 81	References to 5.13 and 5.14 should be added in the text.
Page 82	should read "...for particles 0.5 mm and larger ..."
Page 83	the phase (See Figure 5.16)
Page 86	The kink in the profile is due to both differences the angle of repose and segregation. If the angle of repose were the same for the different materials then the profile would be straight. If the material did not segregate, the profile would straight.
Page 87,	The sentence "As in previous experiments the applied field was in the vertical direction." should be added *before* the last sentence in section 6.1.
Page 88/89	The caption should read "Phase diagram for segregation is the angle of showing the difference in particle size of material Δ. r_1 and r_2, represent the size of the non-magnetic and iron particles respectively. ..."
Page 90	Fig 6.6: The caption should read "Phase diagram for stratification showing the difference in angle of repose, δ, between the angle of repose of the non-magnetic θ_1 and magnetic material θ_2.
Page 97	This sentence needs a comma after "bulk concentration" which makes it easier to read.
Page 98	Figure 7.2 word "of" inserted in figure caption
Page 98	The sentence "Again the field direction was vertical." should be added after the second sentence in section 7.2.
Page 106	More mobile particles will roll over less mobile particles which will sink, and so for the purposes of modelling, they can be ignored.
Page 107	The definitions of the symbols should have been explained better and these definitions should be placed after the terms as they are introduced in the text. This can be addressed by the following changes "where n_v is the number of collisions and A is the area of the surface perpendicular to the direction of motion over which collisions can occur and t is time." to be added after equation 7.7 on page 107. "where v_{rel} is the relative velocity of the particles. D can be written as ..." to be added after equation 7.8. The passage *before* equation 7.9 should read "...energy lost through inelastic collision, $\Delta K.E.$" and the following sentence should be added after equation 7.9. "Where g is acceleration due to gravity and h is the height over which the particle falls."

SAND AS A COMPLEX SYSTEM: INTER-PARTICLE FORCES AND GRANULAR MATTER

A THESIS SUBMITTED FOR THE DEGREE OF
DOCTOR OF PHILOSOPHY

By
Sean Hutton B.Sc. M.Sc.

Department of Physics,
Monash University.

May 2002

Acknowledgements

This work was made possible thanks to the support, encouragement and assistance of several people. I would first like to thank my family (Mum, Dad, Kim and Amy) for always being there. I also wish to give a special acknowledgement to my supervisors Charles, who was always encouraging and supportive of my ideas, and Adam, whose enthusiasm for granular materials and science in general has been infectious.

I should give a special thanks Nino in the electronics lab and to the physics workshop staff especially Roger, John and Alan for helping me to build equipment for the experiments. They showed a legendary amount of patience. Despite my alternately cracking, melting, zapping, and on one occasion exploding their equipment, they were always happy to repair it again.

I would also like to thank Professor Martin Rhodes for allowing me to use the resources of the Chemical Engineering Department and his helpful comments with the preparation of papers resulting from this research. Thanks must go to Shan and his students in the Chemical Engineering Department for their help with the fluidisation measurements in chapter 4. Thanks also to my work colleagues at both PCI and Hadland Photonics for their support and allowing me the time to complete my studies. I would also like to thank the many other members of staff at the Monash Physics Department who have from time to time given me help and feedback on my research. Special mention needs to go to Julia Chadwick for her patience and help with the intricacies of LaTeX.

Abstract

In this thesis, a novel method for studying the effect of inter-particle force on granular materials is introduced. By using magnetisable particles in a magnetic field, experiments on the effect of altering inter-particle force between grains were performed. This technique is used to study the effect of inter-particle force on several aspects of dynamic and static granular behaviour and on the surface and bulk properties of the material.

The effect of inter-particle force on the static and dynamic angle of repose is investigated. It was found that both the static and dynamic angles of repose increased linearly with magnetic inter-particle force. The shape of the granular profile is investigated and the fractal dimension calculated and plotted for increasing inter-particle force.

The manner in which inter-particle forces influence packing in granular media is also investigated. The void fraction of the bed resulting from many iron particles being poured into a container at a given magnetic field is measured. The poured packing fraction is found to vary only with the ratio of inter-particle force to particle weight. This, it is shown, is a universal effect not limited to magnetic systems.

The transition from bubbling to non-bubbling behaviour in fluidised grains is examined as inter-particle forces are increased. A transition from Geldart group B behaviour to group A behaviour observed. Aspects of pattern formation in thin granular layers fluidised by vibration are also examined. Experimental observations are made of the effect of inter-particle force on this pattern forming process. It is found that increasing the inter-granular force in vibrated granular layers has a similar effect to increasing the amplitude of vibration.

Finally, segregation and stratification are examined as inter-particle force is altered. It is found that inter-particle force has a significant effect on the segregation and

stratification of granular media. The effect of these forces on avalanche stratification and segregation is examined as well as the effect on radial and axial segregation in rotating drums. Experiments were performed to investigate axial segregation in three particle mixtures. From consideration of the results of these experiments, a model for axial segregation in binary mixtures is proposed.

Preface

Granular materials are everywhere. Examples include food products such as rice, corn, seeds, salt, sugar and flour. Building materials such as sand, gravel, and soil are granular materials as are many industrially important chemicals such as coal, plastics, and pharmaceutical products. A granular material can be defined as a collection of discrete, solid particles dispersed in a vacuum or an interstitial fluid[1]. Many peoples' earliest childhood memories would be likely to include playing with sand and dirt and yet despite this the properties and dynamics of such materials are still poorly understood (see for example (Kadanoff, 1999)).

This lack of understanding is not due to lack of interest. The study of granular materials has a long history. Many of the leading figures in the history of the physical sciences have looked at granular materials including Faraday (Faraday, 1831), Coulomb (Heyman, 1998) and Reynolds (Reynolds, 1885). In recent years, there has been a resurgence of interest in granular matter. This has been due, in part, to the suggestion by Bak *et. al.* (Bak, 1997) that sand piles evolve to a self organised critical state. This self-organised critical state is observed in a wide range of complex systems. Self-organised criticality is one example of the many interesting phenomena recently discovered in granular materials. In this thesis, it is argued that granular materials are best thought of as a "complex system".

Inter-particle forces play an important role in many areas of statistical physics. In many granular systems (eg. fine powders or wet sand), inter-particle forces could be expected to alter the dynamics of the system quite dramatically. One of the aims of this research is to study the effects of inter-particle forces on the behaviour of granular materials. The role of inter-particle forces in altering the properties of

[1] A more precise definition will be given in chapter 1

granular materials and powders is examined.

The breakdown of the chapters is as follows:

- **Chapter 1** introduces granular materials and explains their interest and importance.
- **Chapter 2** looks at granular statics. A novel means of studying the effect of varying inter-particle force is introduced. The effect of inter-particle forces on angle of repose is investigated and the shape of granular profiles examined.
- **Chapter 3** investigates the effect of inter-particle forces on the packing of granular matter.
- **Chapter 4** looks at bubbling in fluidised sand. A novel experimental fluidised bed is used to examine the behaviour of fluidised sand as the ratio of inter-particle force to weight is varied. The transition to bubbling behaviour is examined using high-speed video analysis.
- **Chapter 5** looks at pattern formation in thin vibrated layers of sand. Experiments are conducted to show how the pattern formation process is affected by inter-particle forces.
- **Chapter 6** looks at avalanches and avalanche segregation. Experiments showing the effect of inter-particle forces on avalanches as well as segregation and stratification during avalanches.
- **Chapter 7** examines the radial and axial segregation that occurs in rotating drums. The effect of inter-particle force on mixing is examined as well as the behaviour of drums containing more than two species of granular material.
- **Chapter 8** takes an overview and looks at what has been learned about the effect of inter-particle forces on granular dynamics and statics. It also points to some promising directions for future research.

Certificate of Originality

I hereby declare that this submission is my own work and that, to the best of my knowledge and belief, it contains no material previously published or written by another person nor material which to a substantial extent has been accepted for the award of any other degree or diploma of a university or other institute of higher learning, except where due acknowledgement is made in the text.

[redacted]

Sean Hutton

May 10, 2002

Contents

List of Tables

List of Figures

CHAPTER 1

Sand as a Complex System

"To see the world in a grain of sand... "

William Blake

Auguries of Innocence

Many children have handled sand and experienced the joys of building sandcastles and knocking them down. In contrast when physicists and engineers handle and experiment with sand they find the properties of sand to be complex. Materials science can deal adequately with the physical properties of most types of sand grain and the dynamics of an individual grain can be accurately described by Newtonian physics. However, when the aggregate of interacting grains is considered, properties emerge which cannot be explained simply in terms of the properties of the individual grains. Sand is not the sum of its grains. In recent years a branch of science has emerged which attempts to look at how properties of systems can emerge from the interactions of their constituent parts. The science (Coveney and Highfield, 1993) is known as "complexity" and systems which demonstrate emergent behaviour are known as "complex systems" (Kauffman, 1993) (Kauffman, 1995) (Lewin, 1993). In the following chapters I demonstrate, using examples, that granular media are an excellent example of a complex system.

1.1 Definitions

First let us define what is meant by granular media. *Granular media* may consist of one of several distinct types of material.

- A *granular material* is composed of discrete particles that are in physical contact most of the time. Granular gases or granular media that have been fluidised are generally not included in this definition.
- A *granular solid* is defined as being composed of granules of between 100 μm to 3000 μm.
- A *broken solid* is a granular material in which most particles are larger than 3 mm
- *Powders* generally consist of particles less than 100 μm in diameter. This classification is further broken down into *granular powders* (10 to 100 μm), *superfine* powders (1 to 10 μm) and *hyperfine* powders (0.1 μm to 1μm).[1]

In this discussion the term *granular material* will be used to cover all materials which are not fluidised, including powders. The terms *granular matter*, *granular media* and *particulate materials* will be used interchangeably to refer to all of the above classes of material including granular gases and fluidised grains.

1.2 Why is Studying Granular Materials Important?

Many of the leading figures in the physical sciences have investigated granular media including Coulomb (Grasselli and Herrmann, 1997), Galileo (Galileo, 1968) and Faraday (Faraday, 1831) to name just a few. Despite this interest there are, as yet, no continuum equations of motion for particulate materials[2]. While most of our understanding of fluids can be captured by the Navier-Stokes equation most of our knowledge of how to handle particulates is empirical and no general approach to analysing these flows exists (Jaeger et al., 1996). This gap in our understanding has important implications for industry.

Particulate materials are used extensively in industry. The annual production of various grains and aggregates around the world is estimated to be approximately 10 billion metric tonnes. In the chemical industry, granular media comprise roughly one-half of the products and at least three-quarters of the raw materials (Gennes, 1999). After water, the second most manipulated material, as measured in tons, is granular matter. Yet, despite this, granular matter remains difficult and sometimes

[1]These definitions follow those given in (Duran, 2000).

[2]Such equations may not be possible or even useful. See (Kadanoff, 1999).

dangerous to work with. Landslides cause a minimum of 1.5 billion dollars of property damage and at least 25 fatalities in the United States annually. Each year over 1,000 silos, bins, and hoppers fail in North America alone (Knowlton et al., 1994), often with fatal consequences. In addition to this, many fine powders are prone to explode or can be hazardous if inhaled.

Another troubling aspect of granular solids handling is the inefficiencies involved (Ennis et al., 1994). Approximately 10% of global energy goes into processing granular materials. A six-year study of 40 solids processing plants in the U.S. and Canada found that 80% of the plants experienced solids handling problems. These plants were slow in coming on-line and once startup began, the plant performance was typically 40-50% of the design performance. In Mexico, 5 million tons of corn is handled each year, 30% of which is lost due to poor handling systems. Even with these incentives a poor understanding remains of how these materials behave. It is clear that there are important practical benefits to improving our understanding of these materials.

1.3 A Unique State of Matter

From a physicists point of view, the most compelling reason for studying granular matter is its complexity. In particular, granular materials provide new challenges for many body theory and statistical mechanics (Ball, 1999b). The inelastic nature of collisions between grains makes granular dynamics very different to other many body systems. The dependence of granular dynamics on grain shape, size distribution, inter-particle force and surface properties make the behaviour of granular matter very complex.

1.3.1 A Strange Solid

In terms of the state of matter, granular matter is difficult to classify. Since the matter consists mostly of solid particles one might think that granular materials would be best thought of as a solid. Like a solid, granular materials can support a load. However, granular materials at rest have many features that are unlike most solids. For example, granular materials display both vaulting and arching. Voids and spaces in the material are created within the material just as an arch or vault

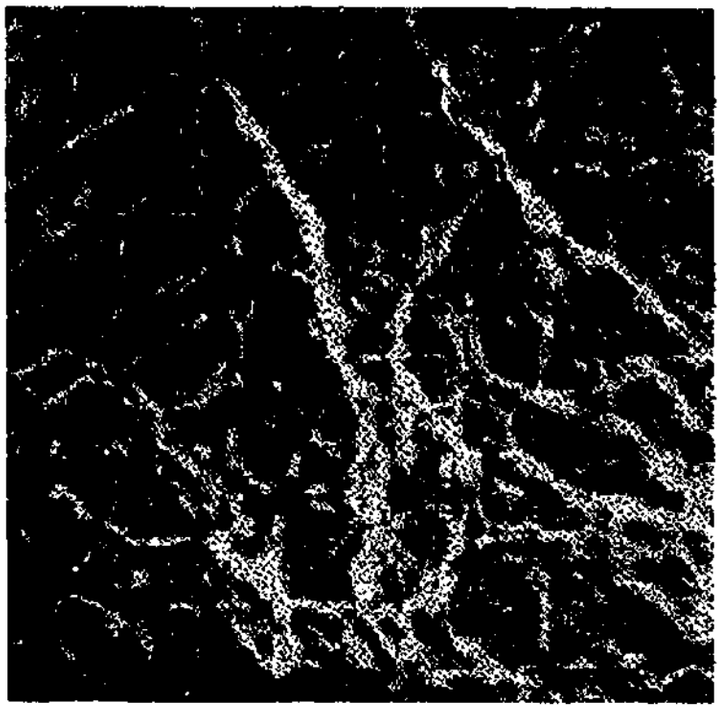

Figure 1.1: Stress patterns in granular materials (from (Jaeger et al., 1996))

can be created by carefully stacking stones or bricks. In a random assembly of particles, we inevitably find a large proportion of voids caused by the vaulting of grains. Compressing or vibrating a granular material leads to more efficient packing, less vaulting and arching and subsequently less voids. Once the assembly is well packed, grains will be unable to move without the material expanding (Jaeger and Nagel, 1992).

Forces within an assembly of grains build up along characteristic chains (Radjai et al., 1999), (da Silva and Rajchenbach, 2000) (see figure 1.1). The resulting web of forces directs loads on the material outward to the walls of the container holding it (Jaeger and Nagel, 1997). In view of their unique properties, it has been suggested (Liu and Nagel, 1998) that granular materials should be considered as an example of a separate state of matter known as 'fragile matter'. Such materials are fragile because even a slight change in the direction of applied stress will change the entire structure of the force chains within the material.

1.3.2 A Weird Gas

Like a gas, granular matter can be compressed. However, granular matter has properties quite unlike ordinary gases. Consider the situation where granular matter

is placed in a container and subject to vigorous shaking[3]. Imagine that the container has a partition in the centre with a hole in it and that the granular material is initially distributed homogeneously throughout the container. The hole is large enough to allow particles to move between the partitions, but small enough to reduce particle flow between the two halves of the container. Inelastic collisions between the particles, the wall and each other lead to clustering and clumping. The particles will therefore accumulate in one partition, leaving the other partition relatively empty (Shinbrot and Muzzio, 2001). This situation is very different from a perfect gas, which tends towards a uniform density.

1.3.3 An Unusual Fluid

Like a liquid, granular materials can flow, ie. they can be poured and will undergo spontaneous flow if piled too steeply. However, any similarity with liquids is only superficial. Unlike a liquid, the pressure head of a granular material in a tall container is not dependent of height. In avalanching sand, for example, this flow is confined to a narrow boundary layer of the sand pile and the pressure will grow until it reaches a maximum value which is height independent[4].

Granular flows have some interesting features. When granular matter is poured from a funnel, density waves can be observed to propagate either with or against the direction of flow (Baxter and Behringer, 1990). An example of such density waves occurs in the flow of sand through a hopper. Density waves in sand flowing through a hopper seem to depend upon the nature of friction between the grains and also on the slope of the sides of the hopper. Experiments on smooth grains, for example, do not appear to show density waves (Baxter et al., 1989).

A distinguishing feature between flows of granular materials and other solid-fluid mixtures is that in granular flows, the direct interaction of particles plays an important role in the flow mechanics. Thus, much of the energy dissipation and momentum transfer in granular flows occurs when particles are in contact with each other or with a boundary.

[3]This experiment is similar to the famous Maxwell's demon thought experiment in thermodynamics. See (Eggers, 1999) for details.

[4]This is why an hourglass uses sand, rather than liquid, to mark time. Sand flow through the neck of an hourglass proceeds at a constant rate.

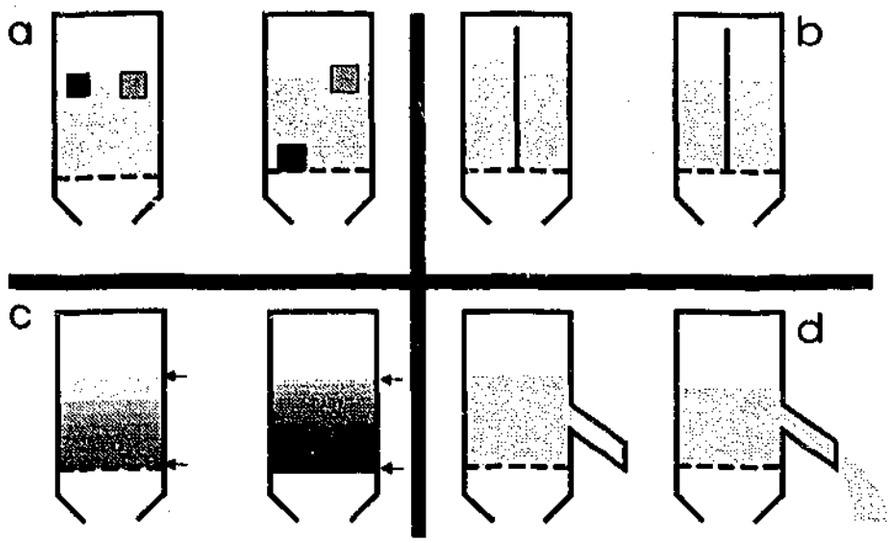

Figure 1.2: Some properties of fluidised beds. *Clockwise from top left*: Dense objects sink and light objects float, two connected volumes will equalise their heights, the pressure will increase non-linearly with depth and fluidised material flows without jamming through an outlet.

1.3.4 Traffic Flows and Jams

The density waves in granular flow have much in common with density waves in highway traffic, with the individual grains behaving in a similar way to cars on the road. Even in steady traffic flow, one sometimes encounters the situation when cars are forced to slow as the traffic ahead slows apparently for no reason. As fast moving cars meet the slower cars ahead of them they brake and a relatively dense "wave" of braking cars which propagates against the direction of traffic flow. Such traffic density waves appear when small fluctuations in the speed of vehicles are amplified (Gaylord and Nishidate, 1996).

Another property of granular materials, which shares similarities with traffic, is jamming. If a granular material is compressed it will jam into a solid like state. If the granular material is shaken, its density will increase slowly approaching an equilibrium value. A model describing this approach has been developed using the analogy of cars parking. In this theory, a parking space becomes available when many small spaces are assembled together (Kadanoff et al., 1989). The density, ρ, as a function of the number of car movements (or, in the case of granular matter,

Group A	Size: $30 - 100\mu m$	exhibits both bubbling and non bubbling fluidisation regimes
Group B	Size: $40 - 500\mu m$	bubbles immediately on fluidisation
Group C	Size: $30v < \mu m$	powders are cohesive and do not fluidise
Group D	Size: $600 > \mu m$	produce deep spouted beds

Table 1.1: Properties of Powder Groups

shakes), t, can be given by

$$\rho(\infty) - \rho(t) = A/\log(1 + t/\tau) \tag{1.1}$$

where the acceleration A, $\rho(\infty)$ and τ all depend upon Γ the maximum acceleration relative to g.

1.3.5 Bubbling Sand

A granular material can be fluidised by injecting fine jets of air though it from below. When in this fluidised state granular matter takes on properties that are reminiscent of those found in fluids (Kunii and Levenspeil, 1991). Objects can be made to float on the surface of the material or sink depending upon the density of the object. In some granular media bubbles will form which behave in a similar way to bubbles in a liquid (see figure 1.2).

The behaviour of fluidised granular matter is quite complex in itself and fluidised granular matter and powders can be classified into several different powder groups which have sharply differing bubbling behaviours (Geldart, 1973) (see Table 1.1). Some powders will bubble spontaneously upon fluidisation (Group B). Some powders fluidise but do not bubble (Group A) and other powders do not bubble at all (Groups C and D).

A complex system is a system consisting of many interacting parts, which exhibits self-organisation and emergent behaviour. By emergent behaviour, it is meant that, when the considered as a whole, the system exhibits properties and behaviour, which

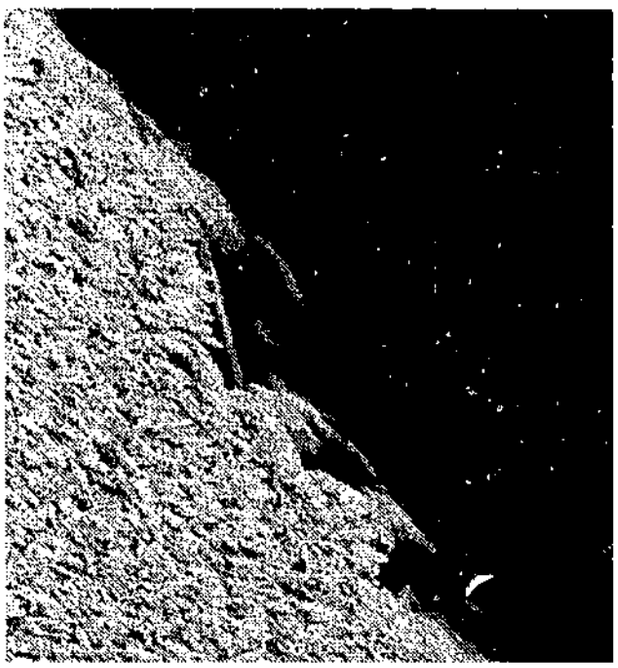

Figure 1.3: Avalanching rice exhibits Self Organised Criticality (from (Frette et al., 1996))

would not be expected from consideration of the properties of the constituent components alone. Given its complex emergent behaviour and properties, granular matter could perhaps be best described as an example of a complex system. Let us consider some examples of self-organisation and complexity in granular media.

1.4 Patterns and Dissipative Structures

One interesting feature of granular materials is the property of inelastic collapse (Kadanoff, 1999). Collisions in granular materials are nearly always inelastic (ie. involving some dissipation of energy). As an example of how this dissipation can affect the behaviour of particulate matter consider the following simple model. Imagine a ball (grain particle) bouncing on a spot on the ground. If the speed of the ball after the mth bounce is s_m, then the speed on the next bounce is

$$s_{m+1} = r s_m \tag{1.2}$$

where r is a constant representing the energy loss per bounce. The heights of the mth bounce obey

$$h_m = s_m^2/(2g) \sim r^{2m} \tag{1.3}$$

Figure 1.4: Oscillons combine to form patterns in vibrating layers of granular materials (from (Umbanhowar, 1996b)).

The speeds approach zero as a geometric series

$$s_m = s_0 r^m \tag{1.4}$$

The time between collisions, which is proportional to h/s_m approaches zero as r^m. Theoretically, we can get an infinite number of collisions in a finite time. This property of granular matter is known as *inelastic collapse* and it leads to clumping and clustering of particles. This behaviour makes it unlikely that granular media can be adequately described by hydrodynamic type equations since dissipative collisions lead to clumping rather than the equilibrium state needed for the usual derivation of hydrodynamic equations. The system therefore shows a strong dependence upon history. If the granular clustering experiments are re-run, different outcomes are obtained with each run (Luding and Herrmann, 1999).

Dissipation appears to be involved in the creation of many non-equilibrium structures in nature (Prigogine, 1980) and in granular materials dissipation appears to play a role in forming patterns.

1.4.1 A Pattern Language

When rigid container of sand is shaken in a horizontal plane unexpected order emerges from the collisions between the grains (Umbanhowar, 1995). Striking patterns emerge including stripes, spots, squares and hexagons (see Figure 1.5). Associated with this pattern formation process are small, stable excitations known as *oscillons* (Umbanhowar, 1996) (see Figure 1.4). Oscillons[5] consist of groups of particles which oscillate between forming a peak above and crater below the surface of the layer of vibrated sand. Vibrating the sand at around 30 Hz and then reducing the acceleration from above to 2.5g can create oscillons (Umbanhowar, 1996a).

Experiments on these strange excitations have shown some interesting results. Small imperfections in the base of the container can cause oscillons to drift. Two oscillons that drift close to one another can interact in unexpected ways. If they are in phase two oscillons will repel each other. However if they are out of phase oscillons will attract and, when they meet, become bound together. With many oscillons it is possible to create stable chains, triangular "molecules" and even stable lattices. In fact, oscillons can be thought of as atoms for the formation of all other patterns. For sufficient densities of oscillons squares, hexagons and all the other patterns so far observed in vibrating sand can be created (Chown, 1997).

In three dimensions the pattern formation is even more complex and is still poorly understood (Shinbrot, 1997). A better understanding of pattern formation in granular materials may give insight into pattern formation in other systems (Ball, 1999a).

1.4.2 Self-Sorting Sand

Another, quite different form of patterning in granular materials involves the grain sorting and segregation. One might think that shaking or rotating a container filled with different types of particles would tend to mix the particles increasing the systems disorder. In granular materials the opposite occurs. Different particles tend to separate and the system becomes increasingly ordered (Makse, 1997), (Shinbrot and Muzzio, 2000). When a granular material is shaken larger particles rise to the

[5]Oscillons only occur in ***driven*** dissipative systems and so differ from other non-linear phenomenon, such as solitons.

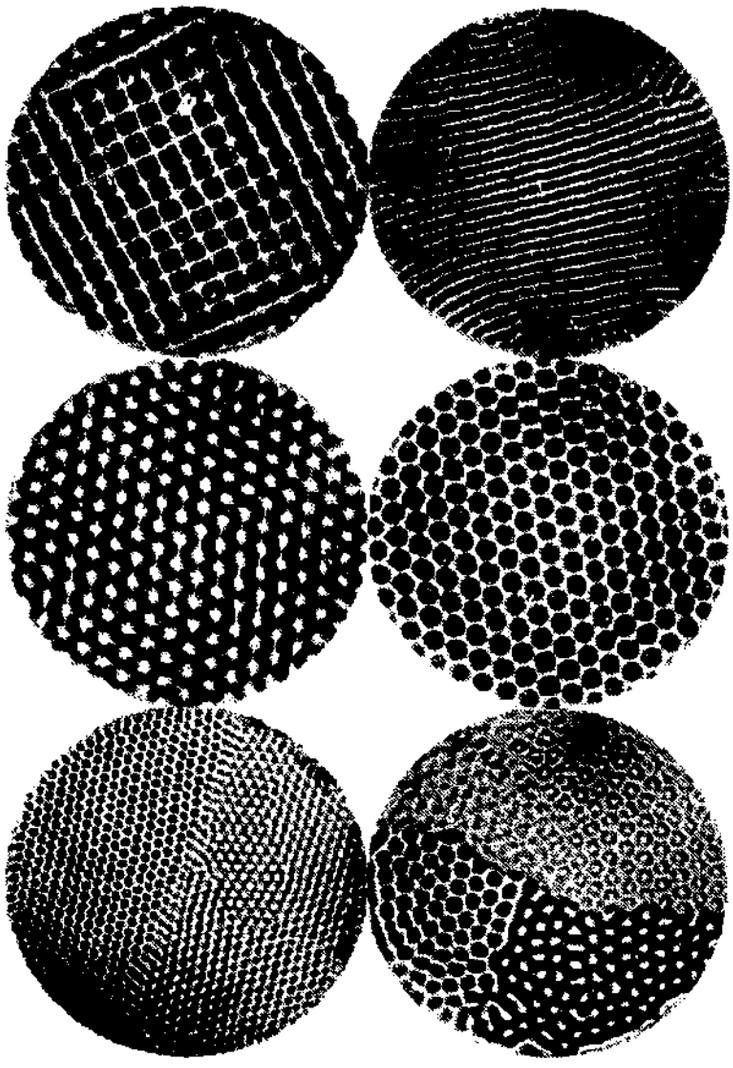

Figure 1.5: Patterns observed in vibrating layers of granular materials (from (Umbanhowar, 1996b)).

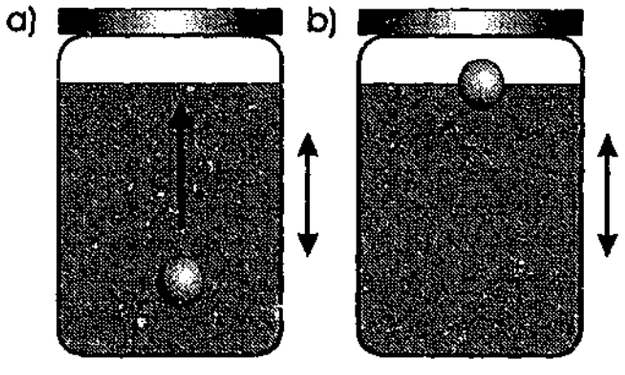

Figure 1.6: The Brazil nut effect

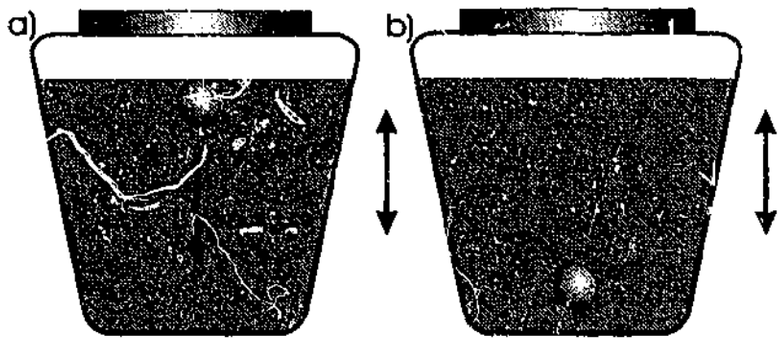

Figure 1.7: The Brazil nut effect in a container with angled sides

top, regardless of their density (see Figure 1.6))[6]. This is known as the "Brazil nut effect" (Duran, 2000), after the way these nuts rise to the top of a jar of mixed nuts. This segregation can be both useful, if different particles need to be separated, or problematic, if different powders (say, for example, pharmaceuticals) need to be mixed to a fixed consistency. This sorting is associated with the formation of convection rolls in the granular flow. Large grains appear to follow the convection rolls to the top of the container but are unable to sink back down again with the smaller grains. These convection rolls can be seen by filling a container with layers of different coloured sands and shaking it. Studies on such an arrangement show that the vibrations cause the sand to crawl up the sides of the container, move across the top and then sink again in the middle. It is found that different shaped containers will produce different sorting behaviour. A conical container, which is wider at the top than the base will, for example, when shaken, caused larger particles to congregate at the bottom of the container instead of the top (see Figure 1.7).

Another segregation effect related to the "Brazil nut effect" is the "Hex nut effect" (Shinbrot and Muzzio, 2000) illustrated in Figure 1.8. Consider a container filled with salt. Two objects, one heavy and one light, are placed in the container. If the jar is shaken vertically, the heavy object will rise rapidly to the surface and the light object will sink. However, when shaken horizontally, the heavy object will sink and the light object rise.

Particle segregation can also occur in rotating drums. Long cylindrical drums containing well-mixed peas and rice will, when rotated, separate into striped patterns

[6]All figures by the author unless otherwise stated

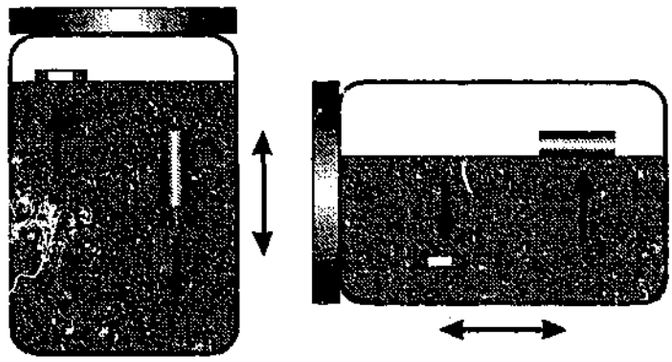

Figure 1.8: The Hex nut effect

of peas and rice along the length of the drum[7].

One other interesting example of segregation occurs in avalanching. If a random mixture of particles is poured onto a sand pile, the pile will build up until it reaches a critical angle. Above this critical angle, the sand will begin to flow. The pile will build up until it reaches a stable *angle of repose* about which it tends to stay (Grasselli and Herrmann, 1997). Particles with different size, shape and/or surface friction, when piled, will tend to have different angles of repose. In general smaller and smoother particles will have a lower angle of repose than larger and rougher particles. If a mixture of particles is poured into a heap then spontaneous stratification occurs[8]. A cross section through such a pile shows a layered appearance (Makse et al., 1997). In general, the smaller and smoother particles will be found below the larger and rougher grains. When the larger grains are the smoother of the two grain types in the mixture, segregation is not observed to occur. This stratification could explain the existence of "long run out" rock slides (Fineburg, 1997). In these rockslides, the slide does not stop at the bottom of the hill on which it occurs, but continues for some considerable distance more. These rock slides often result from a catastrophic event such as an earthquake and can cause a great deal of devastation. In such events particle segregation could cause the smoother rocks and particles to move to the bottom of the slide where they act as a lubricant.

[7]This will be investigated further in chapter 7

[8]This will be further discussed in chapter 6

1.4.3 Avalanches, Earthquakes and Extinctions

Besides their ability to segregate particles, avalanches have some fascinating dynamics in their own right. In fact, the humble sand pile has been used as a paradigm example of a process known as self-organised criticality which is postulated to occur in a very wide range of physical phenomena. Bak *et. al.* (Bak et al., 1988) have argued that sand piled at the angle of repose is in a critical state in the sense of a second order phase transition. They also argued that this state is an attractor for the systems dynamics.

To illustrate the principle Bak and his colleagues (Bak et al., 1987) created a cellular automata model of a sand pile (see Figure 1.9). A lattice is constructed whose values, $z(x, y)$ represent the height of the pile (or alternatively the number of particles of equal size) at the point (x, y). If the slope of the pile becomes too large at a point (x, y) on the pile then the pile avalanches. By avalanche, it is meant that the height at that point, $z(x, y)$, decreases by four units and the height of the neighbouring points $z(x \pm 1, y)$ and $z(x, y \pm 1)$ increase by one unit each. In other words, the system is updated synchronously according to

$$z(x, y) \rightarrow z(x, y) - 4 \tag{1.5}$$

$$z(x \pm 1, y) \rightarrow z(x \pm 1, y) + 1 \tag{1.6}$$

$$z(x, y \pm 1) \rightarrow z(x, y \pm 1) + 1 \tag{1.7}$$

The boundary values of the pile are set to zero so that particles can fall off the sides. Beginning with random conditions such that $z \gg z_c$ where z_c is the critical value, the system evolves until all values of z are less than z_c. When this experiment is repeated, the clusters of sites which are affected by the avalanching process are found to obey (Schroeder, 1990)[9]

$$D(s) \sim s^{-\tau} \tag{1.8}$$

[9]This model is a member of a class of avalanche models that exhibit Self-Organised Criticality (see (Kadanoff et al., 1989).

where $D(s)$ is the size of the avalanche and $\tau \approx 1$.

Self-organised criticality has been put forward as an explanation for the distribution of earthquakes, the electrical behaviour of certain semi conductors, the formation of landscapes and river networks and for the pattern of extinction of living species (Bak, 1997)[10]. For sand piles in the self-organised state avalanches occur at all scales, from tiny spills involving only one or two grains to massive falls involving the entire surface of the sand pile. The plot of the avalanche frequency, f, versus the size of the avalanche is found to follow a $1/f$ law with small avalanches overwhelmingly more frequent than large ones (Maslov et al., 1999). Bak *et. al,* have proposed that SOC is a general explanation for the existence of both $1/f$ noise and fractals in the physical world (Bak and Chen 1989).

The phenomenon is called self-organised since, as the sand pile steepens, large avalanches tend to dominate causing the slope to fall again. If the slope becomes too shallow then small avalanches dominate, large avalanches are rare and the pile steepens again. The pile thus settles into a steady state where the 1/f law is obeyed. Self-Organised Criticality has been observed in experiments on real sand piles (Held et al., 1990) and in experiments on rice piles (Frette et al., 1996) (Malthe-Sorenssen et al., 1999) but, only under certain idealised conditions. Real granular systems generally show more complicated avalanching behaviour. Some avalanches occur as material flows down the slope undermining the material above it. This *undermining* propagates upward from the base of the pile (Daerr and Douady, 1999). In other cases *slumping* occurs where large clumps of material build up then avalanche together as a whole (Held et al., 1990) in a more or less periodic behaviour. It appears then that the dynamics of real granular materials contain both critical and non-critical behaviour.

1.4.4 Fingering in Granular Flows

Pouliquen *et. al.* have observed fingering in granular flows (Pouliquen et al., 1997) (Pouliquen and Vallance, 1999). In experiments conducted on avalanching granular flow, an initially uniform avalanching front is observed to break up into "fingers"

[10]There is still much debate in the literature over the legitimacy of SOC as an explanation for these phenomena. This is by no means a settled issue.

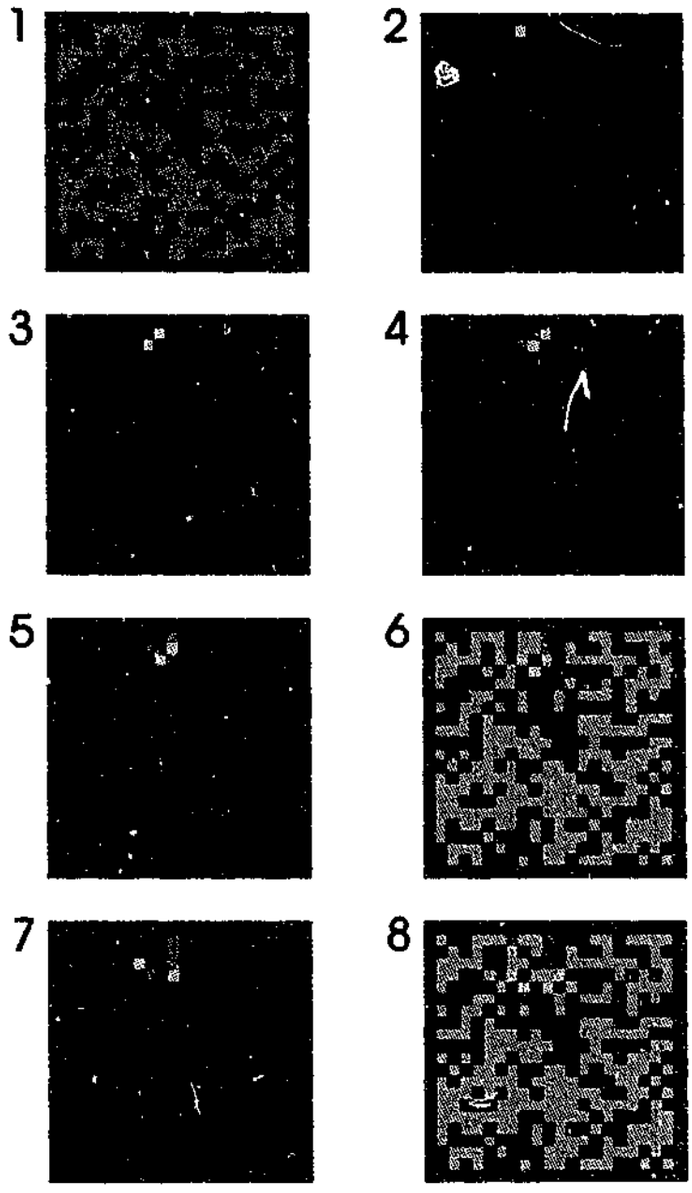

Figure 1.9: The sand pile model of self organized criticality showing an avalanche evolving over time. See appendix C for program listing.

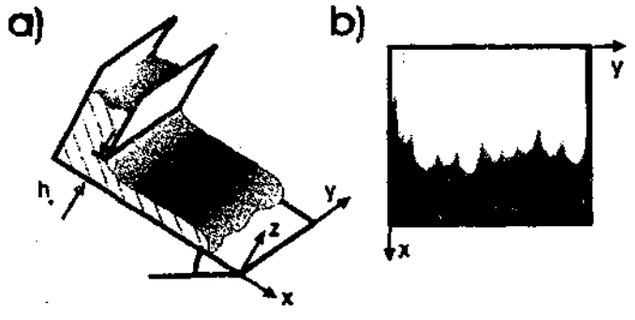

Figure 1.10: Fingering in granular flows (from (Pouliquen et al., 1997)). (a) The apparatus and (b) the view through the transparent base.

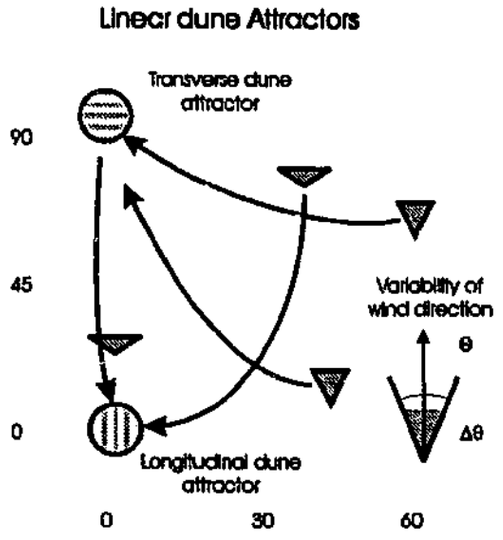

Figure 1.11: Phase diagram for dune formation showing the attracting states. After (Werner, 1995).

Figure 1.12: Ripples in sand

as the flow proceeds down an inclined plane. The experiment is shown in Figure 1.10a. The bottom of the apparatus is transparent glass that has been roughened by gluing a layer of glass beads to it. The fingering is observed when the apparatus is viewed from below (Figure 1.10b). In appearance, these instabilities are similar to those found in viscous fluids. In fluid flow the instabilities are driven by surface tension, however in granular flow there is no surface tension. The dynamics are instead driven by size segregation which develop during the flow.

1.4.5 Ripples and Dunes

One common feature of wind blow sand is the appearance of ripples (Ball, 1999a). The formation of ripples involves some interesting features. Imagine a flat sandy surface that is buffeted by a steady wind. The wind blows on the sand and shifts

it downwind. Imagine that the plain has a small bump. The windward side of this bump will be hit by more wind blown grains than elsewhere on the plain. Conversely the downwind or "lee" side of the bump is protected and is hit by fewer grains. The bump will therefore grow and a ripple is formed. The formation of one ripple leads to the formation of another downwind of the first. As wind blows across the plain the plain rapidly self organises into a series of ripples (see figure 1.12).

Interestingly these ripples show size segregation of sand grains. The coarsest grains appear on the crests of the ripples. Anderson *et. al.* (Anderson, 1996) have shown that as wind blown grains crash into the surface they produce a granular "splash". During these impacts, small grains are scattered further than the larger grains. Over time smaller grains are preferentially effected by collisions from the crests of the ripples leading to segregation.

Sand dunes come in a variety of forms, which also show a tendency to self organise. These forms include long ripple like dunes, which line up perpendicular to the prevailing wind. Other dunes, known as longitudinal dunes, run perpendicular to the prevailing dunes. Barchan dunes are crescent shaped and curve down wind. These can merge to form wavy crests known as barchanoid ridges. There are also star dunes, which have several arms radiating in all directions (see figure 1.11).

Werner (Werner, 1995) has developed cellular automata models of dune formation is which reproduces all these major dune formations from a few simple assumptions. In this model grains are scattered at random across a rough stony surface. They are picked up at random and carried by the wind. The model takes into account the fact that sand bounces more readily off stony ground than off sandy surfaces. It assumes that probability of wind blown sand being deposited on the sandy surfaces is greater than that deposited on stony ground. Werners' model suggests that these dune varieties act like attractors of the system. Regardless of the initial conditions, the system seems to inevitably produce these forms.

1.4.6 Sound Producing Sand

Some sand dunes are musical (Sholtz et al., 1997b). Under highly restricted conditions in several places in the world sand has been observed to avalanche in such a way as to produce a loud distinctive and sometime musical booming sound. This

bizarre behaviour has been reported for over 1,500 years and is usually accompanied by strong seismic avalanching of the dune surface. The grains of sand dunes that have been observed to boom are unusually well sorted, polished and rounded. It is thought that coherent oscillations within the flowing sand are responsible for the sound produced but, as yet, no detailed mechanism has been discovered. A related phenomenon is squeaking sands (John F. Lindsay and Criswell, 1976). Like booming sands these naturally occurring sands are usually well sorted and well rounded. Unlike booming sands, which are found in desserts, squeaking sands are found on beaches and are not highly polished. Squeaking sands get their name from the squeaking noise they make when walked upon. Again the reasons for this remain mysterious, however there are reasons for thinking that the mechanisms for both booming and squeaking are similar (Sholtz et al., 1997a).

1.5 Aims and Objectives: Inter-particle Forces

The above summary suggests that inter-particle forces are important in understanding many of the above phenomena. Inter-particle forces play an important and often crucial role in many of the complex behaviours and properties observed in granular matter. These inter-particle forces include:

- Friction and mechanical forces
- Liquid bridging (where surface tension of small amounts of liquid between grains acts to bind them together.)
- Electrostatic and Van der Waals forces. These forces can be quite complicated and can be influenced by such things as adsorbed surface layers[11].

The main aim of this research is to investigate the effect of inter-particle forces on the properties and behaviours of granular media. In the next chapter, a novel system for investigating the effect of inter-particle forces on particulate materials is presented. In subsequent chapters, this is used to investigate the effect of inter-particle forces on granular behaviour in a variety of situations.

[11] see (Israelachvili, 1992)

CHAPTER 2

Building on Sand

Granular materials are subject to many kinds of inter-particle forces such as friction, Van der Waals and liquid bridging forces. In order to examine how these forces influence the properties of granular media it would be advantageous to be able to alter these forces in a controlled manner. Unfortunately, for most of these forces, this is difficult, if not impossible. In this chapter, the effect of inter-particle forces on the properties of granular media is examined using a novel method. A magnetic field is applied to a pile of iron shot. The field induces a magnetic dipole in the iron particles altering the inter-particle force between them. This method, it is shown, has several advantages over other methods of altering inter-particle force. For example, the induced magnetic inter-particle force can be easily controlled by altering the field strength. Using this technique, the static and dynamic angles of repose are studied as functions of inter-particle force. The change in the shape of the granular profile as inter-particle force increased is also examined.

2.1 Overview: Static Behaviour in Granular Materials

2.1.1 The Angle of Repose

When a powder is poured onto a flat plate, it forms a conical shaped heap. Once the powder has reached an equilibrium state, the average angle the sides of the cone make with the plate is called the *static angle of repose*[1]. The angle of repose depends on such factors as the packing history (Alonso et al., 1998), size (Pilpell, 1958), density (Grasselli and Herrmann, 1997), surface roughness and level of moisture of the powder (Tegzes et al., 1999), (Forsyth et al., 2001c), as well as the surface

[1]Generally referred to as simply the *angle of repose*

roughness of the plate (H. Kalman and Ben-Dor, 1993).

A sand pile will keep its shape as long as the sides of the pile or *free surface angle* (Grasselli and Herrmann, 1997) do not exceed the maximum *angle of stability.* Above this angle the surface of the pile becomes unstable and undergoes avalanching. An avalanche generally stops once the free surface angle reaches the *static angle of repose.* Between these two angles, there is a region of complex bi-stable behaviour that depends upon how the pile was prepared.

The static angle of repose can be measured in several ways, though not all methods will give the same angle (H. Kalman and Ben-Dor, 1993). It is therefore necessary to refer to the method used when describing angle of repose measurements. For instance, a flat-bottomed box can be filled, and the powder allowed to flow out through a hole in the bottom of the box. The angle that the remaining powder forms with the horizontal, once flow has ceased, is the *draining crater* or *discharge static angle of repose.* A second technique is the so called *injection method.* In this method, the material is poured onto a plate through a funnel. Assuming that the pile forms a perfect cone, the angle of repose can be calculated by knowing the diameter of the base and the height. A third method, *the tilting method*, involves placing the material in a narrow drum and tilting it until avalanching occurs. Tilting is then stopped and the angle of repose then measured. The final method that will be considered is the *poured angle of repose.* This involves pouring the material into a narrow box and measuring the angle of repose of the pile (see Figure 2.1). The internal angle of the crater formed in draining crater method is generally larger than the external angle of the conical pile formed by the injection method. The difference between the angles is expected to decrease as the radius of curvature of the pile and crater are increased. The angles obtained in both the draining crater[2] and poured methods will be influenced by container dimensions, increasing slightly[3] as the container size increases.

The static angle of repose will be influenced by many factors but one of the dominant influences is the inter-particle friction force. Consider the slope of a granular pile to consist of sheets of granular material laid on top of each other. These sheets

[2] see for example (Grasselli and Herrmann, 1997) p302

[3] $\approx 1^o$

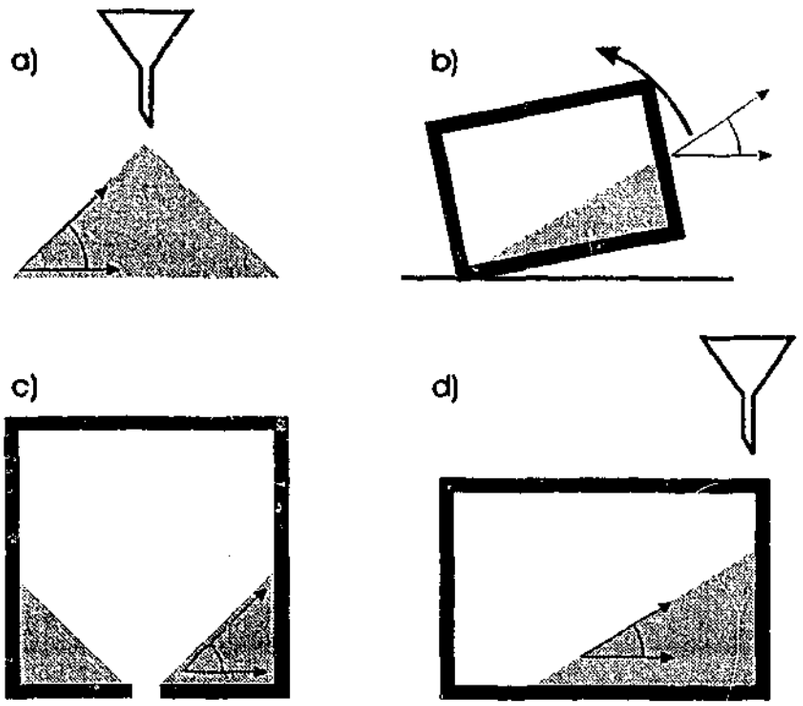

Figure 2.1: Methods of defining angle of repose. (a) discharge (b)tilting (c)draining crater and (d)poured

cannot slide past each other unless the angle of inclination of the slope exceeds $\tan^{-1}\mu_s$ where μ_s is the coefficient of static friction (Duran, 2000).

2.1.2 Dynamic Angle of Repose

Consider a drum filled with a granular material. As the drum is rotated, the free surface angle undergoes avalanching. For a very slowly rotated drum, avalanching occurs intermittently. The angle that the surface of the avalanching slope makes with the horizontal will be steeper before each avalanche than after it. These two angles are known as the *starting (or maximum)* and *stopping (or minimum)* angles. As the rotation speed is increased, the avalanching becomes less intermittent. At a critical value of rotation speed, the avalanching surface undergoes continuous flow, forming a constant angle with the horizontal known as the *dynamic angle of repose*[4]. At very low rotation speeds (0.01 rotations per second) the free surface makes and angle θ_e with the horizontal (known as the *embankment* angle). This angle is not a steady, well defined angle however, and if examined carefully it is found to vary. It is found to increase to θ_m (known as the *angle of movement*), after which a small

[4]This term is strictly speaking self-contradictory. However, it is commonly used terminology and so we will follow the convention in this discussion.

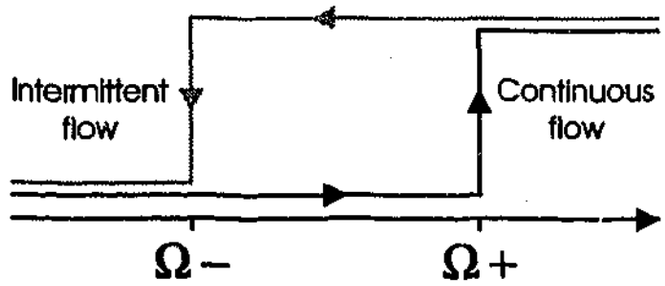

Figure 2.2: Hysteresis for dynamical angle of repose

avalanche takes place and angle drops to θ_r (the dynamic angle of repose). The relaxation angle is defined such that $\delta = \theta_m - \theta_r$ and is typically about 2° for dry granular materials (Duran, 2000). For low rotation the angle oscillates between θ_r and θ_m. This flow is intermittent. As the speed increases, a point, Ω_+ is reached where the flow becomes continuous. If the rotation speed is decreased from above Ω_+ however a different and lower speed Ω_- is obtained, where the continuous flow becomes intermittent (see Figure 2.2).

As the speed of the drum is increased the angle of repose increases. At high speeds the surface profile distorts and is no longer a constant angle (Hill and Kakalios, 1995). The surface takes on an "S" shaped profile seen in Figure 2.11. The way in which the angle of repose varies with velocity appears to depend upon the material.

2.1.3 Cohesive Forces and Liquid Bridges

When building a sandcastle, experience quickly teaches us that damp sand is a much better building material than dry sand or very wet sand. This is especially true if the castle is to have steeply sloped (or vertical) sides.

If one attempts to use dry sand, the sandcastle will have gently sloping sides, usually less than 25°. The gravitational force on the particles acts to flatten the pile, and the only force resisting this is the weak inter-particle friction. Adding water to the sand provides an inter-particle force in the form of liquid bridges. It is this inter-particle force that allows the sand to form structures with steep sides. In order to investigate the dependence of granular statics and dynamics on inter-grain friction, experiments were conducted on iron shot placed in a magnetic field. The idea behind these experiments was that the magnetic field would induce a magnetic dipole on the iron particles and cause them to stick together. For low field

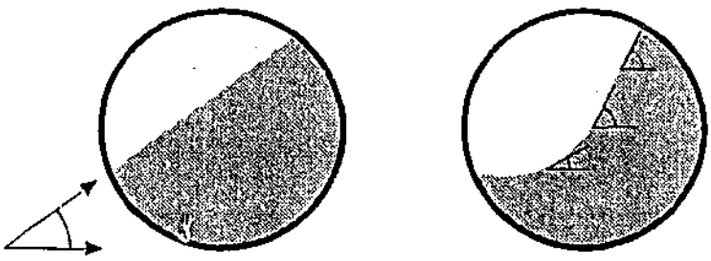

Figure 2.3: The dynamic angle of repose is hard to define for large rotational velocities

strengths, this produces the magnetic analogue of friction. The induced dipoles reduce the tendency of particles to roll over one another and so should influence such properties as the angle of repose. At high field strengths, the dipoles tend to align themselves strongly with the field, clustering takes place and so the analogy with friction breaks down.

The cohesive properties of powders depend upon a variety of factors such as size, density, surface roughness, presence of liquid and degree of compaction. Rather than examine each of these variables in isolation, the widely suggested idea that competition between the inter-particle forces and the inertial forces determines granular behaviour will be used (see for example (Rhodes et al., 2001)). As the ratio of inter-particle force to inertial forces increases, the powder becomes more cohesive and the angle of repose increases accordingly.

For smooth dry powders, the dominant inter-particle force is the Van der Waals interaction. This increases linearly with particle size, while inertial forces increase as the cube of the particle size. Hence, the effect of the Van der Waals force is best seen for small particles. For instance, coarse dry beach sand is free flowing, and forms piles with a very low angle of repose. On the other hand, fine powders such as corn flour and icing sugar are typically cohesive, and piles of these materials can support more steeply sloped sides. Compaction will also have the effect of making a powder more cohesive. The Van der Waals interaction for macroscopic particles falls off as the square of the inter-particle separation (Israelachvili, 1992). Compaction decreases the average inter-particle distance and hence increases the Van der Waals force. Compacting the powder also increases the "coordination number" of the particles within the powders. For example, in a loosely packed powder each particle may be, on average, in close contact with only six other particles. In a

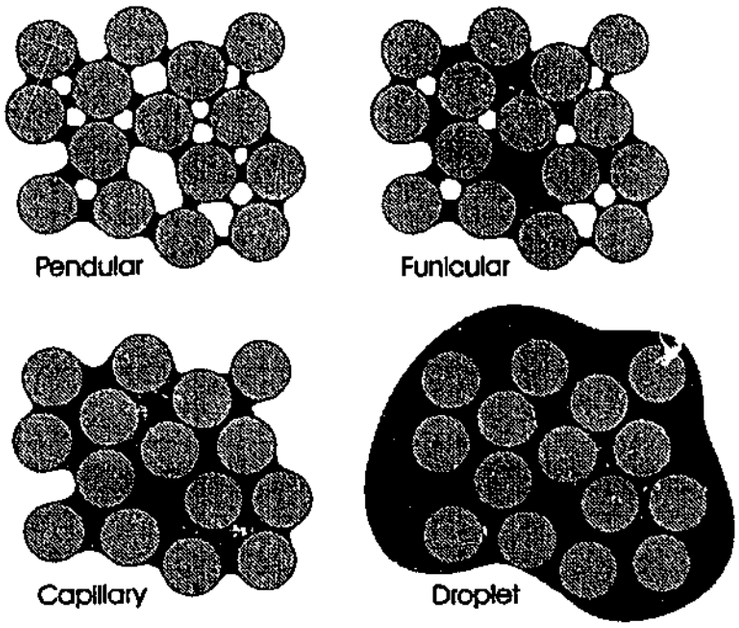

Figure 2.4: Different states of saturation for wet granular materials.

closely packed state, they may be in contact with 8 to 12 particles, with 12 representing the, in practice unobtainable, hexagonal close packed state.

The addition of liquid to dry powders will cause a transition in behaviour. Damp sand is better for making sand castles than dry sand, due to its cohesive properties. The inter-particle force in this case is caused by the formation of liquid bridges. When a small amount of water is added to a granular material the liquid coats the grains forming small liquid bridges at the point of contact between grains. The surface tension of the liquid in these liquid bridges provides a force that pulls the grains together. The concave nature of these *pendular* bridges creates a capillary action that allows us to create steep sided castles. If more liquid is added some of the bridges merge, forming the so-called *fenicular* state. When the liquid content is further increased, a capillary state is reached where, the interstices are filled with liquid, but the concave liquid surfaces hold the material together (see Figure 2.4). When the liquid is increased further, the concave liquid surfaces disappear and the material is said to be in a *droplet* state. In this state, the surface curvature of the liquid is no longer concave and the capillary action disappears. This explains why it is difficult to make sand castles with either completely dry[5] or sand which is un-

[5]Sand castles on the beach are able to retain their shape when dried. This is due to salt, which crystallises out of the seawater, forming solid bridges between grains.

derwater. In both instances there is no surface tension to hold the grains together[6].

2.1.4 Methods for Examining Cohesive Forces

To examine in detail the transition from non-cohesive to cohesive behaviour, a method for varying the ratio of inter-particle force to inertial forces is needed. We shall discuss briefly methods used previously and note the disadvantages associated with each.

One way of altering inter-particle force is to change the ratio of inter-particle force to inertial force by altering the particle size since smaller particles tend to be more heavily influenced by Van der Waals forces. This leads to several complications. For instance, particles might not be available in the desired size. Commercial batches of say $250\mu m$ and $500\mu m$ may not have the same relative size distribution. Most importantly however, it is difficult to obtain the same initial experimental conditions with different particle sizes. While particles larger than approximately 250μm pack under normal gravity with roughly the same voidage, for particles smaller than this the voidage increases with decreasing particle size (Feng and Yu, 1998)[7].

Several groups (Albert et al., 1997), (Hornbaker et al., 1997), (McLaughlin and Rhodes, 2001) have added liquids of varying surface tensions and viscosities to dry powders to observe the increase in inter-particle force. Work has also been done on examining the effect of liquid on packing of mono-sized coarse spheres (Feng and Yu, 1998). There are several limitations with this method. Firstly, adding liquid increases the inter-particle force in a step-wise manner. It is also difficult to remove liquid in a controllable way. Adding liquids to dry powders not only increases the inter-particle interaction, but also the interaction between the powder and the wall. This complicates the analysis further since the walls of a container can support a large fraction of the weight of the powder inside and increase the angle of repose. Perhaps the most important limitation of this method is that it is difficult to relate the quantity of liquid added to the inter-particle force.

To avoid these complications, the packing of iron spheres within a magnetic field was

[6]damp sand acts like a *tensegrity* structure (Fuller, 1975). Unlike conventional structures, these structures are held together mostly by tension rather than compression.

[7]This will be examined in more detail in chapter 3.

examined. Varying the strength of the field allowed induced inter-particle magnetic force to be continuously varied. As the walls of the vessel are non-magnetic perspex, the particle-wall interaction was unchanged. As the same particles under the same packing conditions are used for all of the experiments, it was ensured that the initial conditions were as uniform as possible.

If it is assumed that the particles are magnetically linear, it follows that the inter-particle force between two particles F_{mag} will vary in proportion to the square of the applied magnetic field ($F_{mag} \approx B_0^2$) (Jones et al., 1989). Rather than rely on a calculation of the field from theory, the ratio of inter-particle force to weight was measured directly, as described below. A plot of measured force against field strength squared was approximately linear, and a linear calibration curve was prepared to allow the inter-particle force to weight ratio for any given field strength to be determined.

The interactions between particles in the magnetic field will, in general, be non-linear. Recent research, however, seems to suggest that the systems can be treated as linear in a wide variety of circumstances. Tan *et. al.* (Tan and Jones, 1993) have conducted experiments on the induced magnetic force between individual and/or regular configurations of magnetically non-linear spherical particles. While there was a slight tendency for particles to form chains and a tendency for layers of chains to repel, they concluded

> "...we have not perceived a radical difference in results between the two particle and multi-particle arrangements. In light of our experimental results the two particle chain seems to warrant a role as the basic building block in modelling the strong particle interactions of more complex systems."

2.2 Experimental

The experimental set-up is shown in Figure 2.5. To measure the static angle of repose, a narrow rectangular box of width 4 mm, length 300 mm and height 150

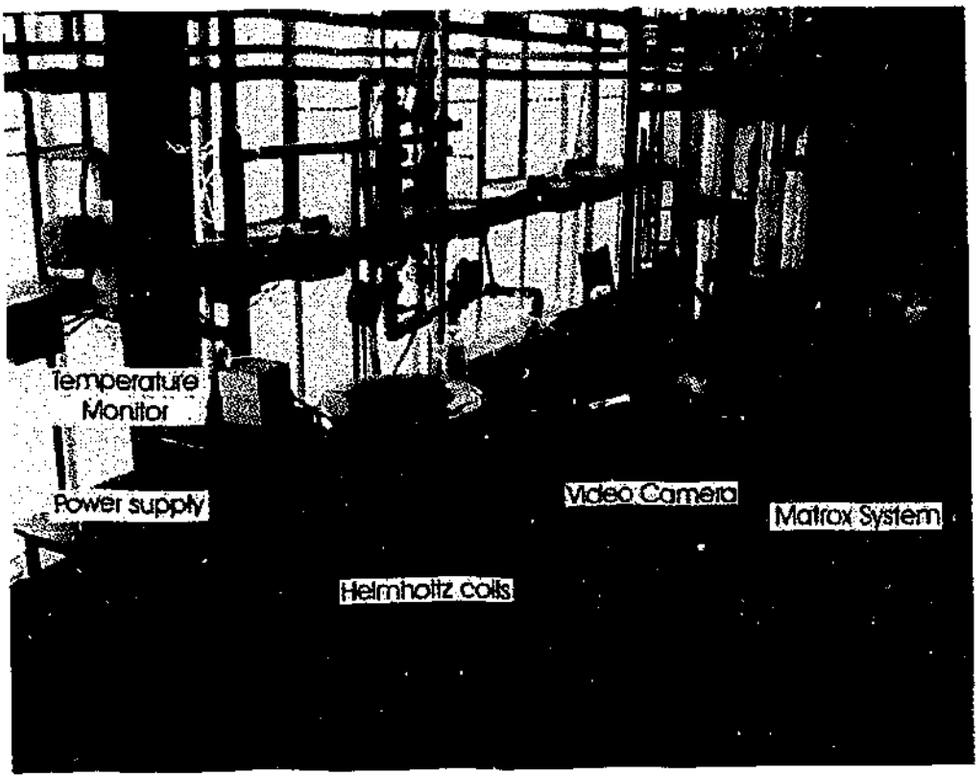

Figure 2.5: The laboratory setup showing Helmholtz coils and imaging system.

mm was filled with iron spheres[8] of mean diameter $800\mu m$[9] from a funnel with a stopcock attached. The stopcock was used to control the flow-rate.

To measure the dynamic angle of repose, a narrow perspex drum of diameter 150 mm and thickness 10 mm was placed horizontally on a set of aluminium roller supports and driven by an electric motor. The rotation speed was kept at 24 rpm. Due to the presence of the magnetic field, only non-magnetic materials were used in construction of the roller supports, and these were connected to the electric motor via a long belt. The drum was approximately half filled with iron spheres.

2.2.1 Particles

The iron particles used in these experiments were essentially spherical and were sieved using a set of standard "Endecott" brand sieves (see appendix A for details). The particles were sieved into fractions differing by approximately $\pm$ 5% of the mean particle diameter. When sieving the particles, care was taken to ensure that the layer of material covering the sieve was only one particle deep. This allowed

[8] see appendix A for details of suppliers.

[9] The particles were sieved to various size ranges - details of the exact size ranges can be found in Appendix A.

any small particles present to pass through the sieve. In these experiments iron particles of size ranges 350-425 μm, 800-900 μm and 1.6-1.8 mm were used. In the discussions which follow the convention of quoting the smallest sieve size when describing the particle diameters will be adhered to.

2.2.2 Helmholtz Coils

The magnetic field for this experiment is supplied by a pair of Helmholtz coils. These coils have an inner diameter of 456 mm, an outer diameter of 568 mm and a thickness of 76 mm. The formers were constructed from nylon, and were each wound with 1.1 km of 2.24 mm diameter insulated copper wire. The coils were powered by a 16 A, 16 V stabilised DC power supply, and have a total resistance of 2.2 Ω. Thermal sensors on the inner wall of the coils provided information about temperature within the coils. The power supply was designed to automatically switch off if the temperature rose above a preset value. Additional cooling was provided by a water jacket, but this was not found necessary for these particular experiments. The magnetic field axis orientation was in the vertical direction and was measured as a function of current by a Bell 240 series Gaussmeter. The field was found to vary less than 10% throughout the volume between the coils, and by less than 5% within a sphere of diameter 140 mm centred on the axis of symmetry, midway between the coils. The variation in magnetic field intensity with current is shown in Figure (2.6).

To directly measure the inter-particle force between two particles as a function of field strength, the following method was used. An iron sphere of the appropriate size was glued to a plastic spatula and positioned on the axis of symmetry at the point midway between the coils. With the field at full strength (approximately 6400 A/m) a second particle of the same size was brought into contact with the fixed sphere. Due to the strong magnetic force between the two particles, the second particle became suspended from the first. The current in the coils, and hence the magnetic field strength, was slowly decreased until the suspended particle fell from the fixed particle. At this point, the inter-particle force is equal to the weight of the particle. This measurement (and all subsequent measurements) were repeated several times for accuracy. The weight of the particle was measured with a sensitive

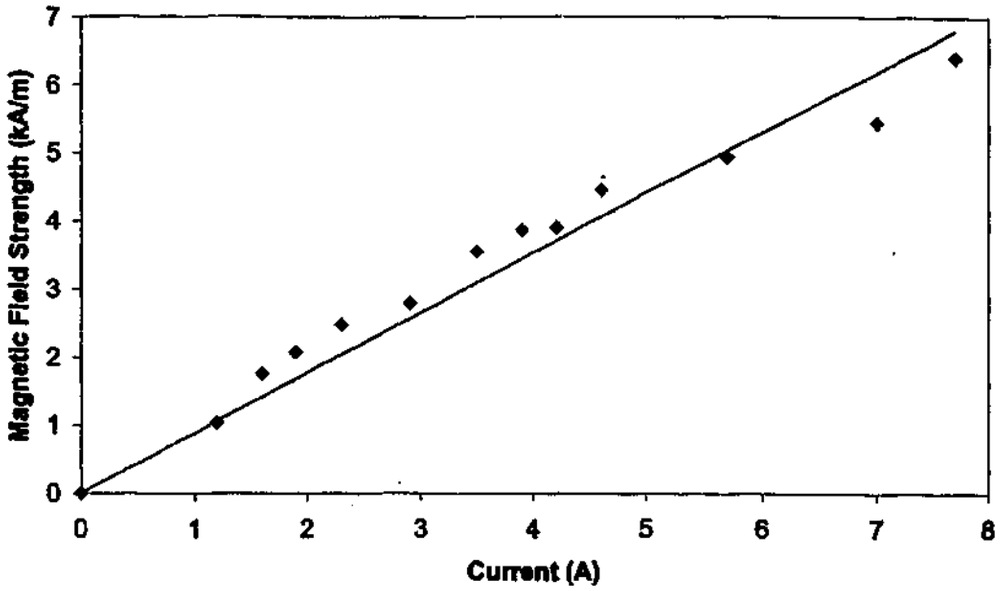

Figure 2.6: The variation in magnetic field intensity with current for the Helmholtz coils

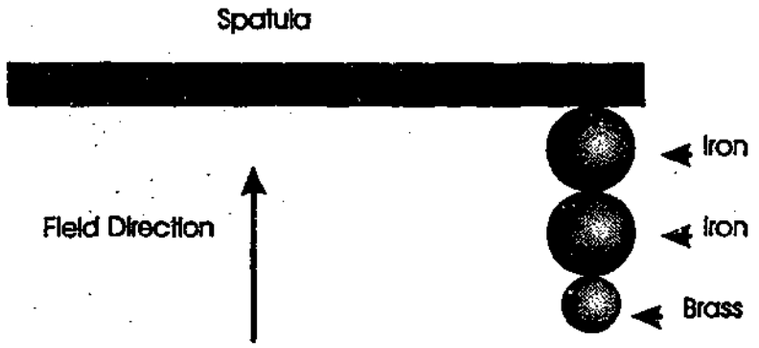

Figure 2.7: Method of measuring inter-particle force

laboratory balance.

To obtain further points for the graph, small ($500\mu m$) bronze spheres were carefully glued to the "bottom" of the particle to be suspended. This served to increase the weight of the particle without significantly altering the inter-particle force. This new particle was weighed, and the measurements repeated, making sure that none of the bronze particles became dislodged when the suspended particle fell (see figure 2.7). The weight of the particle was then plotted against the square of the field at which it fell. By dividing through by the weight of each particle, the ratio of inter-particle force to weight can be obtained, as shown on the right hand axis of figure 2.8.

Ramping the field down slowly serves two purposes. First, it allowed the current

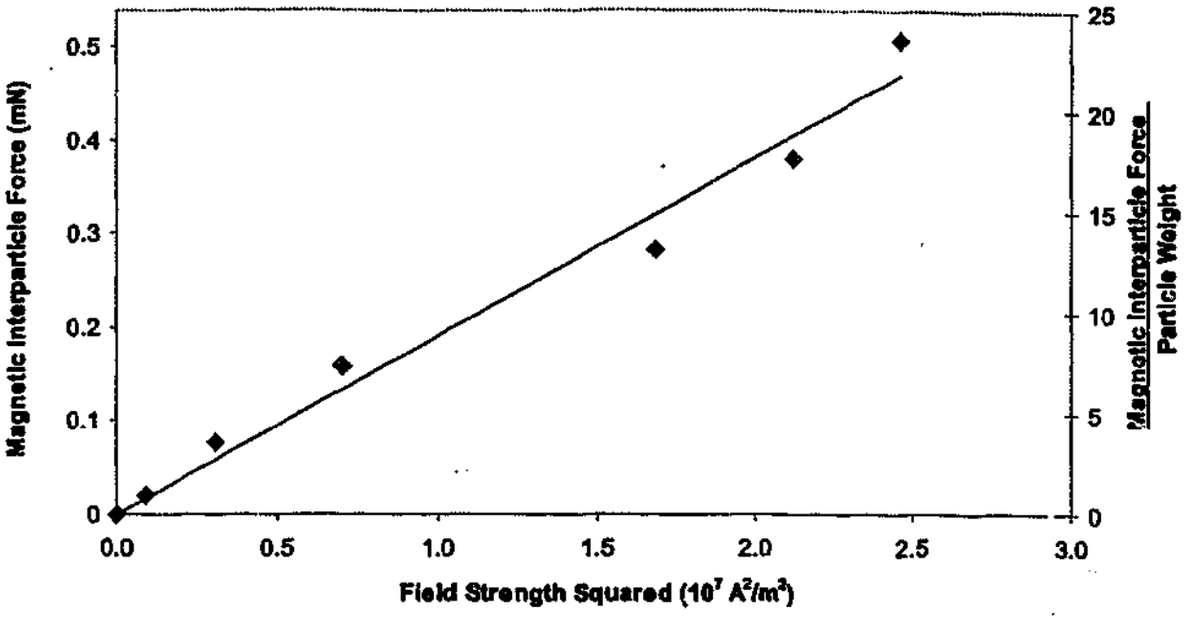

Figure 2.8: Graph of magnetic inter-particle force with field strength squared

and hence field at which the inter-particle force and gravitational forces become equal, to be accurately determined. Secondly, it allowed the magnetic field induced in the iron spheres to relax, so that the force was representative of the present field, rather than the higher field it was at moments ago.

An image recognition system consisting of a commercial digital camera attached to a Matrox card was used to capture the images and our own software used to analyse the results. Lighting was controlled by backlighting, using a diffuser to ensure uniformity of the lighting conditions. Pre-processing to remove noise and unwanted artefacts was applied to all images.

A set of experiments were conducted to measure the angle of repose for different values of inter-particle force[10].

2.3 Results and Discussion

The increase in dynamic angle of repose with increasing inter-particle force can be clearly seen in Figure 2.12. The angle of repose was determined by first segmenting the image, and the angles were determined using a Hough transform. This approach

[10]The results of the authors experiments have been published in (Forsyth et al., 2001a) and (Forsyth et al., 2000)

is robust to noise and is preferred to other curve fitting techniques (Gonzalez and Wintz, 1987).

The results of the experiments to measure the static and dynamic angles of repose are shown in Figures 2.12 and 2.13. In both cases, the angle of repose increases approximately linearly with increasing inter-particle force. Similar results for the static angle of repose have been demonstrated elsewhere (Albert et al., 1997), (Tegzes et al., 1999), (Hornbaker et al., 1997) for liquid bridge forces, using the draining crater (Albert et al., 1997) method to measure angle of repose.

The dynamic angle of repose measurements were made at the point of continuous flow. Tegzes *et. al.* have defined a series of flow regimes in granular media. They postulate the existence of a granular regime, a correlated regime and a plastic regime. The linear behaviour in these experiments corresponds to the *granular regime* of Tegzes *et. al.* (Tegzes et al., 1999) for wet granular media, where surface flow is homogenous and involves only the top few layers of grains. This behaviour manifests itself at low levels of liquid addition. In the experiments of Tegzes *et. al.*, as the amount of liquid increases, two other regimes become apparent. In the *correlated regime* surface flow becomes strongly correlated in that clumps of many attached grains fall in each avalanche, leading to a cratered surface. In this regime the angle of repose rises more slowly than in the granular regime, though still in a linear manner. In the *plastic regime* surface flow is reminiscent of a viscous fluid in that the surface remains smooth, rather than taking on the cratered appearance that appears in the correlated regime. In the plastic regime, the angle of repose stops increasing with additional liquid content, and indeed in some cases actually decreases.

It is unclear whether plastic or correlated regimes will show up at higher fields. Obviously the angle of repose cannot continue to increase linearly with increasing field, as the angle of repose cannot exceed 90°, and one doubts whether in practice this can even be approached closely. At high fields, the poured angle of repose became difficult to measure due to the cohesive nature of the iron spheres. The iron spheres began to clump, blocking the orifice in the funnel. Theoretical studies

based on stability criteria (Albert et al., 1997) demonstrate that the maximum angle of stability should increase approximately linearly with increasing inter-particle force from about 23°, at zero inter-particle force, up to a little over 80°, at a ratio of inter-particle force to weight of 1. At ratios above one the graph tails off towards the maximum angle of repose at 90°. The work of Albert (Albert et al., 1997) considered liquid bridge forces as the inter-particle cohesive force. The theory is based on the maximum angle of stability for stationary particles, rather than the poured angle of repose measured here.

In essence, this corresponds to taking a flat surface of particles and very slowly tilting it until flow begins. The particles in this experiment have been dropped from an average height of around 10 cm, and gain a velocity of the order of 1 ms^{-1} before impacting on the surface of the pile. This energy must be dissipated before the particle comes to rest, and obviously allows the particle to come to rest further down the slope than it would if it were placed gently at the top of the pile.

It is perhaps not surprising that the angles of repose measured here rise more slowly with increasing inter-particle force than theory based on liquid bridge forces would suggest. One limitation of the system used here is that the force is a dipole interaction rather than an isotropic force such as the Van der Waals force. Not only is the magnetic force anisotropic, particles situated next to one another (in the same horizontal plane) will actually repel one another. If it is assumed that the pile is packed in a cubic state, all particles on the surface of the pile will have a neighbour on the same plane up-slope, but not necessarily a corresponding neighbour down-slope. This results in a net force F_{cub} attempting to push the particle further down the slope, lowering the angle of repose. If the packing was perfectly hexagonal close packed, the net horizontal force on a particle at the surface would be zero. In practice, the packing is random, and the net horizontal force on particles at the surface somewhere between zero and F_{cub}.

Only the maximum inter-particle force F_{max}, obtained when the particles are touching and aligned with the field is given here. It can be demonstrated (Israelachvili, 1992) that (at least for separations large compared to the dimensions of the dipole) that the interaction energy for particles aligned in the direction of the field is twice

Figure 2.9: Magnetic "sand castle"

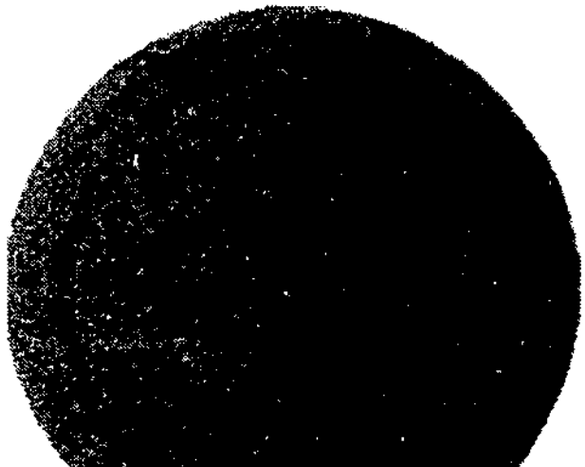

Figure 2.10: Picture in the "sand"

that of two dipole aligned parallel to each other at the same separation. When the line joining the centres of our particles is aligned with the field our dipoles attract, and repel when the line joining the centres of the particles is perpendicular to the field lines. The average force felt by the particles will overall be attractive, but less than F_{max}. Hence, the ratio of inter-particle force to particle weight is over estimated.

Like the magnetic force, the liquid bridge force is also anisotropic. The liquid bridge force is always attractive, and acts along a line joining the centres of two particles. This results in a net horizontal force towards the slope, rather than away from the slope as in the magnetic case. One would therefore expect that the angle

of repose for wet powders would increase more rapidly as a function of the ratio of inter-particle force to particle weight than in the magnetic case, and so perhaps better reflect the theory of Albert *et al* (Albert et al., 1997).

It is difficult to quantitatively compare our data to those experiments done using liquid bridges to supply the inter-particle force as there is at this stage no robust manner in which to calculate the inter-particle force due to liquid bridges without resorting to fitted parameters. The work of Hornbaker *et al* (Hornbaker et al., 1997) plots static angle of repose obtained by the draining-crater method(Brown and Richards, 1970) versus the average liquid layer thickness. The angle of repose rises approximately linearly with increasing liquid layer thickness. Albert *et. al.* (Albert et al., 1997) demonstrate that for slightly rough particles, the liquid bridge force $F_{liq} \approx V^{\frac{1}{3}}$, where V is the volume of the liquid bridge. Hence, the liquid bridge inter-particle force is proportional to the thickness of the liquid layer. Qualitatively, this gives the same behaviour seen using magnetic forces, that angle of repose increases linearly with increasing inter-particle force.

Basic stability criteria (Albert et al., 1997) would predict an angle of repose at zero field of approximately 23^o. Our angle of repose is significantly higher ($\approx 31^0$). The difference can possibly be attributed to the narrow box used for the experiments. It has been shown that wall effects can add several degrees to the angle of repose (Dury et al., 1998). Repeating our experiments at zero field with boxes of width 6 mm and 8 mm gave angles of repose of 30^0 and 28^0 respectively. Zero field experiments were performed on iron spheres that had not previously been magnetised to ascertain whether residual magnetisation was the cause. No effect due to residual magnetisation was found.

The dynamic angle of repose at zero field (47^o) is considerably higher than the static angle of repose at zero field (31^o for the 800μm particles). The motion of the drum carries the particles up the wall, leading to a higher angle of repose. As for the static case, the dynamic angle of repose rises linearly with increasing inter-particle force, though more slowly than predicted by theory (Albert et al., 1997) due to the inertia of the particles.

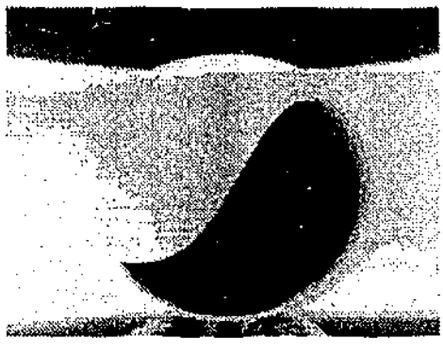

Figure 2.11: Typical Ying-Yang shaped interface for a powder in a rotating drum at high rotational velocities.

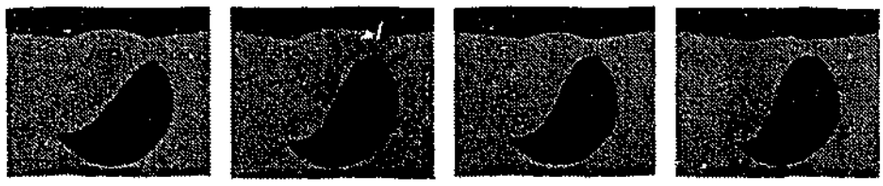

Figure 2.12: Dynamical angle of repose at high rotational velocities. From left to right the figures represent coil voltages of 0V, 2 V, 4V and 6V

Figure 2.13: Angle of repose for iron shot at intermediate rotational velocities for increasing values of coil voltage and hence field strength. From left to right the figures represent coil voltages of 0V, 2 V, 4V and 6V

2.3.1 Sand Castles

A simple experiment carried out with this system illustrates the difference between the liquid bridging and magnetic forces. A small "sandcastle" was built from iron shot in the magnetic field. Because the iron spheres were quite heavy, when compared to sand of a similar particle size, this required that the applied field be high. Unlike a regular sandcastle, the anisotropic nature of the applied magnetic force meant that to be stable the sandcastle had to have rather thin walls. When the walls were thickened, the structure became unstable. Repulsive due to the grains being aligned with the field tended to weaken the structure. At lower fields, this was less of a problem. However, the sandcastles at low field were very small. When the field was turned off completely the castle crumbled and disappeared.

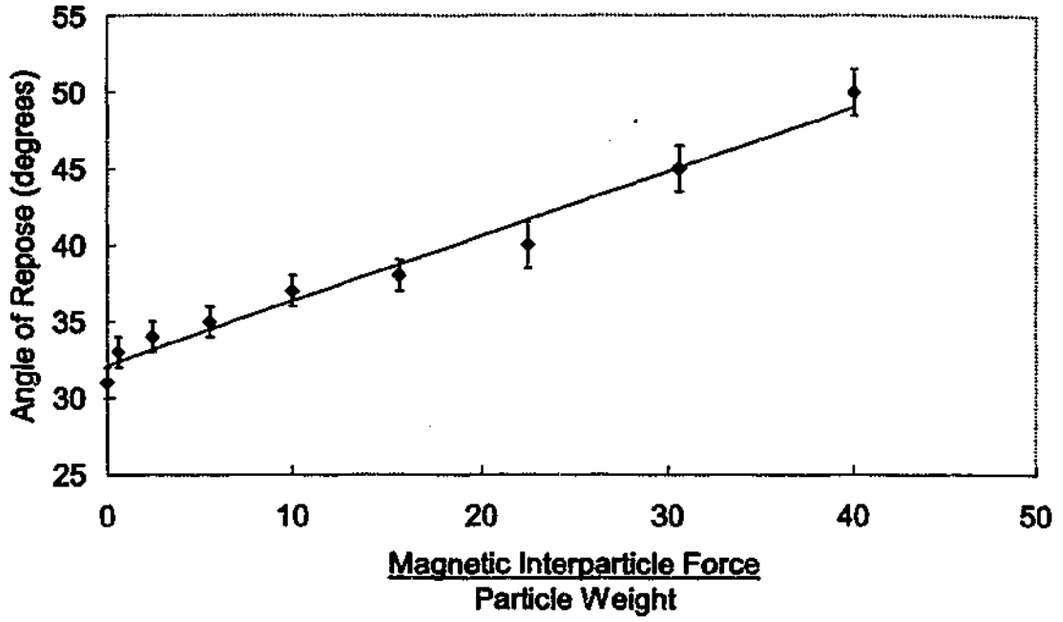

Figure 2.14: Graph of static angle of repose vs the ratio of inter-particle force to weight.

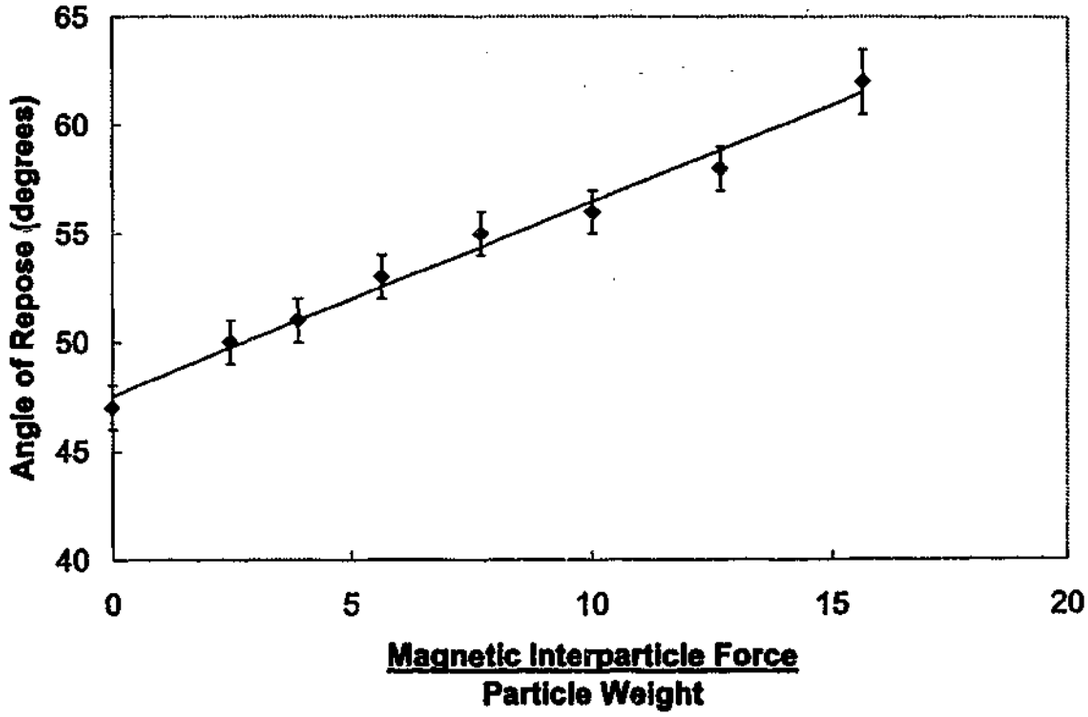

Figure 2.15: Graph of dynamic angle of repose vs the ratio of inter-particle force to weight squared.

It was found that it was easy to write messages in the material, even at low field. Again, when the field was turned off the messages almost completely disappeared.

2.4 Effect of Inter-particle Force on Granular Profile

At low field, the grain profile of the poured iron shot was a relatively smooth slope. As the field was increased however, the profile became increasingly irregular, taking on an increasingly bumpy or "fractal" appearance. This made the angle of repose more difficult to define for high inter-particle force[11]. Similar irregularities in granular profiles can be seen in powders such as flour and icing sugar where Van der Waals forces are presumably responsible. This irregularity in grain profile has some interesting implications for self-organised criticality. Self-organised criticality was originally proposed as an explanation for 1/f noise and as a mechanism for the formation of fractals in nature. Commenting on the rice experiments of Frette *et. al.* (Frette et al., 1996), Bak explains[12]

> "In the stationary state, the rice grains get stuck in intricate arrangements where they lock into each other, allowing for steep slopes, even with overhangs. An analysis of the surface profile shows it is a fractal structure just like the coast of Norway, with bumps and other features of all sizes[13]"

In order to investigate the variation of the profile with inter-particle force, the following experiments were performed. The narrow perspex box used to measure the poured angle of repose was used. The iron shot was poured into the box by means of a stopcock. The flow rate was such that only one or two grains were allowed to fall into the box at a time. A granular profile was thus obtained for small, medium and large sized particles for various different values of the field.

Using a CCD camera images and strong back lighting of the pile profiles were obtained. The images were processed to remove noise and converted to black on white profiles using a threshold function and an edge detect algorithm. The fractal

[11] This was not really a significant problem for the previous experiments.
[12] see (Bak, 1997) page 71
[13] see figure 1.3 and 2.16

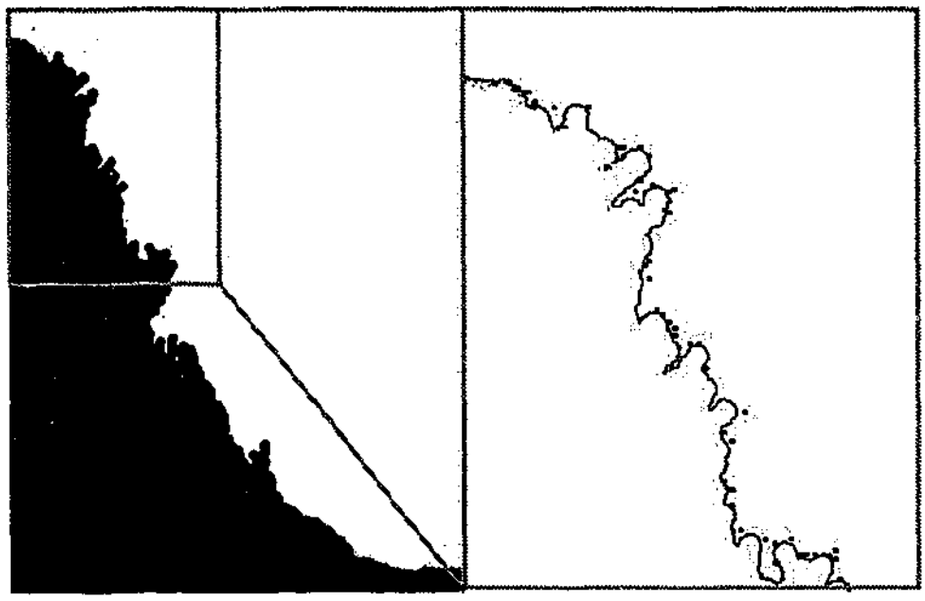

Figure 2.16: Fractal granular profile.

dimension was calculated using a box-counting algorithm and the Hausdorff dimension found (Schroeder, 1990). This was plotted against the applied field. The results are shown in Figure 2.17.

One interesting feature to note is the fact that the smaller particles take higher applied field values to show irregularities. This is due to size. More small particles are needed to bind together to produce a noticeable change in the granular profile. Another feature is the falling-off of the fractal dimension with increasing particle size. This may be due to a change in the flow characteristics of the material. As the inter-particle force increases, particles tend to cluster together. Large clumps tend to break off and slide together. This leads to a smooth flow down the slope. Smaller avalanches become less likely and the fractal dimension of the profile stops increasing. The transition to this new flow regime appears to depend upon the mass of the particles. This new flow regime is similar to the correlated regime found by Tegzes *et. al.* (Tegzes et al., 1999).

These observations suggest that inter-particle force will have a significant effect on avalanche size distributions. This could explain why critical dynamics have only been observed in rare circumstances in experiments on granular matter. Rather than being a robust state, the self-organised critical state should only occur for

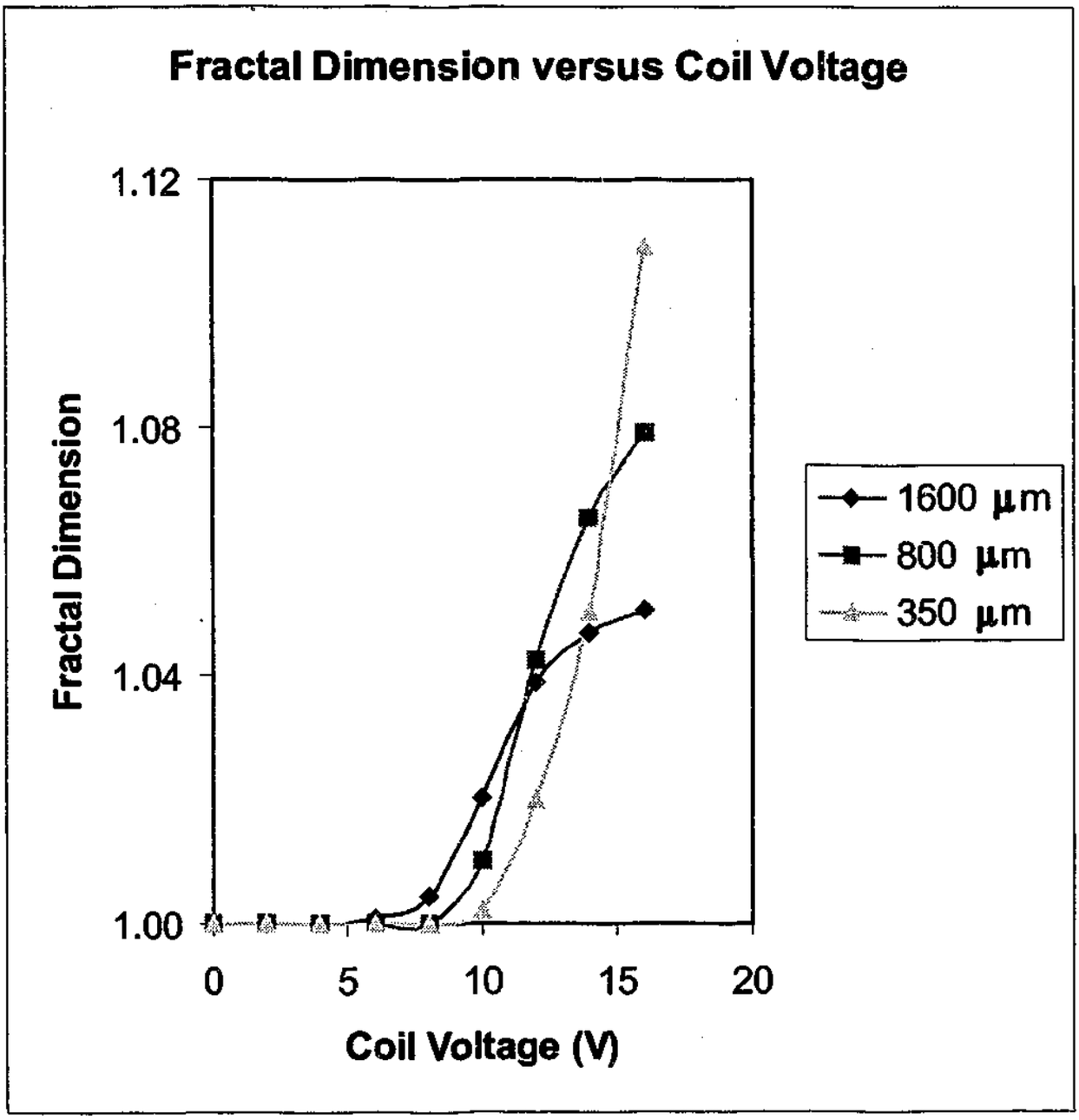

Figure 2.17: Graph of fractal dimension vs coil voltage.

systems where inter-particle force falls within a narrow range of values. The inter-particle force must be strong enough for the granular profile to undergo intermittent flow and weak enough so that large avalanches don't dominate the dynamics.

Experiments on real world sand-piles have shown that the issue of the existence of self-organised criticality in real sand piles is far from simple. First, the method by which avalanches are measured can influence the distribution of avalanches. Experiments in rotating drums (Jaeger and Nagel, 199?) have found that the number of small and large avalanches follows a characteristic pattern of behaviour. Initially there are many small and intermediate avalanches. However, during a large avalanche, once grains have begun moving they would gain momentum until the angle of repose was a few degrees below the critical angle. The surface would then build up, before undergoing collapse again. This leads to oscillatory behaviour that is quite unlike the self-organised critical behaviour. Similar results have been found for experiments by Held *et. al.* (Held et al., 1990) in which grains were piled on a plate and weighed to measure the amount of material spilling off the plate. These experiments also suffered from another shortcoming in that they did not measure the more frequent internal avalanches on the surface of the pile. Experiments on rice piles carried out by Frette *et. al.* (Frette et al., 1996), however, have shown self-organised critical behaviour for large grained rice. The larger surface of the grains, it is thought, suppressed inertial effects by increasing friction.

2.5 Conclusions

A novel system for examining the effects of inter-particle force on the behaviour of powders has been presented. This system offers a way of studying the effects of inter-particle forces in isolation from other factors. Examination of these effects on both the static and dynamic angles of repose has shown a linear increase with inter-particle force. In experiments on the static angle of repose, it was found that the increase with inter-particle force was accompanied by an alteration of the profile geometry. The fractal dimension of the profile was found to increase with the applied field. This leads to questions about how robust the self-organised critical state is in poured granular piles.

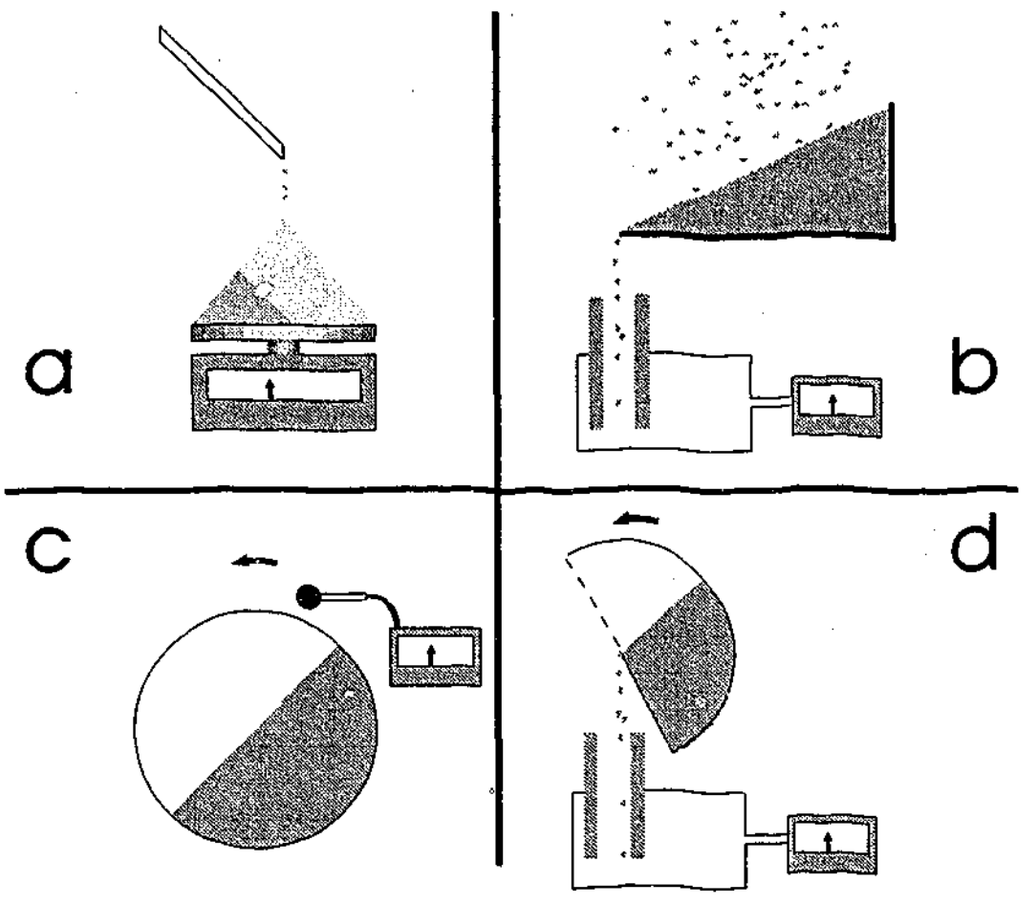

Figure 2.18: Several methods used to study avalanching in granular matter. (a)The variation in mass of the pile undergoing avalanches was measured. (b) The number of particles falling off the pile was measured using capacitance as particles were added from above. (c) Avalanches were detected via the noise they made using a microphone. (d) The number of particles falling off the pile were measured using capacitance as the surface was inclined.

In the following chapters, this method will be used to investigate the role of inter-particle forces in the behaviour and dynamics of granular materials. In the next chapter the bulk properties of static granular materials is investigated.

CHAPTER 3

Packing and Voids

The study of granular packing has a long history dating back to Kepler (Kepler, 1976). In addition to its theoretical interest, understanding how particle properties affect packing arrangements in powders is of great practical importance. Examples range from the formation of tablets from complex particulate mixtures in the pharmaceutical industry, through to the manufacture of sintered metal products from metal powders and to the apparently simple task of ensuring that a certain amount of a powder product will fit into the appropriately sized bag for distribution and sale. In this chapter, the effect of altering inter-particle force on packing fraction is examined.

3.1 Static Behaviour in Granular Materials

The properties of static or near static granular materials are more complex than would be guessed at from a study of the properties of the individual grains. One of the more significant features of granular assemblies is the formation of arches and voids throughout the material. For centuries, builders have constructed bridges, vaults, doorways and windows by placing one stone on top of another to form an arch. A carefully placed keystone at the top of the arch gives the structure stability by distributing the weight above it horizontally (see Figure 3.1).

The densest possible packing of identical spheres is an orderly close packed hexagonal array in which only 26 percent of the structure is empty space. 74 percent of this structure is taken (Jaeger and Nagel, 1992) up by the spheres. A random packing of spheres would be far less efficient in filling space. A close examination of random assemblies of sand grains, for example, would show numerous arches, vaults

and voids. If this assembly of sand grains were subject to vibrations designed to dislodge keystones and remove some of the arches and voids it would undergo a relaxation toward the "random close packed limit". Most granular materials tend toward this limit in which only 64 percent of the available space is taken up by solid matter (Finney, 1970). Once a granular material is well packed, it becomes impossible for the material to move without expanding. This property of granular matter is called *dilatancy* and was first noted by the physicist/engineer Osborne Reynolds in 1885 (Reynolds, 1885).

Friction plays an important role in the formation of vaults and arches in most granular matter. One might think, at first, that purely frictionless beads would not pile but the issue is not that simple. Consider a pile of frictionless beads placed on a rough surface. If the grains are stacked in orderly close packed layers much like oranges are often displayed in a grocery store then the pile cannot move without expanding. Any expansion will however be opposed by gravity. Therefore, the pile must be stable after all. The issue of whether a frictionless pile can support itself is still not completely resolved. It has however been shown that if a bead pack is piled up one bead at a time it can not hold itself up without rearrangement of the beads.

3.1.1 Relaxation

Vibration can reduce the free surface angle of a pile of granular material (Kadanoff, 1999). It is found that when a pile of granular material is vibrated the free surface angle falls logarithmically with time. Logarithmic relaxation with time has been observed in a variety of systems including amorphous ferro-magnets, high temperature super-conductors and the magnetisation of spin glass (Jaeger and Nagel, 1992).

Besides surface relaxation effects, there are also relaxation effects which operate throughout the bulk of granular materials. For example, vibrating or tapping on the sides of cereal packet will cause the contents to settle and the volume to decrease significantly. This internal settling is due to small internal avalanches that

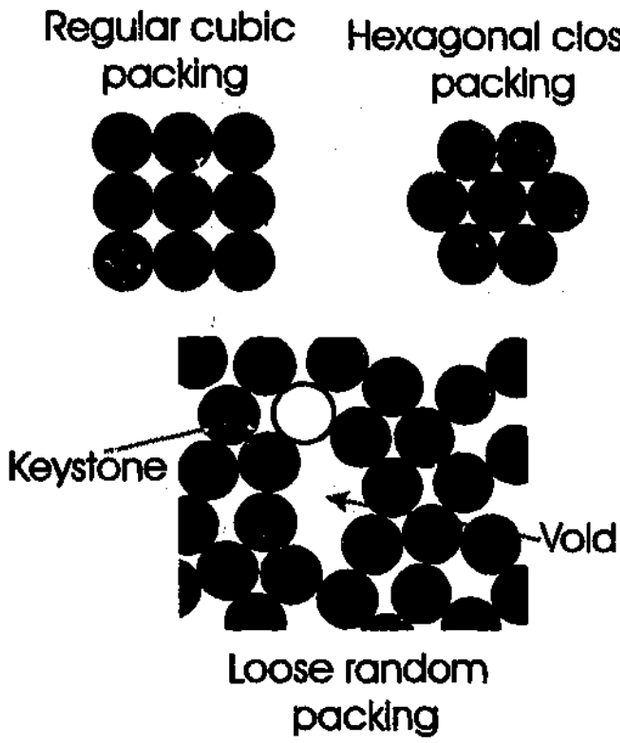

Figure 3.1: The void fraction for dry powders increases with decreasing particle size

occur in the bulk of the material. Computer models of this process have been proposed which are based on the computer game Tetris[1]. Packing fraction (ρ the ratio of space filled by particles to empty space) in particulate materials is affected by particle size distribution, particle shape and inter-particle forces. In general, for random packing arrangements, packing fraction increases with increasing size distribution, increased particle sphericity and decreasing inter-particle cohesive forces. The increase in packing fraction with increasing size distribution is due to smaller grains being able to fit into interstices between the larger grains[2].

In the absence of inter-particle forces a powder will attain a packing fraction somewhere between the loose random packing limit (≈ 0.58) and the dense random packing limit (≈ 0.63) (Cumberland and Crawford, 1987). These values correspond to void fractions ($\varepsilon = 1 - \rho$) of 0.42 and 0.37 respectively. Inter-particle forces allow "vaulting" to occur, leading to large (on the scale of the particles) voids within the

[1] In this game odd shaped blocks fall from the top of the screen. The object of the game is to pack the blocks so as to leave no spaces. If there are no spaces in the row of blocks, the row disappears, otherwise the pile of blocks grows.

[2] It is possible to have a fractal packing in which the interstices between large grains are filled with smaller grains and the interstices between these smaller grains are filled with still smaller grains and so on. See (Schroeder, 1990).

powder, and hence a greater void fraction. It is well known that for dry powders the range of possible packing densities under normal gravity increases with decreasing particle size (Geldart and Wong, 1984), (Geldart and Wong, 1985), (Feng and Yu, 1998). For dry powders the dominant inter-particle force is Van der Waals, which increases linearly with particle diameter (Israelachvili, 1992), while inertial forces increase with the cube of the particle diameter. Consequently, with dry powders the inter-particle cohesive forces become more dominant with decreasing particle size. Hence, the void fraction for dry powders increases with decreasing particle size as was discussed in the previous chapter. This effect is demonstrated in Figure 3.6 with data taken from Feng and Yu (Feng and Yu, 1998). Several groups (Albert et al., 1997), (McLaughlin and Rhodes, 2001), (Hornbaker et al., 1997) have added liquids of varying surface tensions and viscosities to dry powders to observe the effect of the resulting increase in inter-particle force. Work has also been done on examining the effect of liquid on packing of mono-sized coarse spheres (Feng and Yu, 1998). As discussed in the previous chapter this method suffers from several limitations[3].

3.2 Experimental

Using the methods outlined in the previous chapter the variation of the voidage fraction with inter-particle force was measured[4]. As the walls of the vessel used were perspex, the particle-wall interaction was unchanged. The standard method for the measurement of the poured packing fraction of dry particles (Svarovsky, 1987) was used, with slight modifications described below. With B set at a particular level, iron shot was poured into a standard container, approximately 4 cm in diameter and 10 cm in high (volume 128 cm^3), through a funnel with a stopcock attached to regulate flow. The height of the stopcock was kept constant at a level of 5 cm above the top of the container. Once the container was full, excess particles were levelled off and the sample weighed. This was repeated for a number of particle sizes and field strengths. Using Figure 3.4 as a calibration curve, the void fraction is plotted

[3] see section 2.1.4

[4] The results of the authors experiments, as outlined here, have been published (Forsyth et al., 2001b), (Forsyth et al., 2000) and (Rhodes et al., 2002)

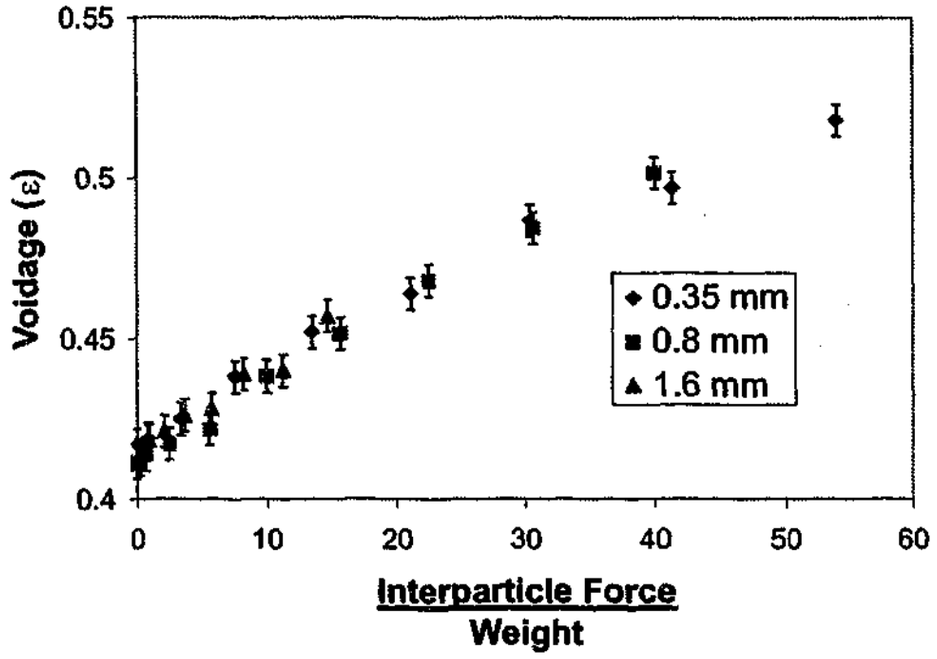

Figure 3.2: Void fraction versus the ratio of inter-particle force to weight for 0.35 mm, 0.8mm and 1.6 mm iron spheres in a magnetic field.

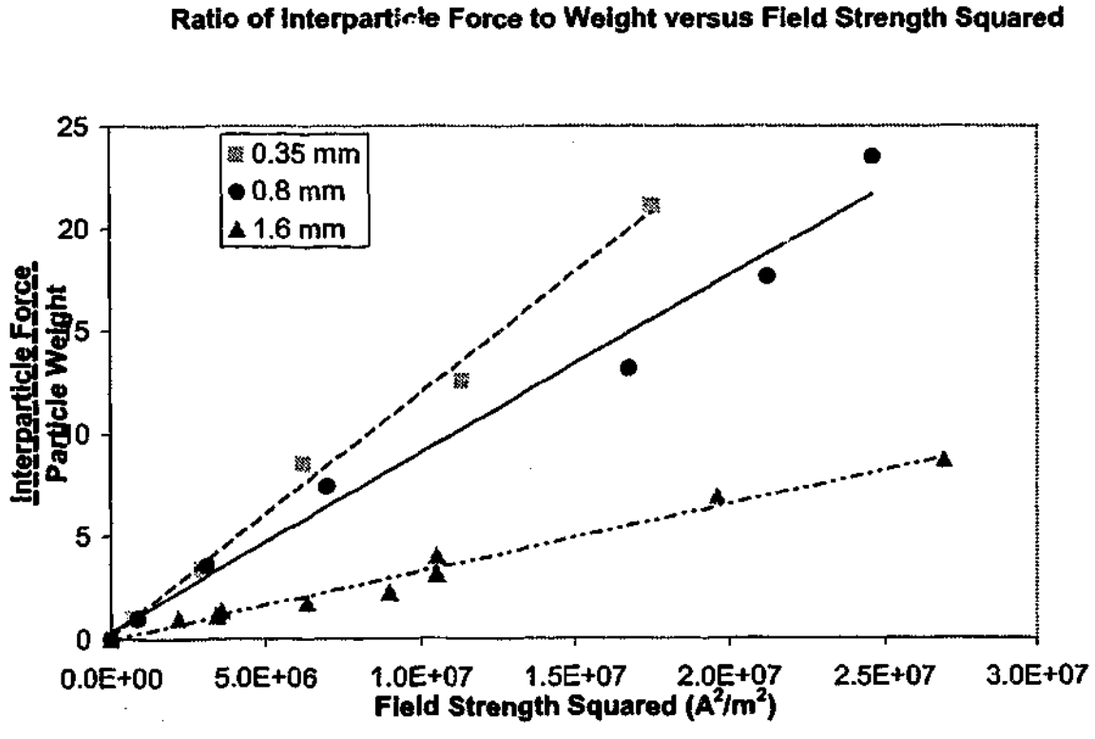

Figure 3.3: Ratio of inter-particle force to weight versus field strength squared

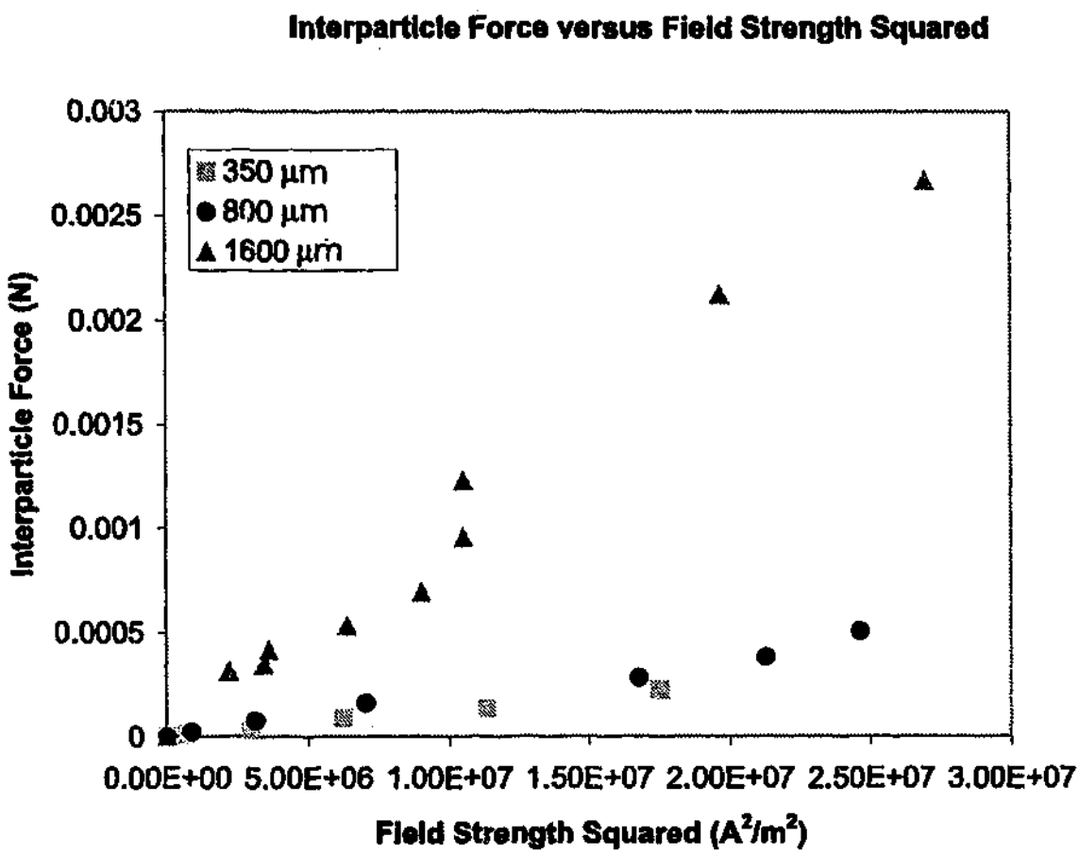

Figure 3.4: Inter-particle force verses field strength squared

against the ratio of inter-particle force, F_{ip}, to particle weight, mg, for each of the particles.

3.3 Results and Discussion

The results of these experiments are shown in Figure 3.5. The void fraction was now plotted against the ratio of inter-particle force, to particle weight, F_{ip}/mg, it was found that the data for the three different particle sizes fell on the same curve, as shown in Figure 3.2. This demonstrates that the poured packing fraction, under normal gravity, is a function only of F_{ip}/mg .

One might argue that perhaps this only holds for our magnetic system, so let us now consider dry, non-magnetic, powders. We shall assume that void fraction is only dependent on F_{ip}/mg. We shall also assume that the relationship is universal - that is that the void fraction for dry powders varies in the same manner with F_{ip}/mg demonstrated for the magnetic system. From Figure 5, it is apparent that the void

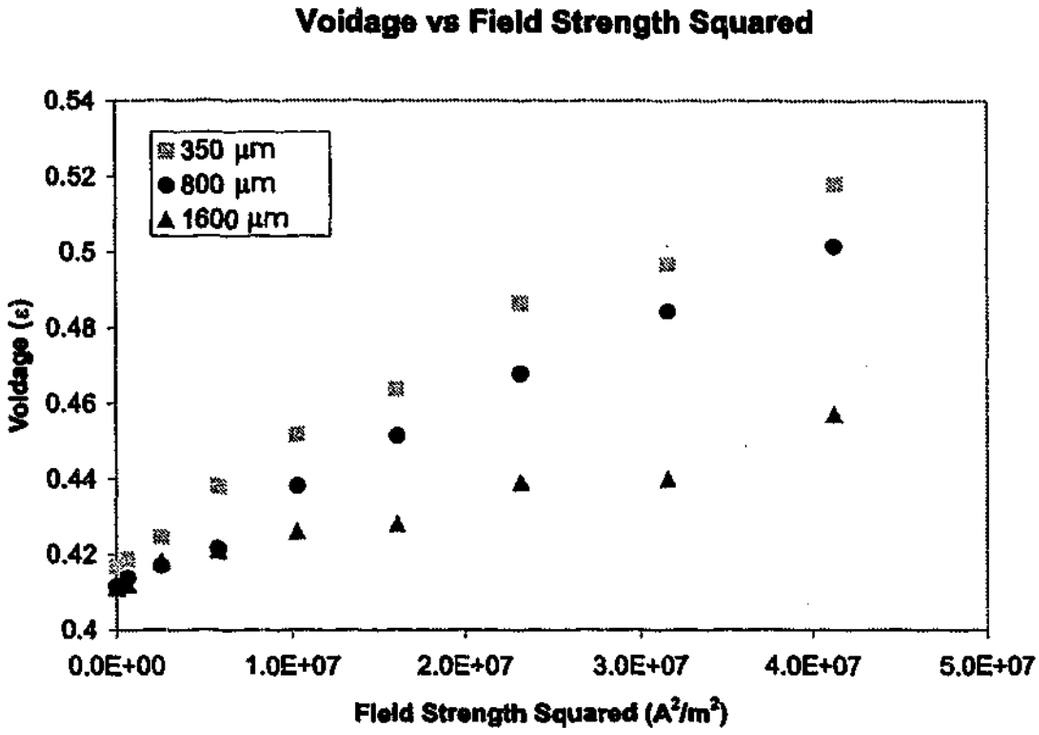

Figure 3.5: Field strength squared verses the ratio of inter-particle force to particle weight

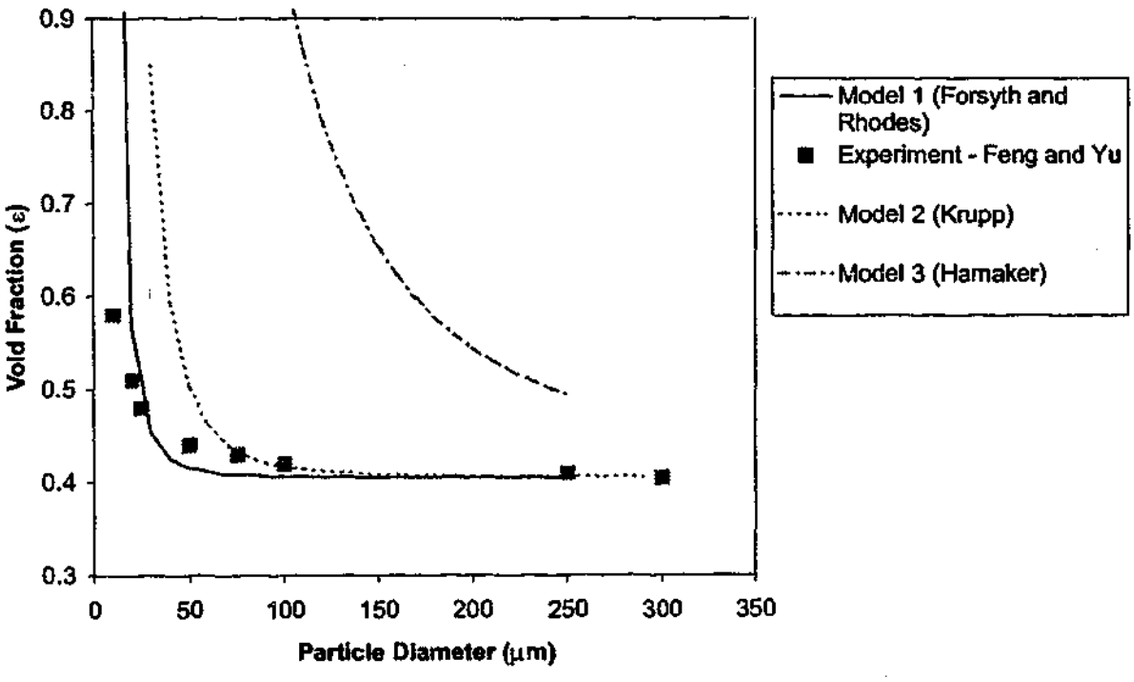

Figure 3.6: Variation of void fraction for dry powders with particle. with data from (Feng and Yu, 1998), (Forsyth and Rhodes, 2000), (Krupp, 1967) and (Hamaker, 1937).

fraction rises approximately linearly with increasing F_{ip}/mg. We shall assume that the void fraction increases according to

$$\varepsilon = \varepsilon_0 + k\left(\frac{F_{ip}}{mg}\right) \tag{3.1}$$

where ε is the void fraction, ε_0 is the void fraction at zero field, k is the rate at which void fraction increases with increasing F_{ip}/mg. For dry, non-magnetic, powders the dominant inter-particle force is the Van der Waals force. Asperities, or protrusions from the particle surface, play an important role in determining the Van der Waals force, so we shall use an expression for the force between 2 particles (eg. glass spheres) developed previously by Forsyth et. al. (Forsyth and Rhodes, 2000).

$$F_{ip}(d) = -\frac{2Ar^3}{3d^2(d+2r)^2} - \frac{2AR^3}{3(d+r)^2(d+r+2R)^2} \tag{3.2}$$

where d is the particle separation, A is the Hamaker constant (Hamaker, 1937), r is the asperity radius (assumed to have a spherical profile) and R is the particle radius. We take our asperity and separation data from Molerus (Molerus, 1982), with $d = 0.4$ nm and $r = 0.1$ μm. The Hamaker constant for glass is approximately 1.6×10^{-19} J (Israelachvili, 1992), and we take the density of glass to be 2950 kg m^{-3}. The values of k and ε_0 were calculated from Figure 3.2, giving approximately 2×10^{-3} and 0.41 respectively. Using this data, we can now estimate how the void fraction for dry powders should vary with particle diameter. The prediction is shown in Figure 3.6, with the experimental data of Feng and Yu (Feng and Yu, 1998). Predicted curves using the models of Hamaker and Krupp to model the inter-particle Van der Waals force are also shown. Krupp's model considers only that asperities contribute to the inter-particle force and hence underestimates the force (Forsyth and Rhodes, 2000). All parameters in Krupp's model were taken from Molerus (Molerus, 1982). The predictions of Forsyth and Rhodes (Forsyth and Rhodes, 2000) provides good agreement with experiment for particle diameters larger than about 25 μm. For particles smaller than 25 μm the void fraction is overestimated. This is due to a linear dependence between void fraction and F_{ip}/mg being assumed. Obviously this approximation must break down at high values of F_{ip}/mg. By definition, the void

fraction can never exceed unity, and in practice, void fractions never even approach this value. For a 20 μm particle, F_{ip}/mg is approximately 137, which is far beyond the maximum ratio examined by our magnetic system (approximately 54). Hence, it is not surprising that the model breaks down for very small particles. At 25 μm, the ratio of inter-particle force to weight is down to 70. In fact, one can see the data in Figure 3.2 rises more and more slowly as the inter-particle force increases. By choosing a relationship between voidage, ε, and F_{ip}/mg that does not rise linearly, the experimental data could be modelled more closely. Until a better theoretical understanding of the effect of inter-particle force on void fraction is obtained, the form of the curve will be completely arbitrary, and will require the introduction of extra parameters. For instance using a curve of the form

$$\varepsilon = \varepsilon_0 + (\varepsilon_{max} - \varepsilon_0)\,\mathrm{Exp}\left[-k\left(\frac{F_{ip}}{mg}\right)\right] \tag{3.3}$$

where ε_{max} is the maximum attainable voidage can be made to fit the experimental data more closely than the linear model in equation (3.1).

3.4 Conclusions

The results of our experiments are consistent with the idea that the void fraction depends only on the ratio of inter-particle force to particle weight. It was demonstrated that the poured packing of dry powders also depends only on the ratio of inter-particle force to particle weight. This result is surprising since factors that are often thought of as important in granular packing, such as packing geometry, play no role in these results .

In the next chapter, the effect of inter-particle force on bubbling in fluidised granular matter will be examined.

CHAPTER 4

Bubbles

Injecting fine jets of air though beds of granular material causes the material to fluidise. These fluidised beds are routinely used in the petro-chemical, pharmaceutical and energy production industries as well as in the re-processing of nuclear fuels (Gupta and Sathiyamoorthy, 1999). In this chapter, experiments investigating the transition between bubbling behaviour and non-bubbling behaviour in fluidised beds, are discussed. A novel experimental fluidised bed is used to examine the behaviour of fluidised iron shot as the ratio of inter-particle force to buoyant weight is varied. A transition to non-bubbling behaviour from bubbling behaviour is observed using high-speed video analysis and measurements of the pressure drop as the inter-particle force is varied.

4.1 Overview: Fluidised Granular Matter

Fluidised granular matter differs from non-fluidised granular matter in several ways (Geldart and Wong, 1984). For example:

- Objects that are denser than the fluidised material will sink while objects that are of lower density than the fluidised material will float on the surface of the bed.
- A bed that initially has an uneven surface in the un-fluidised state will have a flat or horizontal surface when fluidised.
- The surface level of two connected regions of the bed will equalise when the bed is fluidised.
- When fluidised, granular matter will flow like a liquid through an outlet.

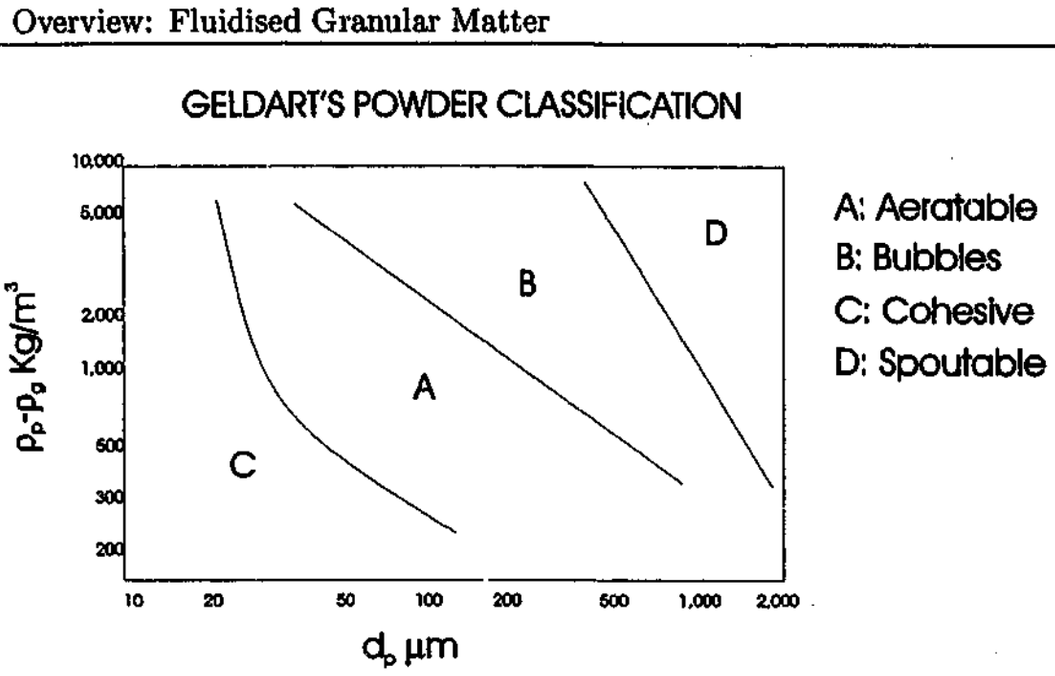

Figure 4.1: Phase diagram for fluidised powders. From (Geldart, 1973).

In some fluidised materials, an increase in the fluidisation velocity results in bubbles forming. These bubbles have some similarities with bubbles in liquids.

Fluidised granular media can be classified into several different phases that depend upon their properties and ability to bubble[1]. A classification scheme was introduced by Geldart (Geldart, 1973) for the fluidisation of dry powders, fluidised by air under ambient conditions (see Figure 4.1). This scheme divides powders into groups (A,B,C and D). The properties of these groups are as follows:

- Group A powders exhibit a non-bubbling fluidisation regime (Figure 4.2a), but will undergo bubbling.
- Group B powders by contrast bubble immediately upon fluidisation (Figures 4.2c and 4.2d).
- Group C powders are cohesive and do not, in the strict sense, fluidise.
- Group D powders can produce deep spouted beds (Figure 4.2e).

Despite a great deal of research into the nature of fluid beds, a unifying theory of bed behaviour does not yet exist (Kunii and Levenspeil, 1991).

Such a theory would be of great practical importance to industry and so much effort has been made towards this goal (Clift, 1993). Attempts to model fluidised beds using molecular dynamics models (Hoomans et al., 1996) are limited by their

[1] As was mentioned in chapter one.

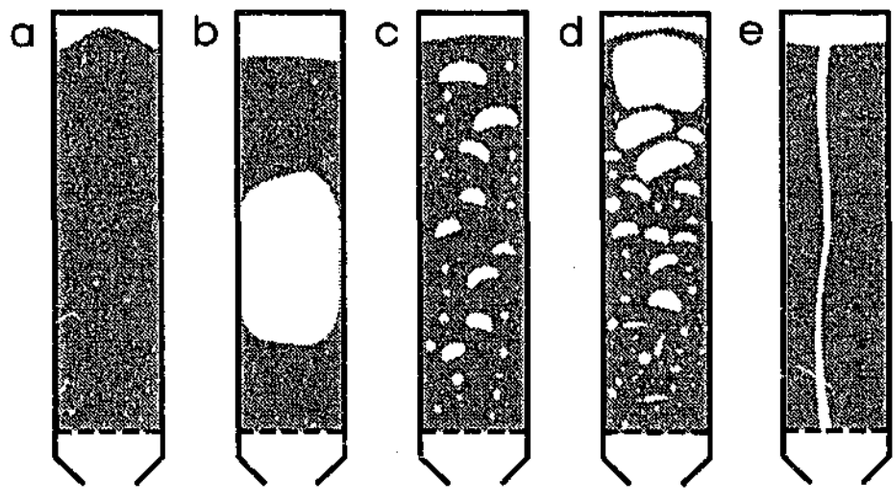

Figure 4.2: Bubbling in fluidised beds *from left to right* (a) stable bed expansion, (b) slugging, (c) bubbling (d) chaotic or turbulent bubbling and (e) channelling.

high computational cost. While computer-processing speeds continue to increase direct Molecular Dynamics (MD) simulations of industrial scale fluidised beds appear likely to remain impractical for some time to come. In order to circumvent the limitations due to computational speed restrictions, cellular automata have also been used to model fluidised beds (van Wachem et al., 1997). This, far less computationally expensive, method has its own limitations. For example, bubbles in lattice gas cellular automata are introduced in an artificial way and the models do not allow large velocity gradients. Other approaches also exist (Ding and Gidaspow, 1990) (Seibert and Burns, 1996), but all these approaches have limitations[2].

4.1.1 Bubbles

If the flow rate of gas through a fluid bed is low then the air will permeate through the interstices between the particles. If the flow rate is large enough to obtain a frictional pressure drop that is greater than the weight of the bed, then the bed will lift. The flow rate at which this occurs is known as the incipient fluidisation rate U_{mf}. The value of U_{mf} for a particular fluid bed will depend upon a wide range of factors.

The typical shape of a bubble in a fluidised bed is roughly spherical with a small wake of particles causing the base to be flattened. The boundary between the interior and exterior of the bubble is generally well defined. The amount of material

[2]see (Clift, 1993) for overview of the strengths and limitations of the various approaches

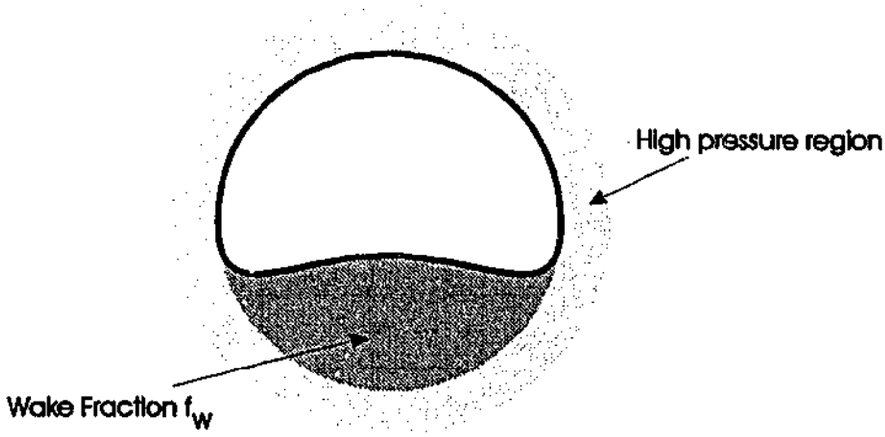

Figure 4.3: Structure of a bubble

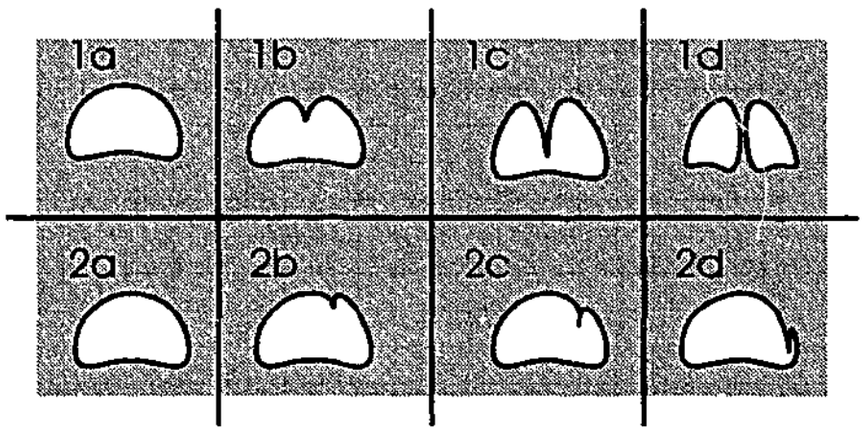

Figure 4.4: (1) How bubbles split. (2) "Knives" of material appear and are transported around the sides of the bubble.

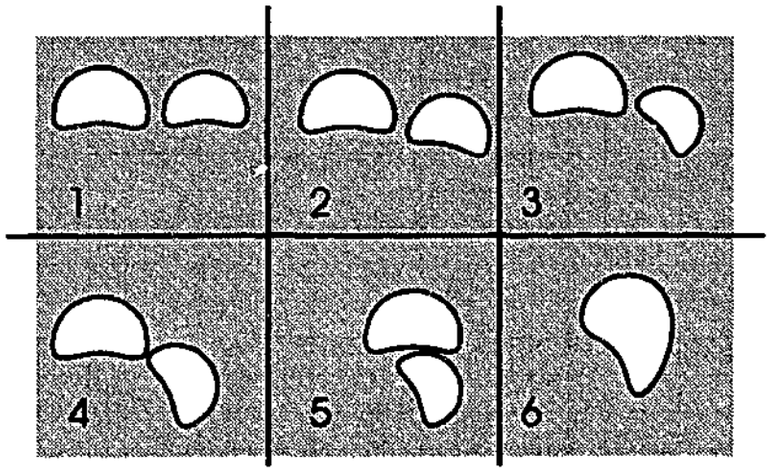

Figure 4.5: How bubbles merge

in the indented base is known as the "wake fraction", f_w, and is generally observed to vary slightly over time as the bubble rises through the bed. Upon reaching the surface of the fluid bed, bubbles do not burst like bubbles in liquids. Instead, the bubbles simply collapse as material from the roof of the bubble falls into the cavity below.

Bubbles are observed to sometimes split in two. It is quite common for downward pointing tips, known as knives, to form in the top of the bubbles (see Figure 4.4.2). These tips commonly travel around the surface the bubble and end up dissolving in the wake. Sometimes however the knives grow so rapidly that they cause the bubble to split in two (see Figure 4.4.1).

On other occasions, two or more bubbles can coalesce. This typically happens in the following manner. If two bubbles are rising side by side, the slower moving bubble will get caught in the wake of the faster moving bubble and dragged underneath where it is absorbed (See Figure 4.5).

Bubbles are observed to undergo significant distortion if bought close together or in close proximity to boundaries or other objects. Shape will also depend significantly on the material being fluidised. Each material will in general have a characteristic bubble shape and different wake fractions so that the shape of bubbles can vary from thin crescents to almost completely spherical bubbles.

4.2 Experimental

4.2.1 Powder Groups and Inter-particle forces

The differing behaviour of the powder groups has been explained as being due to differences in the ratio of inter particle force to buoyant weight. Applying a magnetic field to a fluidised bed of magnetisable particles has long been known to suppress or delay bubbling in the bed (Clift, 1993). The effect has been observed in admixtures of magnetisable and non-magnetisable particles and in gas-liquid-solid beds (Wu et al., 1997). The effect is observed regardless of the field orientation.

By applying a magnetic field to fluidised iron shot, a range of fluidisation behaviours can be induced. In these experiments, two fluidised beds were constructed. The

first, a three dimensional fluid bed (shown in Figure 4.6) consisted of a 140 mm transparent Perspex tube (of wall thickness 5 mm) with a flange attached. The tube was attached to a Perspex windbox using nylon bolts. A distributor was placed between the windbox and the nylon tube. The 8 mm thick distributor was constructed of sintered bronze. To prevent air from escaping from the sides of the bed, the edges of the distributor were coated in PVC glue and the tube and windbox sealed with 140 mm diameter "O" ring seals. The nylon bolts were held apart by spacers that were the same thickness as the distributor (approximately 8 mm). This allowed tight seals between the tube, the windbox and the distributor, but prevented the bolts from being over-tightened. Over-tightening of the bolts could have led to unacceptable stresses occurring in the bed wall, potentially leading to crack formation in the walls.

The three dimensional bed had a shortcoming in that it was difficult to visually observe the onset of bubbling during fluidisation. In order to overcome this problem, a novel fluidised bed was constructed. An annular shaped fluidised bed was constructed as shown in Figure 4.7. This new design allowed the space between the Helmholtz coils to be utilised effectively. The bed was essentially identical to the three-dimensional bed except that there was a 100mm diameter transparent Perspex tube placed in centre. This internal tube was sealed at the bottom and bolted by nylon bolts to the sintered bronze distributor.

The distributor in the annular bed was sealed by PVC glue and the edge and centre. The distributor was also sealed both at the edge and centre by "O" rings. Again, care was taken to ensure the internal regions of the fluid bed were free of PVC glue. The novel design gives what is essentially a two dimensional bed with periodic boundary conditions and allows the bubbles to be examined more closely and the onset of bubbling to be observed. The fluidised material was backlit by placing a light in the centre of the bed. The bed itself was placed between Helmholtz coils[3]. Iron shot was fluidised and its behaviour analysed as the ratio of inter-particle force to buoyant weight was varied, using high-speed video analysis. A rotometer was used to measure the airflow rate. The rotometer allowed for a maximum accuracy

[3]see chapter 2

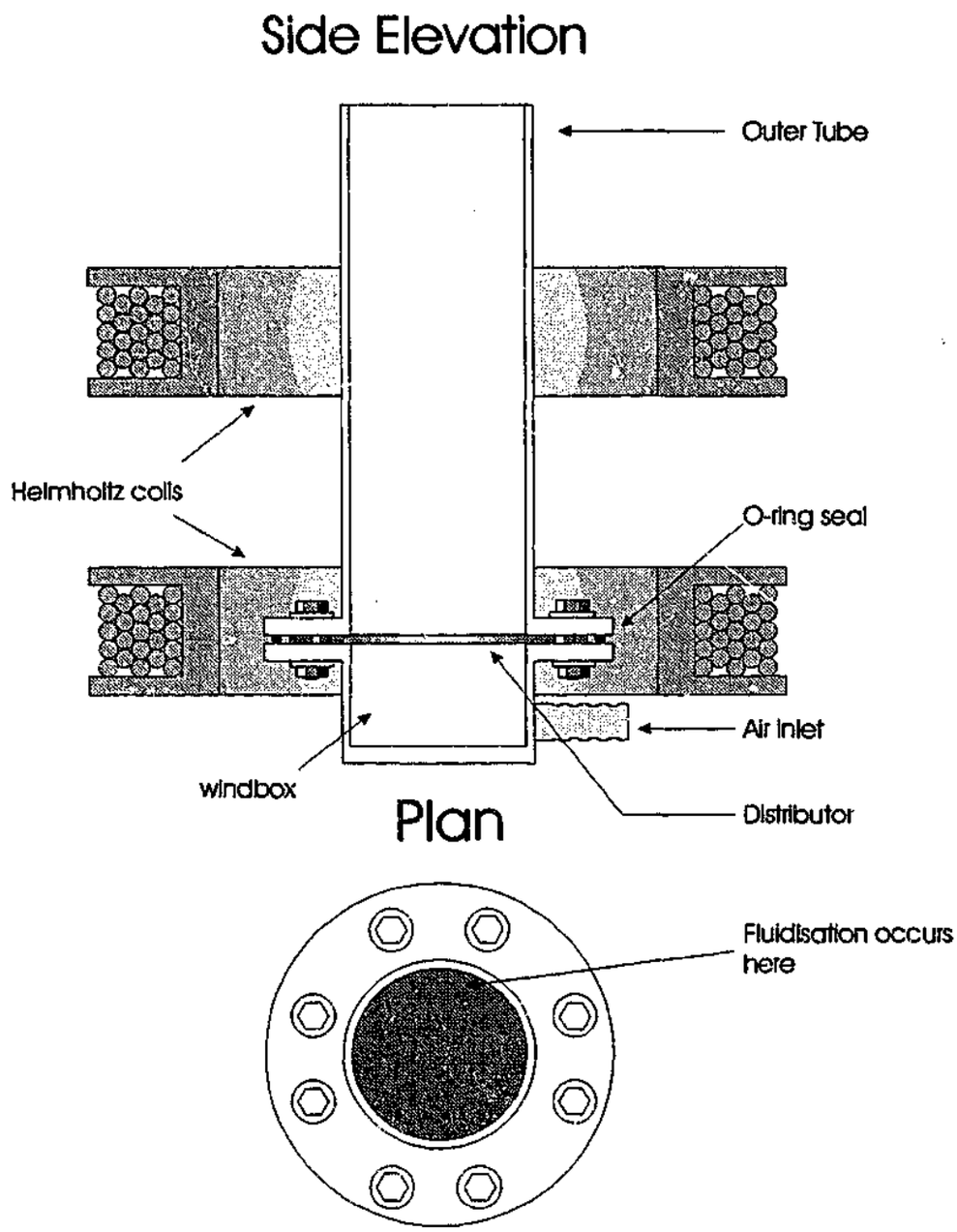

Figure 4.6: Fluidbed design

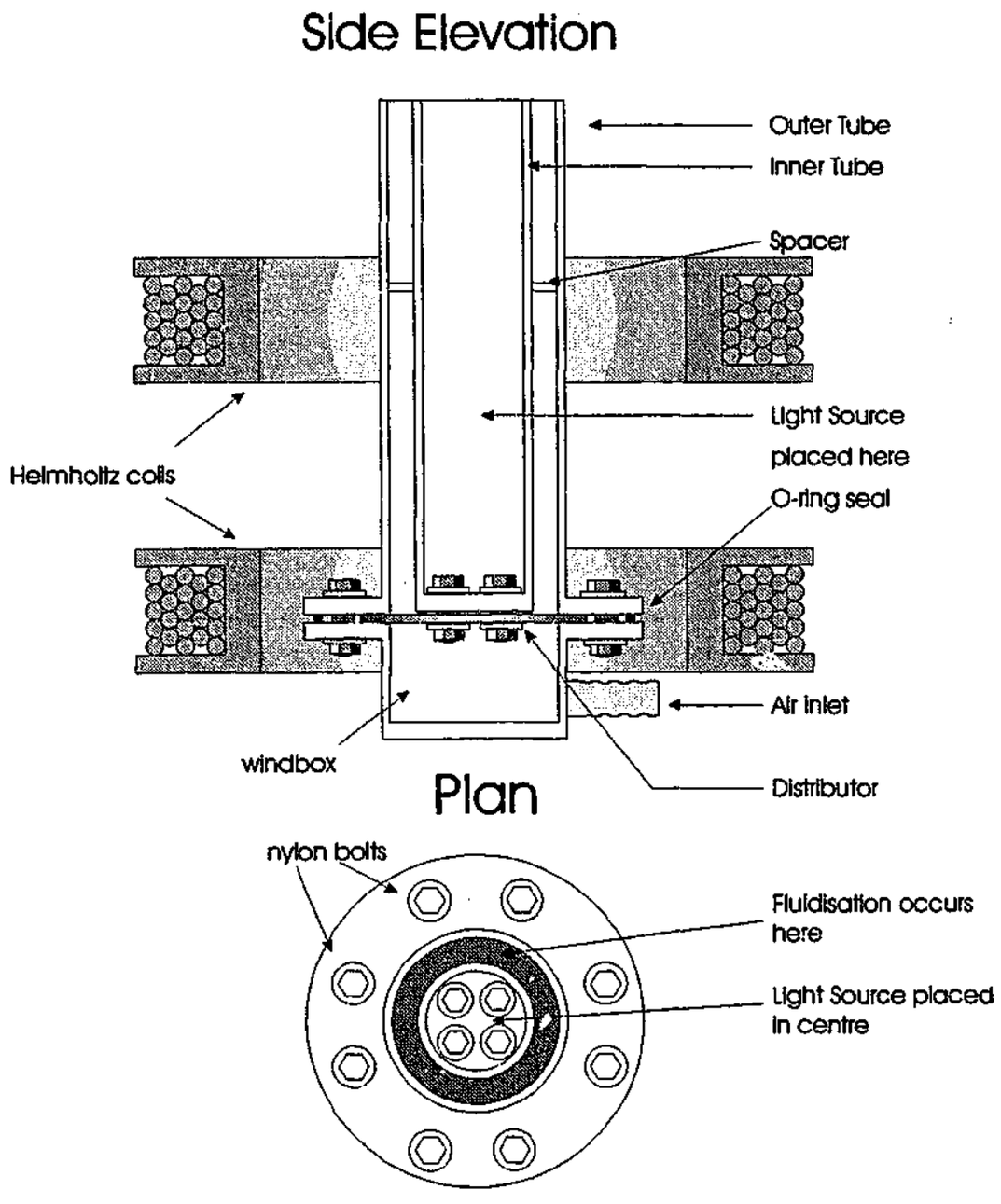

Figure 4.7: Modified Fluidbed design

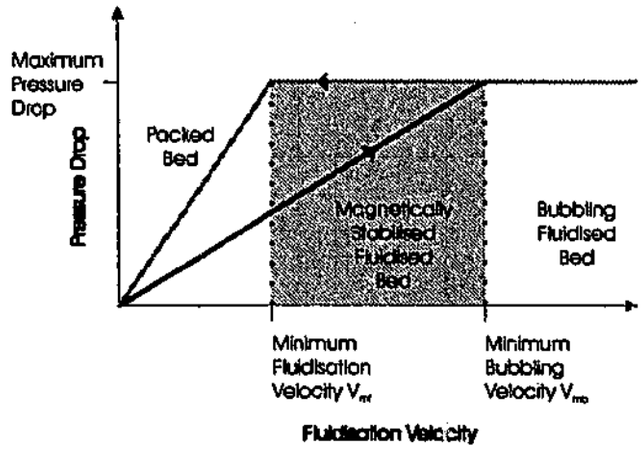

Figure 4.8: The velocity for minimum bubbling can be determined by extrapolating the line for increasing velocity to where it meets the maximum pressure drop.

in determining the superficial air velocity of ± 0.01 m/s.

In addition to visual observations of the bubbling transition measurements of the bed pressure drop were made as a function of the gas velocity for a number of values of the applied field. These experiments were carried out in the fluid bed shown in Figure 4.6. The pressure drop was measured using a differential pressure transducer linked to a computer via an analog to digital converter. The measurement of the bed pressure drop involved an error of about 2% due to uncertainties in calibrating the transducer. The experiment was carried out for both increasing and decreasing air velocity.

4.2.2 Measurement Procedure

In order to accurately determine the minimum bubbling point the following procedure was used

- The field was switched off.
- The shot was vigorously fluidised and the fluidisation velocity slowly reduced to zero so that the bed reached a loose packed state.
- The field was switched on and the fluidisation velocity obtained.
- Care was taken to approach this velocity slowly from below.

This process was repeated until the point of minimum bubbling reached. The point at which bubbling became continuous could then be observed visually. This point could also be found from measurements of the pressure drop. The bed pressure was

Figure 4.9: Bubbling in the fluid bed

observed to increase linearly with gas velocity until the point of minimum bubbling was reached. Above this point the bed pressure remained constant.

4.3 Results and Discussion

The results for various values of the field are shown in figures 4.10 to 4.15 for 300μm diameter iron particles. The bubbling behaviour appeared to depend upon the packing history of the bed. When the fluidisation velocity approached the bubbling transition the bubbling appeared vigorously for 4-6 seconds and then disappeared. Examining the process on high-speed video it was observed that the initial bubble create channels in their wake. These channels allowed the air to escape freely and thus suppressed further bubbling. As the fluidisation velocity was increased, a point was reached where bubbling became continuous.

4.3.1 Bubble shapes and field strength

The shape of bubbles in a two dimensional bed will also differ in cross section to those in a three dimensional bed. The sections of three dimensional bubbles are generally rounder than their two dimensional counterparts. Bubbles in 2D beds tend to be elliptical with the major axis in the vertical direction. The length of the major axis can often be twice that of the minor axis. While particles can be observed inside 2D bubbles these are generally found to be confined to surface of the bed and not in the centre of the bubble itself.

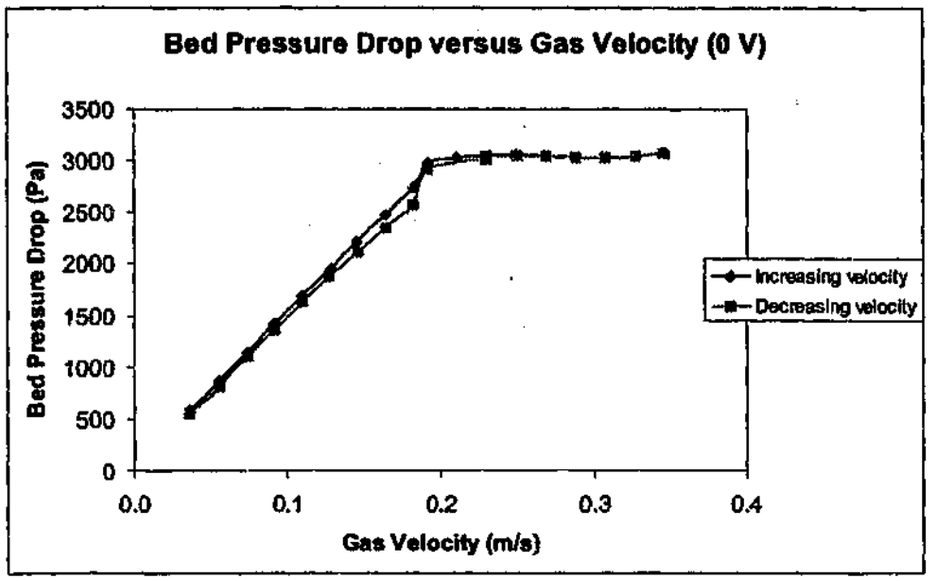

Figure 4.10: The bed pressure drop versus the gas velocity (coil voltage = 0 V)

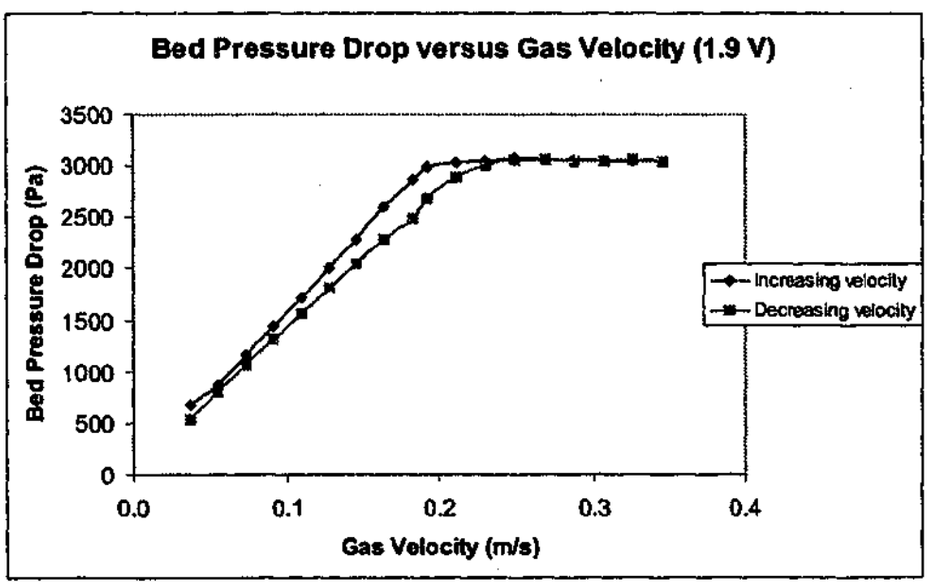

Figure 4.11: The bed pressure drop versus the gas velocity (coil voltage = 1.9 V)

4.3.2 Hysteresis

Examining the results of increasing and decreasing the gas velocity for the various values of the applied field, a hysteresis effect was observed (see Figure 2.2). This effect appears to be due to the packing of particles. For group B powders, the velocity of minimum bubbling, $U_{mb} = U_{mf}$. However for group A particles, $U_{mb} > U_{mf}$. Measuring the transition from group B to A behaviour is therefore a matter of determining U_{mb} and U_{mf}. Visual high-speed video observation were made for

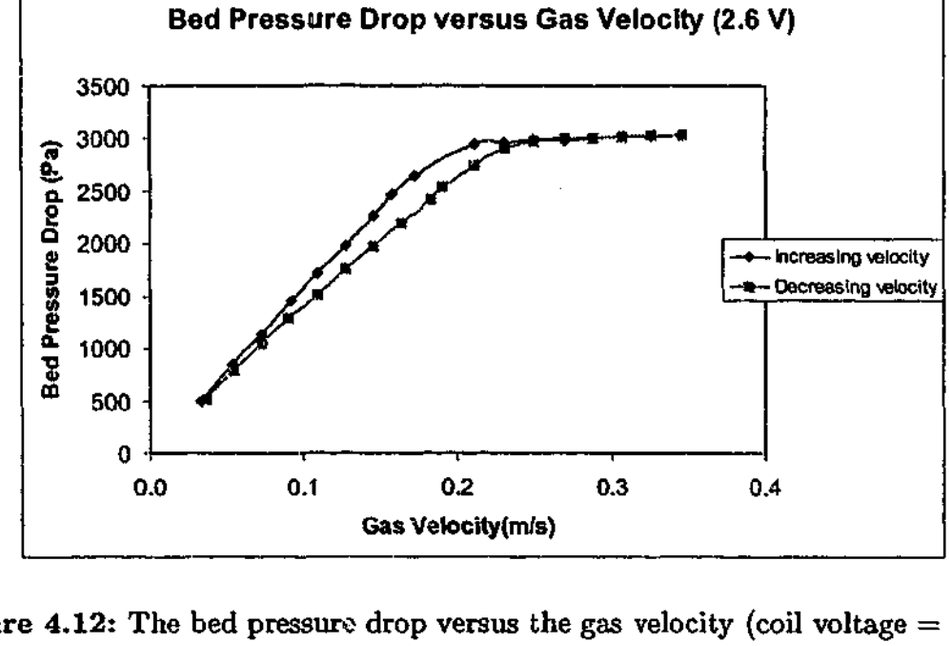

Figure 4.12: The bed pressure drop versus the gas velocity (coil voltage = 2.6 V)

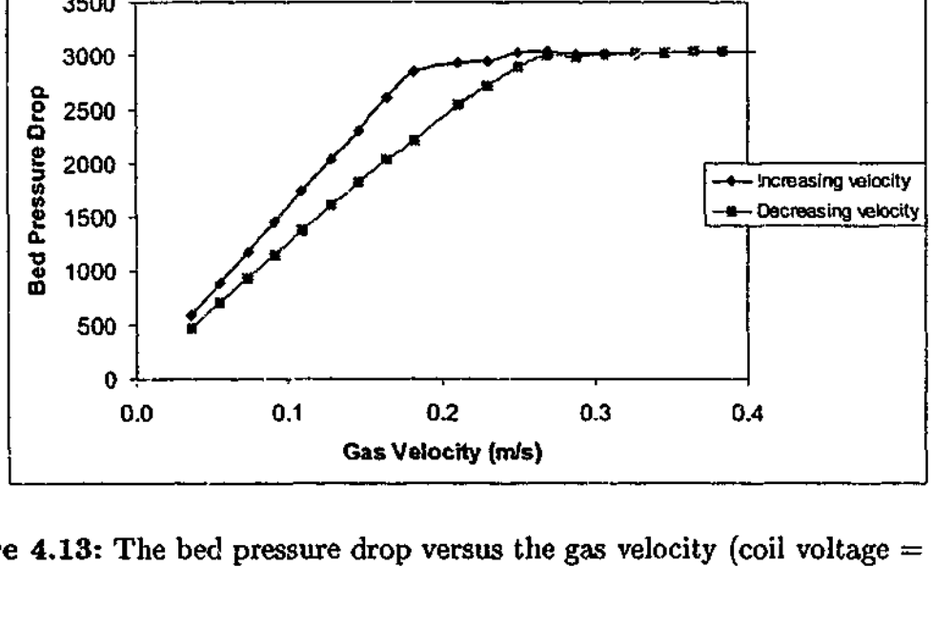

Figure 4.13: The bed pressure drop versus the gas velocity (coil voltage = 4.1 V)

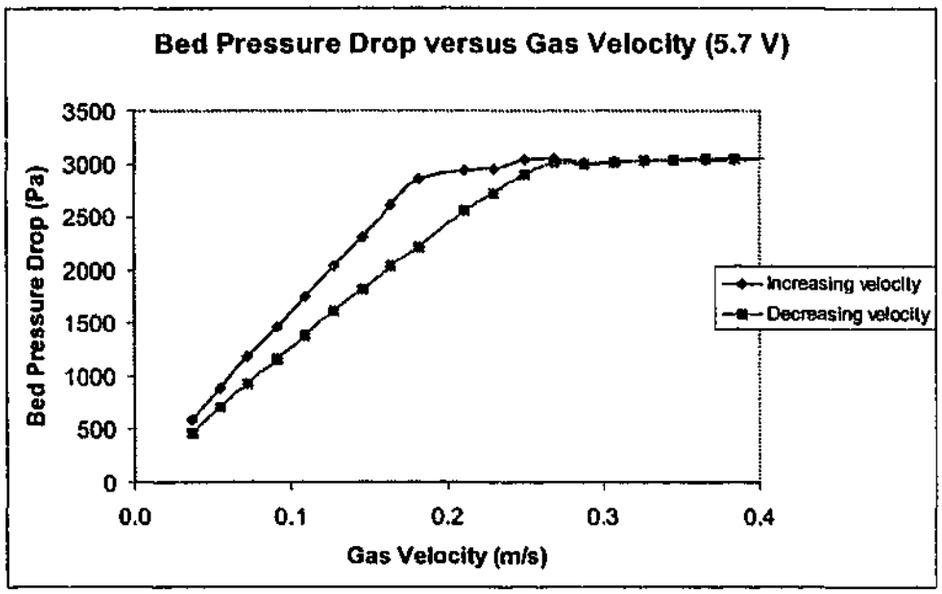

Figure 4.14: The bed pressure drop versus the gas velocity (coil voltage = 5.7 V)

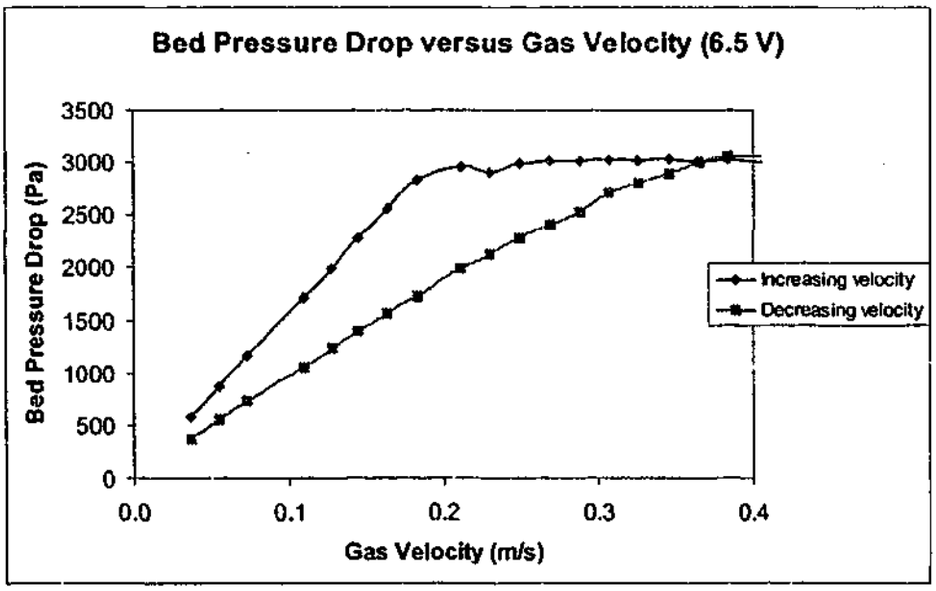

Figure 4.15: The bed pressure drop versus the gas velocity (coil voltage = 6.5 V)

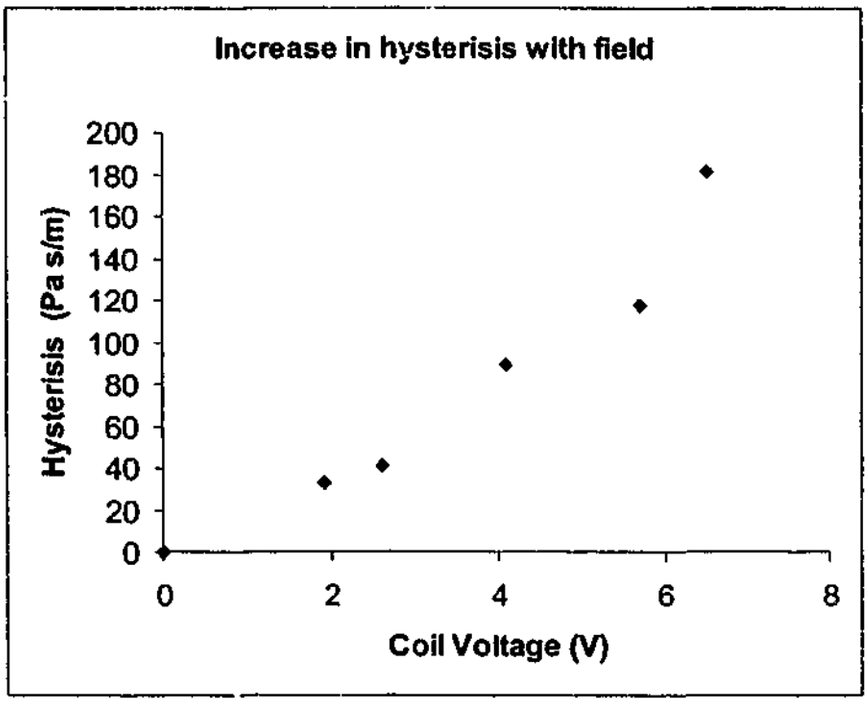

Figure 4.16: The increase in hysteresis with field

H (A/m)	U_{mb}/U_{mf} (300 μm)	U_{mb}/U_{mf} (800 μm)	(U_{mb}/U_{mf} 1600μm)
0	1	1	1
1034	1	1	1
1100	1.05		
1571	1.05		
1750		1	1
1900		1.05	1
2069	1.09	1.09	1
2268		1.13	1.06
2466	1.14	1.17	1.13
2625	1.18		
2784	1.27	1.25	1.18

Table 4.1: The minimum bubbling velocity as a function of applied field for 300 μm, 800 μm and 1600μm diameter particles.

of 300 μm, 800 μm and 1600 μm diameter particles. During these experiments it was found that U_{mf} remained constant, but U_{mb} increased with field. The range of velocities over which the magnetically stabilised bed existed therefore increased with field. From the results (shown in Table 4.1) it can be seen that the transition from B to A behaviour for the 300 μm, 800 μm and 1600μm diameter particles occurs at applied field values of1034 A/m, 1750 A/m and 2069 A/m respectively.

According to Molerus (Molerus, 1982) the B/A transition occurs for fine powders for a specific value of K where K is defined

$$K = \frac{F_{ip}}{F_{drag}} = \frac{F_{ip}}{\pi d^3(\rho_p - \rho_g)g/6} \tag{4.1}$$

where F_{drag}, d is the particle diameter, ρ_p is the particle density, ρ_g is the gas density and g is the gravitational acceleration. Using the results obtained in these experiments for 300 μm particles K is equal to 2.63. From visual observation of the fluidisation transition for particles of diameters 800 μm and 1600 μm, the values for K are 2.34 and 2.29 respectively[4].

These values are consistent with recent discrete element method simulations of two-dimensional fluid beds (Rhodes and Wang, 2002).

4.4 Conclusion

A novel fluid bed has been constructed which enables visual examination of the effect of inter-particle forces on fluid bed behaviour. Using this fluid bed, it has been demonstrated that transitions between Group A and B behaviour can be induced by increasing the inter-particle forces.

Investigations of this transition region have found that transition occurs for F_{ip}/F_{drag} of $\approx$ 2.5 for the three particle sizes investigated. As inter-particle force was increased, the minimum bubbling velocity was found to increase while the minimum fluidisation velocity remained the same.

In the next chapter a different aspect of fluidised granular media is investigated, namely pattern formation in thin vibrated granular layers.

[4]The values of F_{ip} were obtained from the experimental results in chapter 2.

Chapter 5

Patterns

> We forgave Bagnold everything for the way he wrote about dunes. The grooves and the corrugated sand resemble the hollow of the roof of a dogs mouth.' That was the real Bagnold, a man who would put his inquiring hand into the jaws of a dog.
>
> **Michael Ondaatje**
>
> *The English Patient*

Pattern formation in nature obeys a kind of universality (Gollub and Langer, 1999) in that many diverse systems obey similar pattern formation dynamics. Understanding pattern formation in one of these systems can therefore give insights into the same process in other systems. Some of the pattern forming systems which have been the focus of recent research include dendritic growth (Ball, 1999a) (which is observed in bacterial colonies and other physical processes), Turing patterns and models of animal coats (Goodwin, 1994) and the formation of spiral waves (Prigogine and Stengers, 1984) such as occurs in the BZ reaction and slime mould growth (see Figure 5.1).

Granular materials also provide an excellent medium for studying pattern formation. One particularly rich example of pattern formation which has only recently been investigated is pattern formation in vibrated granular layers (Umbanhowar, 1997). Previous experiments (Umbanhowar, 1996b) inter-particle forces have been found to alter these patterns.

In this chapter, pattern formation in thin vibrated layers of granular material is investigated. Using the method outlined in previous chapters the effects of altering inter-particle force on the patterns is examined.

5.1 Pattern Formation in Vibrated Granular Media

A thin layer of granular material is placed in a rigid container and driven sinusiodally with time, t, according to

$$z = A \sin \omega t \tag{5.1}$$

where z is the height, A is the amplitude and $\omega = 2\pi f$ is the angular frequency of the container. The peak acceleration is given by

$$\Gamma = A\omega^2/g \tag{5.2}$$

where g is the acceleration due to gravity and A is the amplitude of acceleration. For various values of maximum acceleration Γ and frequency f complex and elaborate patterns are formed. These patterns include hexagons, stripes, squares as well as chaotic spirals and kinks (some of these patterns are shown in figure 5.2). Extensive experimental investigations of these patterns have been performed by Umbanhowar (Melo et al., 1995), (Umbanhowar, 1996b). Figure 5.3 shows a phase diagram of the pattern behaviour and how the patterns vary with vibration frequency, f, and acceleration, Γ.

5.1.1 Models

There have been several approaches to modelling and understanding pattern formation in vibrated granular layers. In initial investigations, Umbanhowar (Umbanhowar, 1996b) considered a very simple theoretical model in which individual grains collide in-elastically. For low vibration amplitudes the entire granular layer rises and falls in step with the container. Above a critical amplitude however, a period doubling bifurcation takes place. The layer breaks up into stripes at lower frequencies and squares at higher frequencies.

Pattern formation in granular materials can be readily simulated using molecular dynamics models where the motion of each individual grains simulated[1]. This approach, however, is not particularly enlightening as it does not give much insight into general pattern formation mechanisms. Ideally, a continuum model of

[1]see, for example, the simulations by Chris Bizon on Paul Umbanhowar's website URL http://super.phys.northwestern.edu/ pbu/

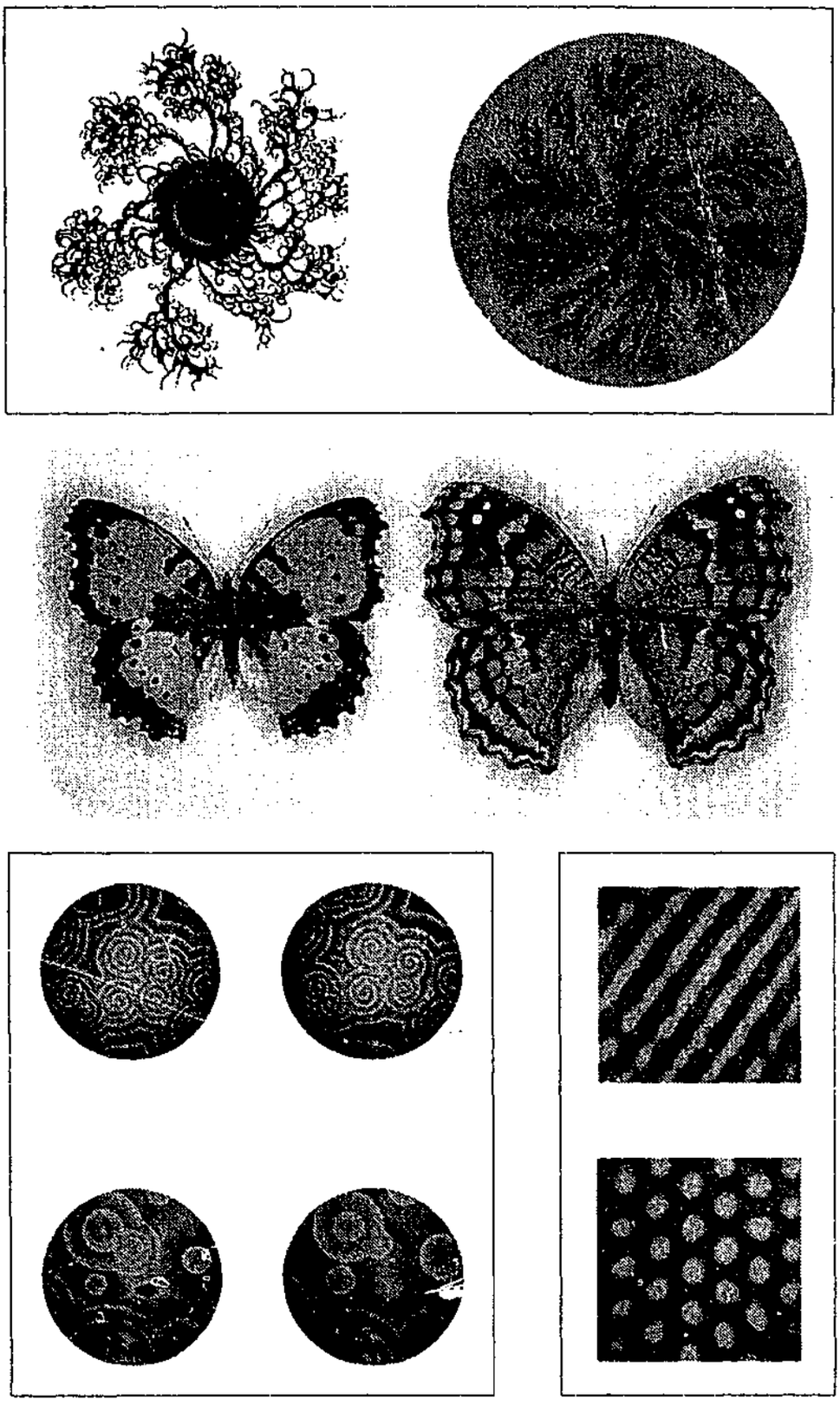

Figure 5.1: Some pattern forming systems in nature. (top) bacteria (center) butterfly wings (bottom left) spiral waves in the BZ reaction and (bottom right) Turing patterns in animal coats (From Ball 1999a).

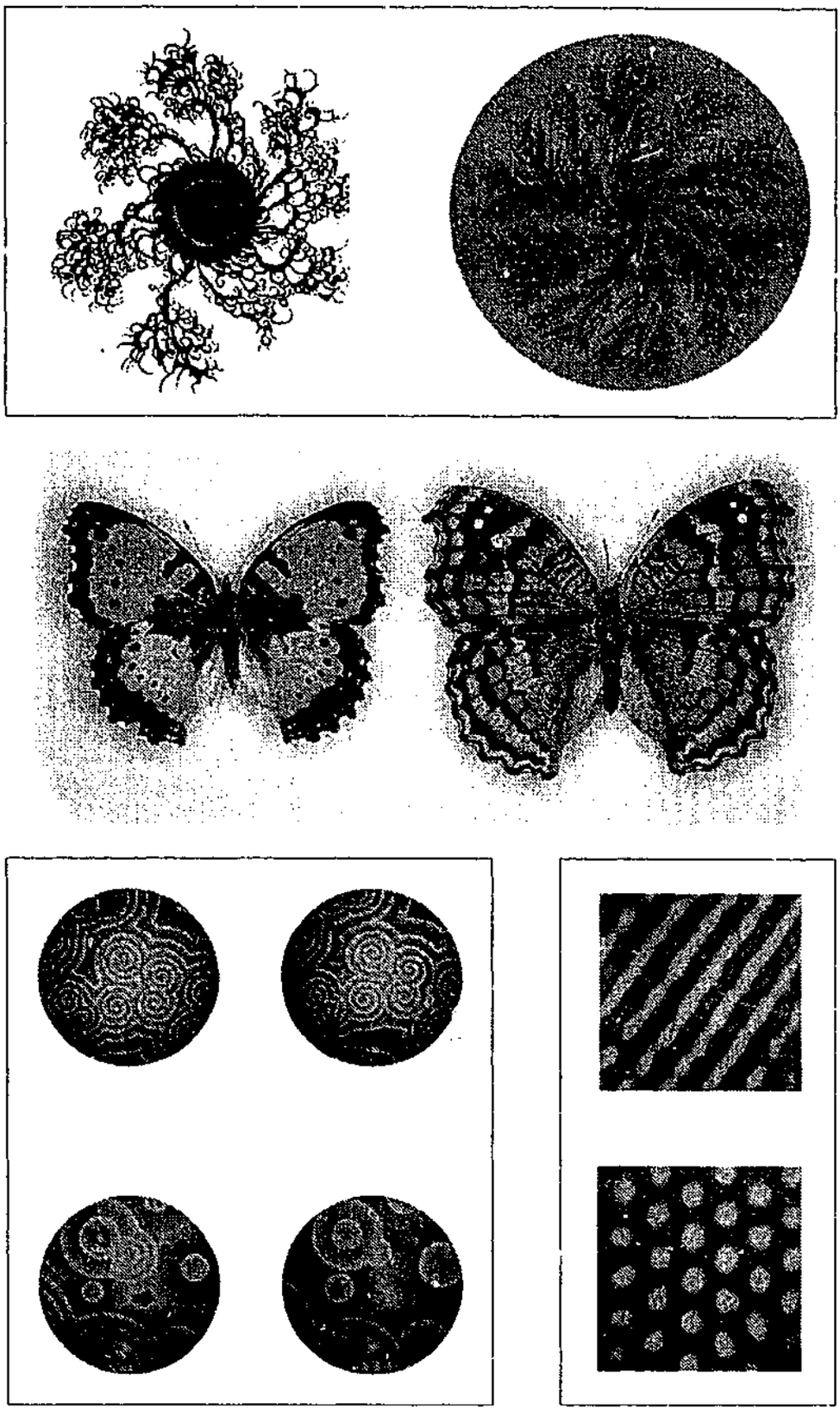

Figure 5.1: Some pattern forming systems in nature. (top) bacteria (center) butterfly wings (bottom left) spiral waves in the BZ reaction and (bottom right) Turing patterns in animal coats (From Ball 1999a).

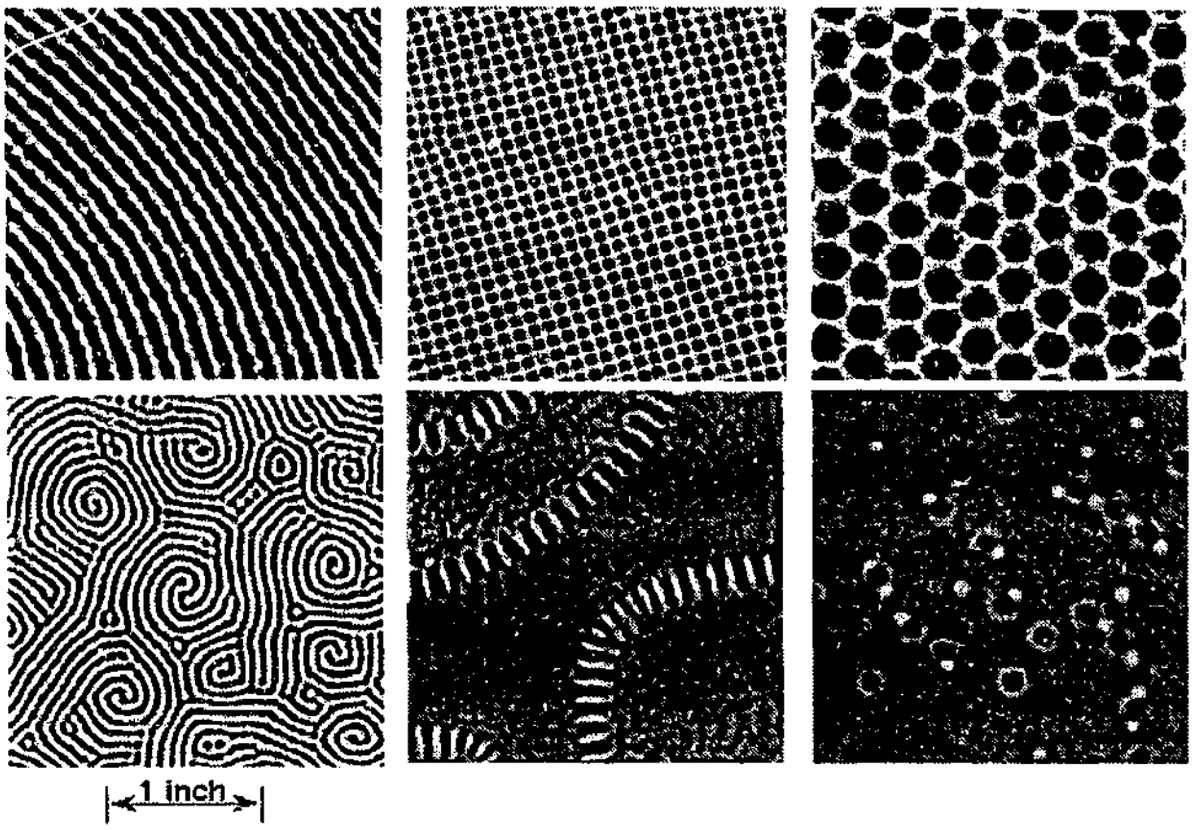

Figure 5.2: Some of the patterns observed in vibrated granular materials. Clockwise from top left, stripes, squares, hexagons, oscillons, decorated kinks and spirals. From (Umbanhowar, 1996b).

the pattern formation process is needed which gives the essential features of the pattern dynamics, independent of the details of individual particle dynamics and interactions. In other non-linear, dissipative, pattern formation systems, such as chemical reactions and hydrodynamic flows, the pattern formation mechanisms are well understood. In these systems analysing the pattern formation process is a simple matter of studying the equations of motion for the system. However, since such equations do not exist for granular matter we cannot do this for patterns in vibrated granular layers.

An interesting model of the pattern formation behaviour in granular systems has been developed by Troy Shinbrot (Shinbrot, 1997). This model ignores the rising and falling of the grains and instead focuses on the horizontal motion of the grains. In the model, grains are given a random kick once each vibration cycle. This models the randomising influence of the collisions with the plate. Grains then collide in-elastically. Despite its simplicity the model is able to account for most of the

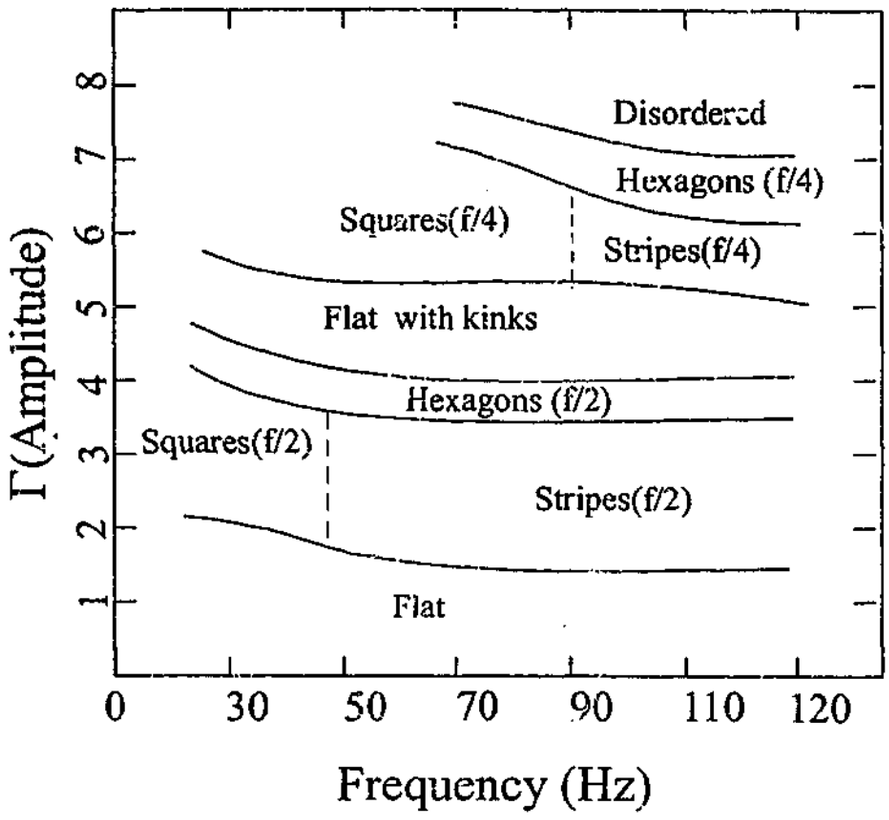

Figure 5.3: Phase diagram of pattern behaviour(from (Umbanhowar, 1996b))

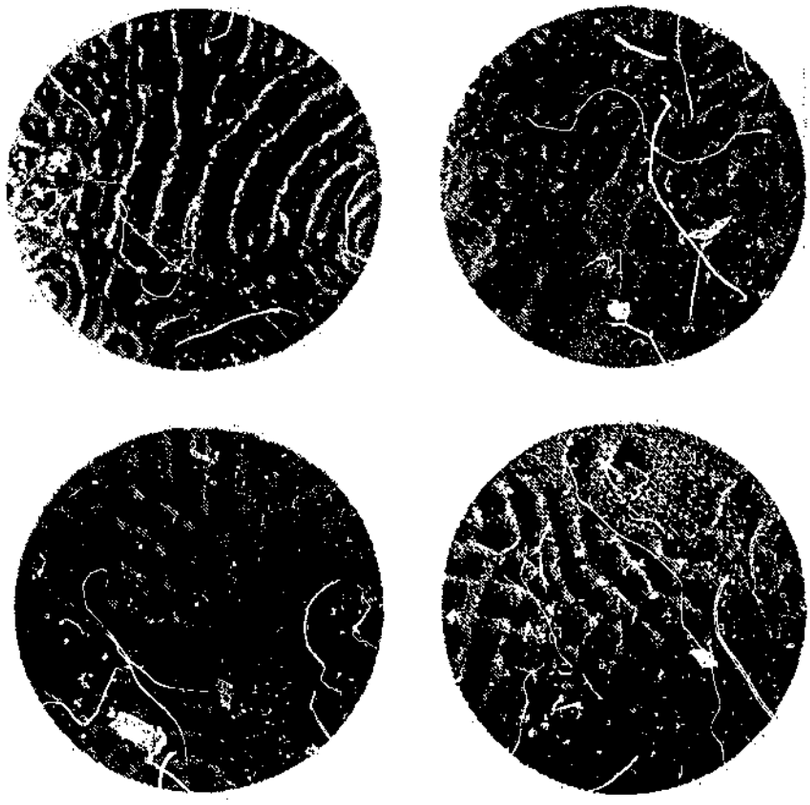

Figure 5.4: Some of the patterns observed the authors experiments on vibrated granular materials

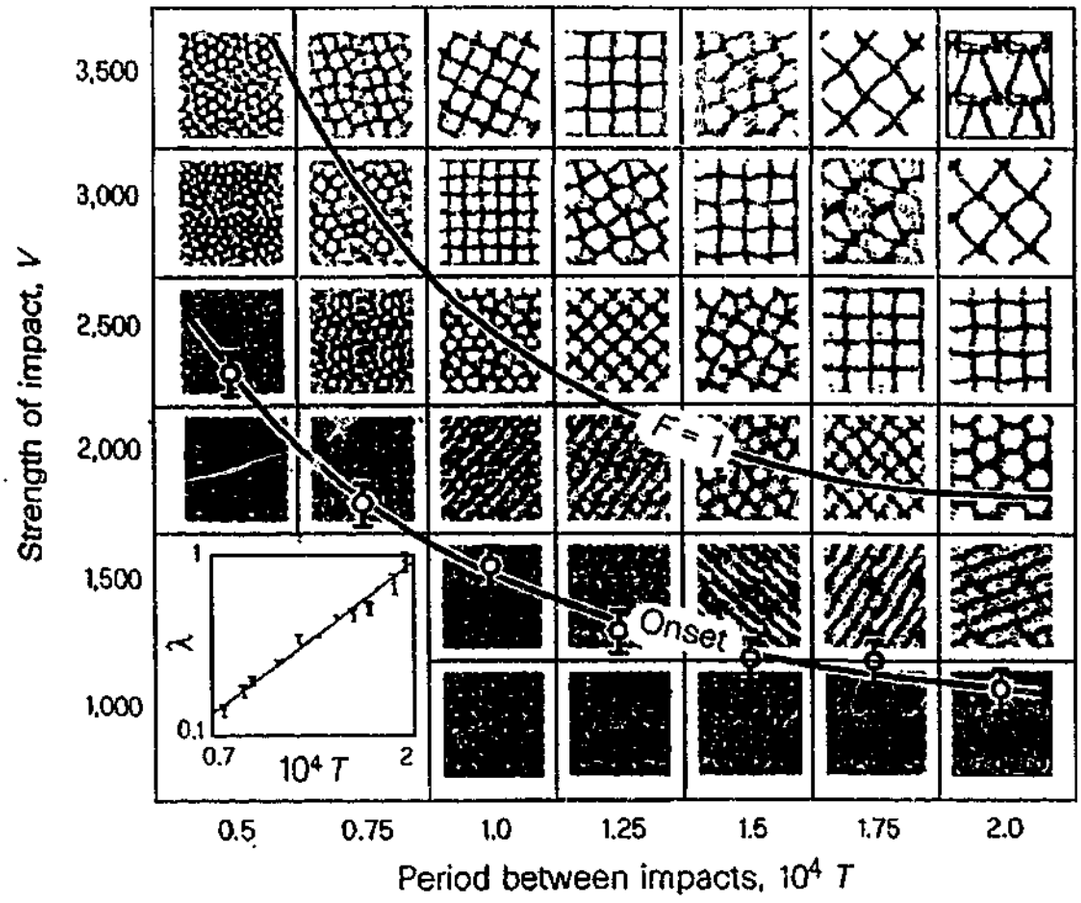

Figure 5.5: Phase diagram of pattern behaviour in Shinbrot's model system (from (Shinbrot, 1997))

patterns found in experiments.

Shinbrots model is a hybrid of both the continuum approach and the molecular dynamics approach. The model suggests that the patterns can be explained in terms of a competition between randomising kicks and dissipative collisions. This model is analogous to chemical reaction - diffusion systems, which are known to have similar pattern formation behaviours. In reaction - diffusion systems, a similar competition occurs between randomisation (in the form of diffusion) and dissipation (in the form of reactions).

Shinbrot's model predicts a number of new patterns that have yet to be found experimentally. These patterns are thought to exist for parameter values which are not yet accessible by experiment (Umbanhowar, 1997).

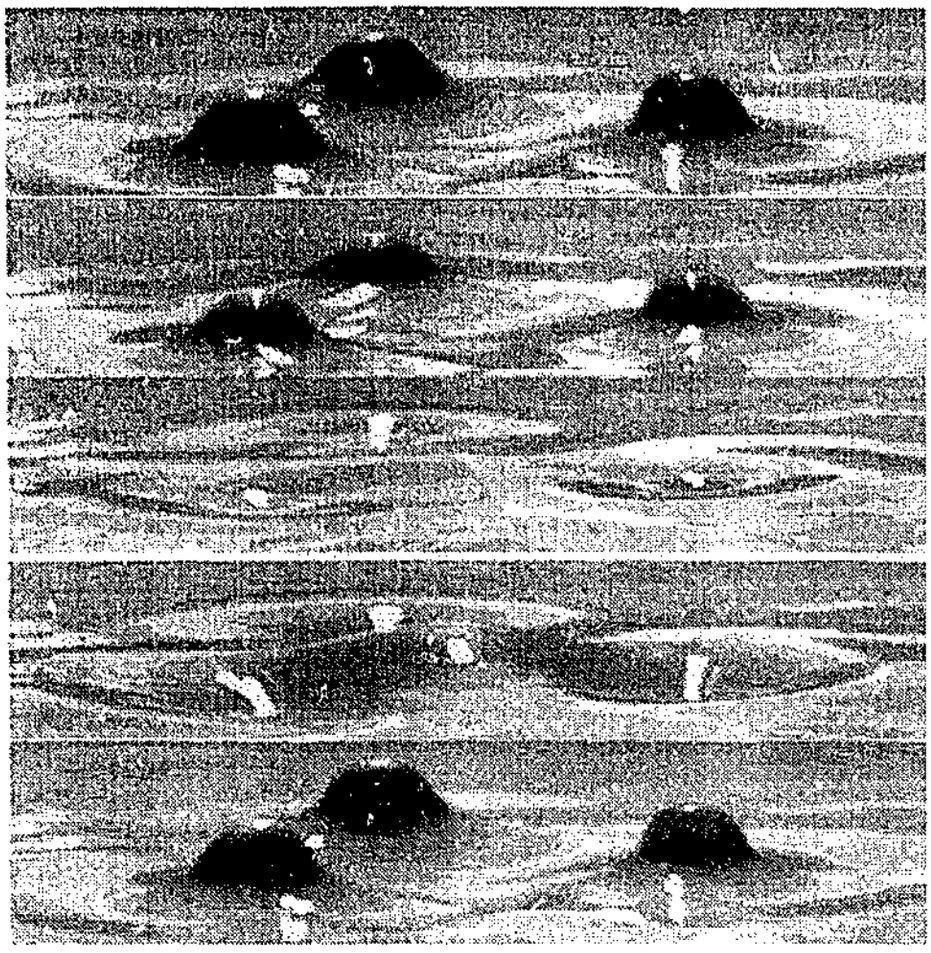

Figure 5.6: Oscillons have recently been observed in clay suspensions. From (Lioubashevski et al., 1999)

5.1.2 Oscillons

Another model for the patterns in granular materials is to consider them as being made up of oscillons[2]. These oscillons have been observed (Umbanhowar, 1996a) in experiments on granular materials and also more recently in vibrated suspensions of clay particles (Lioubashevski et al., 1999) as shown in Figure 5.6. The appearance of oscillons in clay suspensions is interesting since clay suspensions and granular materials are quite different systems. It is possible that oscillons may yet be found in other systems and may even be a universal property of some driven non-linear systems.

In vibrated granular layers, oscillons appear spontaneously for values of Γ in the range between squares and stripes. They are only observed to occur in particle layers more than 13 particles deep. Oscillons can also be created by locally perturbing the

[2]see discussion in chapter 1

layer with a pencil. Oscillons of opposite phase exhibit short range repulsion. Like phase oscillons, on the other hand, attract one another and bind. Experiments have shown that by adding oscillons together more complex patterns can be constructed (Umbanhowar, 1996b).

5.1.3 The Role of Inter-particle Forces

While vibrated particle experiments are interesting, it is possible that behaviours that are even more interesting can be observed in systems into which inter-particle forces are introduced. The methods of altering inter-particle force by adding liquids suffers from the problem that thin vibrated liquid layers also exhibit tendency to form patterns. The pattern forming behaviour of liquids differs significantly for that in granular layers. To avoid this problem, the techniques described in chapter 2, experiments were used out to investigate the effects of inter-particle force on patterns in vibro-fluidised granular layers.

5.2 Experimental

The apparatus consists of an evacuated container in which the thin layer of granular material (5 particles deep) is held as shown in Figure 5.7. This is mounted on a 30 cm aluminium arm, which in turn is attached to an electro-magnetic shaker. Care was taken to align the centre of the drive shaft with the centre of the Teflon sleeve to prevent the shaft from sticking and interfering with the patterns. The container was levelled using a spirit level. This was found to be important as small lateral vibrations lead to particles accumulating in specific areas of the container. If unchecked, this process was found to cause the container to become unbalanced leading to a positive feedback situation. To minimise torques during shaking, the container was carefully balanced about its centre. Lateral vibrations were constrained by means of a Teflon sleeve that was fixed to the base of the device. The base was in turn connected to a large concrete block.

5.2.1 Container

Several containers were trialed during these experiments, including a square container of side length 15 cm and a 20 cm diameter circular container. The size and

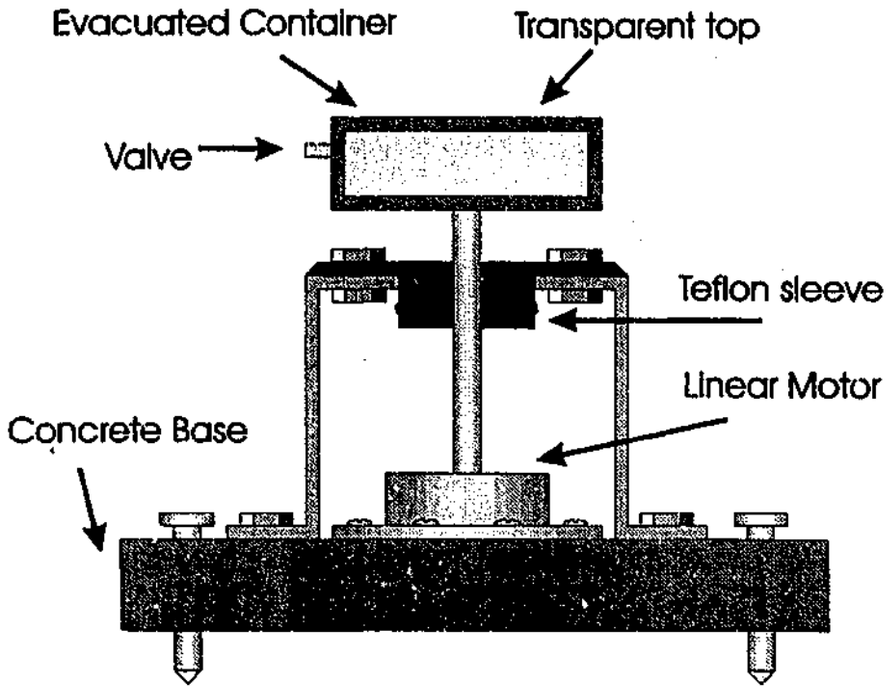

Figure 5.7: Shaker

shape of the container were not found to affect the patterns, which appear to be caused by the interactions between grains and the base of the container. For most of the experiments, a 12.5 cm diameter circular container was used. The base was constructed of 15 mm thick Perspex and the walls made from 5mm thick 12.5 mm diameter Perspex tubing. The container was found to be large enough to give good patterns but small enough to not become unbalanced and introduce lateral vibrations. Anti-static spray was used to prevent charge build up between the particles, which can interfere with the pattern formation process. In the experiments performed with iron shot, the effects of static charge build up were not observed.

The motor used to drive the shaker was an Aura shaker motor assembly (or subsonic actuator)[3]. The motor was powered by a $\pm 35VDC$ ($70V_{pp}$) power supply connected to an AEM6506 power amplifier as shown in Figure 5.8.[4] The frequency and amplitude control was via a Wavetek, model 191, pulse/function frequency generator. The amplitude control was calibrated by measuring the peak to peak displacement of the container as a function of the signal amplitude. This resulted in an accuracy in the determination of the acceleration of ± 5 %.

[3]see appendix A for equipment details

[4]The details of this amplifier can be found in the January 1987 Australian Electronics Monthly

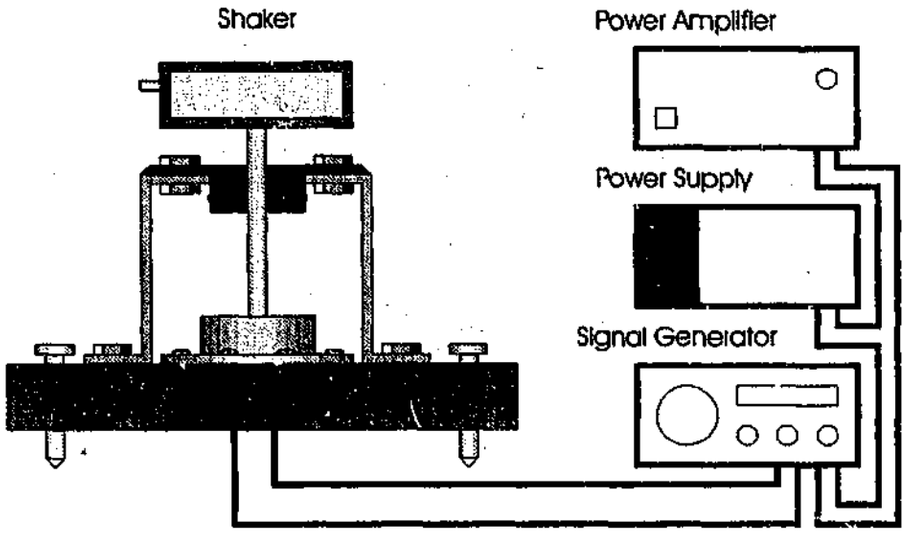

Figure 5.8: Experimental apparatus for pattern formation

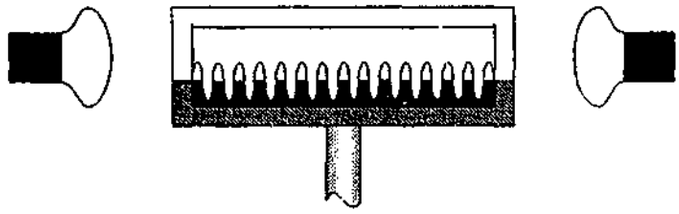

Figure 5.9: Light sources were arranged to illuminate the peaks of the patterns

5.2.2 Lighting

In order to see the patterns clearly, the patterns were illuminated from the sides so as to enhance the peaks of the pattern and leave the valleys in shadow (as shown in Figure 5.9). Bright incandescent lights were used to provide an even and constant illumination. The apparatus was shielded from all external lighting. The light source was found to provide constant illumination even when using high-speed video. The sides of the container were masked off and placed about 10 cm from the light source. Still images were taken using a video camera attached to the matrox imaging system[5].

5.2.3 Heaping

When conducting experiments with fine powders, large heaps of powder emerged in the layer that interfered with the patterns. This heaping was not observed with larger particles. Previous experiments suggest that this heaping is somehow influenced by interstitial gas (Umbanhowar, 1997). It is thought that rising grains

[5]see Appendix A for details

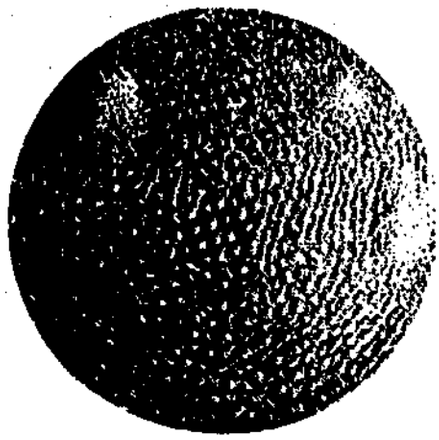

Figure 5.10: Heaping

create a vacuum in their wake, sucking other particles in underneath and forming a heap. To prevent this the container was evacuated and the heaping observed to disappear. This heaping is quite different to the heaping and pattern formation (including surface waves) that is found in deep vibrated beds (Falcon et al., 1999). These processes are quite different to the surface waves in thin layers described here, as they appear to result from convection within the bulk of the material.

5.3 Results and Discussion

5.3.1 Some of the Patterns Observed

The patterns were observed for a range of values of Γ and f using a range of imaging techniques including strobe lighting and high-speed video. As Γ is increased above $\Gamma = 1$ the granular layer was observed to move as a whole. The grains remained well packed and so could not pass each other easily. However, above $\Gamma \approx 2.4$ the granular layer underwent a bifurcation with stripes and squares being observed. The squares occur for $f \lesssim 24$ and $f \gtrsim 40$. For intermediate f values the two patterns compete. The patterns oscillate (ie peaks become troughs and vice versa) with a frequency $f/2$.

As Γ was increased, hexagons were observed to appear and then disappear again. This was followed by the appearance of "kinks". These kinks are twisted walls of oscillating particles that act as boundaries between flat, out of phase regions (see Figure 5.2).

On increasing Γ further, another regime of squares and stripes was observed but this time the frequency of the layer oscillation was $f/4$. Finally for $\Gamma \approx 8$ a disordered regime was reached which consisted of chaotically oscillating waves.

5.3.2 Effect of Grain Shape

Experiments were carried out to investigate the effect of grain shape on patterns. The following results were found.

- irregular particles (sand) gave the same patterns as regular spheres.
- The patterns became less clear when mixtures of two or more different grain sizes were used.
- As the aspect ratio of the grains was increased the edges of the patterns became blurred (possibly due to the fact that there were now two characteristic length scales).

5.3.3 Effects of Inter-particle Force

Experiments were conducted to examine the effects of increasing inter-particle force on the patterns observed. The 12.5 cm diameter circular container was filled with 300 μm diameter iron particles so that the layer was approximately five particles deep. Starting with a stripe pattern with Γ just above onset ($\Gamma \approx 3.3$) the field was increased from zero. These experiments were performed for a range of different frequencies. After each change in frequency, the container was re-levelled. It was found that, for most frequencies, the application of the magnetic field rapidly destroyed the patterns.

For patterns generated from plate frequencies of between 23 and 30 Hz, however, the patterns did not disappear. In this range of frequencies the patterns were observed to change from stripes to hexagons and then to kinks. For this, relatively narrow, range of frequencies, increasing the applied field was observed to have a similar effect to increasing Γ. When the field was decreased again, the patterns were found to transform again from kinks at high field to hexagons and then back to stripes again. It was not found possible to produce stripes from a flat layer by simply increasing the applied field.

Other minor qualitative changes were also observed in the patterns. The peaks

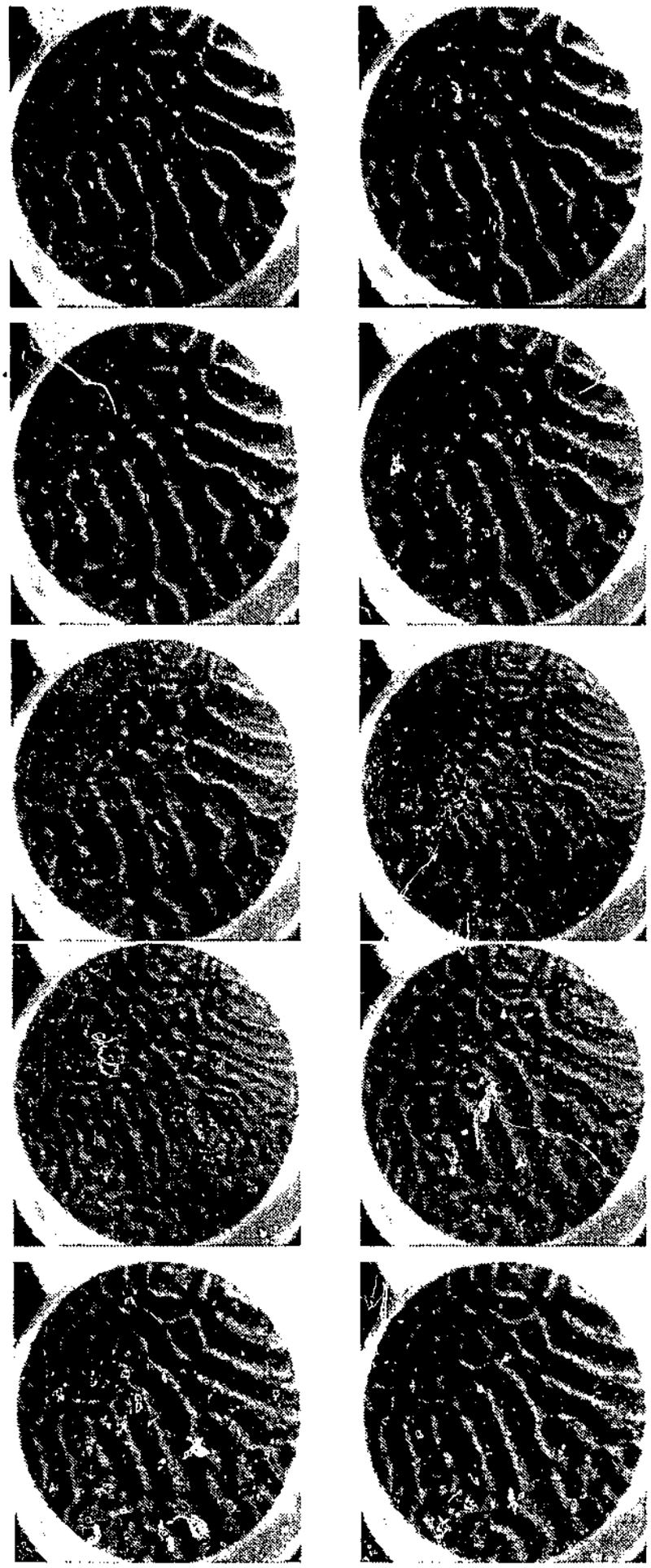

Figure 5.11: Sequence of high speed images showing pattern development

Figure 5.12: Patterns in magnetic field (coil voltage 4V)

of the stripe patterns appeared to sharpen as the particles in the adjacent peaks appeared to repel one another. Figure 5.12 shows the effect on the stripe patterns of increasing the field, but leaving both the frequency and acceleration unchanged. Note the formation of "dots"(small isolated peaks) and corners in the stripes as adjacent peaks appear to repel one another. These features appeared and disappeared rapidly as the magnetic field was switched on and then off again. Applying the magnetic field appeared to suppress the formation of squares. The square patterns rapidly transformed into stripes as the field was applied.

The main effect observed in these experiments is the suppression of the patterns with increasing field. This effect parallels the results of the previous chapters where bubbling was suppressed by increasing the inter-particle force. Experiments were carried out using 800 μm and 1600 μm diameter particles with similar results. It is interesting to compare and contrast the results of these experiments with experiments using glass beads vibro-fluidised in air (Umbanhowar, 1996b). The glass beads acquire static charges during vibration. This alters the inter-particle force and suppressed pattern formation for frequencies above $\approx$ 40 Hz. Experiments were carried out using 0.1, 0.25, 0.5, 0.7 and 1 mm diameter glass ballotini. It was found

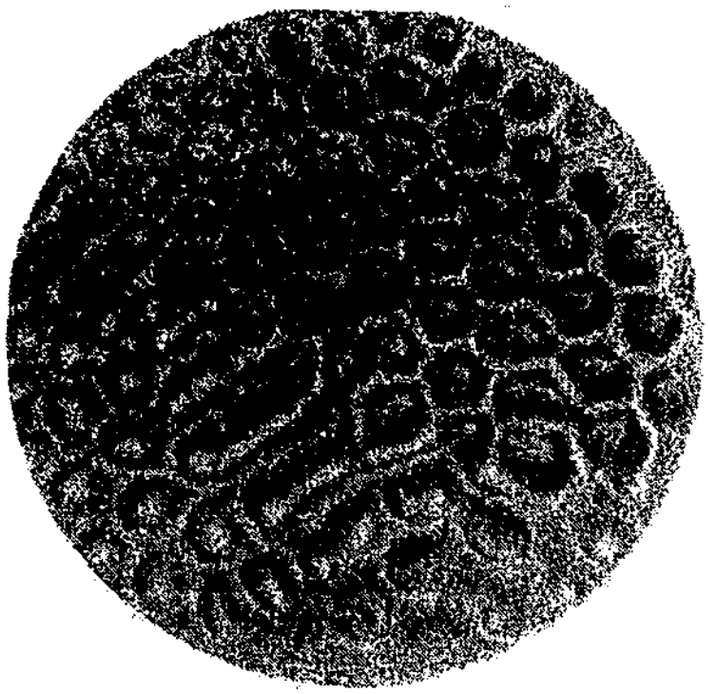

Figure 5.13: Patterns in magnetic field (coil voltage 8V)

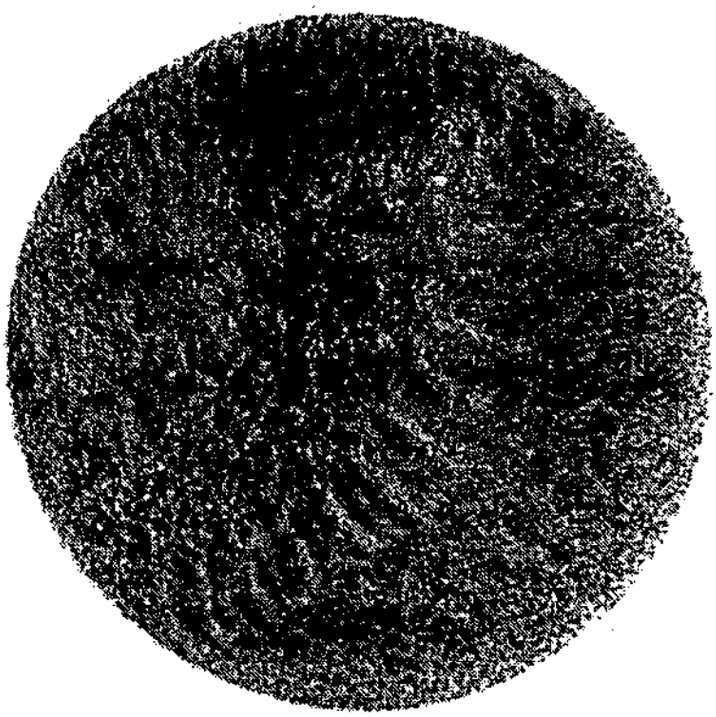

Figure 5.14: Patterns in magnetic field (coil voltage 16 V). The poor contrast is due to the particles aligning with the field and shadowing one another.

that for particles 5 mm and larger the patterns were quite well defined and the effect of static charges appeared negligible. For 1 mm diameter glass particles, however, the pattern formation was strongly suppressed and was complicated by "heaping". The results of the experiments for 0.25 mm glass ballotini performed by the author were very similar to those by Umbanhowar (see Figure 5.15 for a phase diagram of the behaviour for 2 mm glass particles in air.).

Due to problems with lateral vibrations, the length of the shaft driving the container had to be kept relatively short. In the magnetic field experiments, however, this opened up the possibility that the shaker motor was being affected by the applied magnetic field. To test whether the magnetic field was affecting the shaker motor and hence the patterns, the shaker was placed inside the Helmholtz coils and the container outside the coils. Increasing the field with the apparatus in this configuration did not appear to alter the patterns formed in any significant way. This suggests that the effect is due to changes in inter-particle interactions and not interactions between the applied magnetic field and the shaker motor.

A possible explanation for why the patterns were observed to alter as the field was increased lies in the dilation of the layer. In chapter 3, it was found that voidage of poured granular materials increased with increasing inter-particle force. A similar increase in vibrated layer dilation was observed as the inter-particle force was increased although this was not possible to measure in these experiments.

Experiments by Umbanhowar (Umbanhowar, 1996b) have shown that the layer dilation increases linearly with Γ for $\Gamma > 1$ and $f \lesssim 40$ Hz. This effect decreases as the frequency increases. The results of these experiments suggest the converse process of increasing the layer dilation may alter the effective value of Γ. If, how and why this occurs would be an interesting area for further theoretical study.

5.4 Conclusion

The experiments carried out here show that inter-particle force does have a significant effect on pattern formation processes in vibrated granular layers. The most obvious effect of increasing inter-particle force is to suppress the pattern formation process for a wide range of frequencies. The second effect on the patterns that was

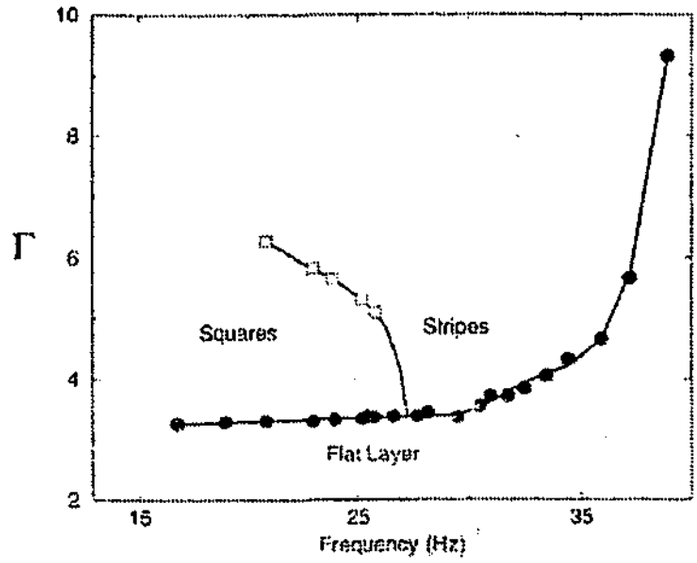

Figure 5.15: Phase diagram of the behaviour for 2 mm glass particles in air. From (Umbanhowar, 1996b).

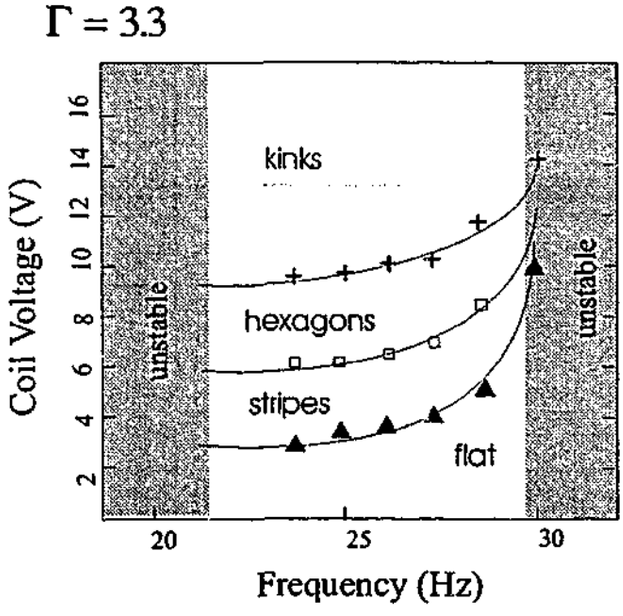

Figure 5.16: Phase diagram of the effect on patterns of applying magnetic fields

noted was for frequencies of between approximately 23 and 30 Hz, increasing the magnetic field was found to have a similar effect to increasing Γ. As the field was increased for these frequencies, stripes were found to change to hexagons and then "kinks". The process was observed to reverse as the field was decreased again.

Further investigation of these effects could have some important implications for understanding the formation of similar patterns in vibrated liquids and clay suspensions, as well as in understanding some seismological processes which have some similarities to oscillons (Umbanhowar, 1997).

In the next chapter, a different form of pattern formation in granular materials is investigated.

Chapter 6

Segregation and Stratification

> How do we know that the creations of worlds are not determined by falling grains of sand?
>
> **Victor Hugo**
> *Les Miserables*

One feature of complex systems far from equilibrium is the appearance of patterns and dissipative structures. One simple pattern formation process in granular materials involves the segregation and stratification of particles. During rock slides and avalanches it is common for larger particles to come to rest at the bottom of the slope while smaller particles accumulate further up the slope. The particles segregate according to size during avalanching. Another segregation process occurs when the angle of repose of the large grains is smaller than the angle of repose of the smaller grains. Under these circumstances, the material will spontaneously stratify into alternative layers of small and large grains. Understanding these behaviours has important implications for industrial processes requiring poured mixtures to remain homogeneous. They may also be important for understanding several geological processes (Makse, 2000), (Fineburg, 1997). In this chapter, the influence of inter-particle forces on avalanche segregation and stratification is investigated.

6.1 Overview: Avalanche Stratification and Segregation

Homogeneous binary mixtures of particles are observed to stratify into layers according to particle size and/or shape when poured between two transparent vertical plates, held a small distance apart, and allowed to avalanche. Further to this, there

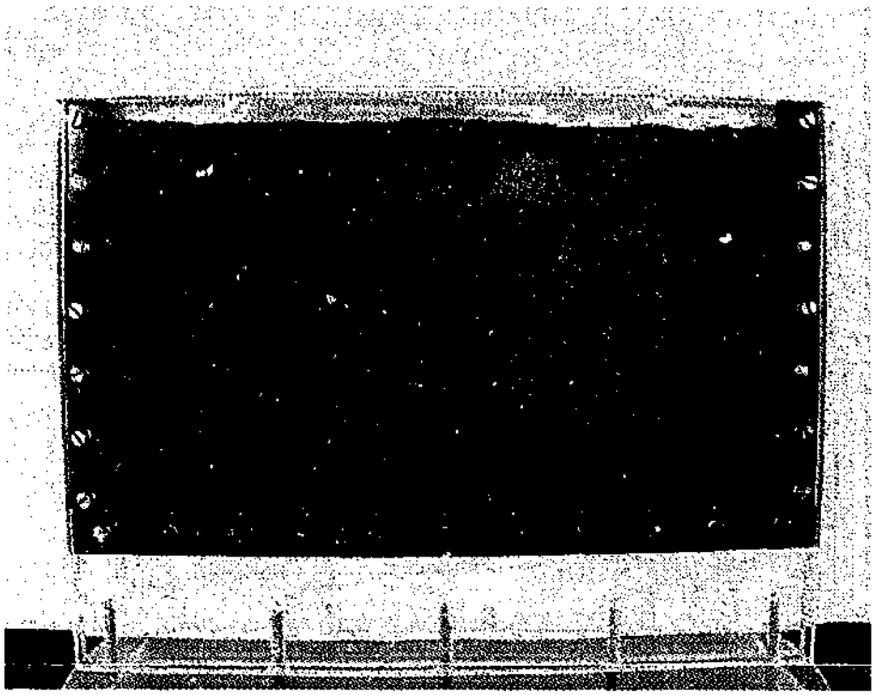

Figure 6.1: Segregation and Stratification.

is segregation between the large and small particles with more of the larger particles tending to collect at the bottom of the plates.

Makse *et al* (Makse, 1997a) performed experiments on a mixture of sand and glass beads and found that the grains formed alternating layers of sand and glass. Working with Boutreux *et. al.* (Boutreux and Degennes, 1997) they also proposed a model that describes quantitatively the segregation and stratification of particles due to particle size and/or shape. Koeppe *et. al.* (Koeppe et al., 1997) have found that the plate separation can also influence the width of the stripes in the stratification process.

The process of segregation appears to be due to the ability of the larger grains to travel faster than the smaller grains across the avalanching surface. Since they have lower inertia, the smaller grains will be more susceptible to being stopped by small bumps and gaps in the underlying grain profile. Stratification, on the other hand, appears to rely upon differences in the angles of repose, of the two materials in the mixture. If the larger particles have the smaller angle of repose, they segregate out at the bottom of the slope forming a kink in the grain profile. As the avalanching grains hit the kink, they segregate across it adding more material to it in the

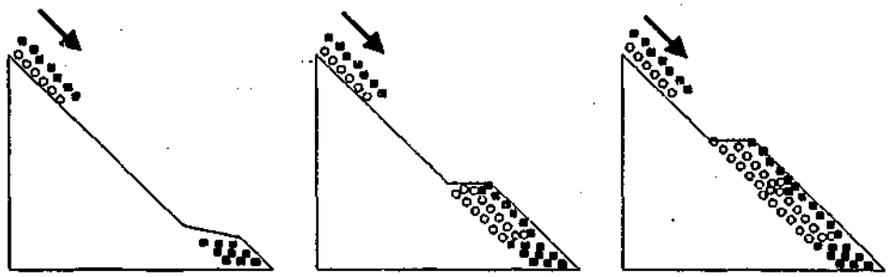

Figure 6.2: (*from left to right*)A kink in the granular profile is formed by differences in the angle of repose of the two grains. Avalanching grains hit this kink and undergo segregation. As avalanching material continues to add to the kink, it rises along the profile forming a stripe.

process. As material is added the kink, it propagates up the grain profile, forming a stripe of segregated material as it grows. Once the kink reaches the top of the pile materials spills down to the bottom of the profile again and the process repeats (Makse et al., 1998).

In this chapter, the effect of altering inter-particle force on segregation and stratification is examined. To observe these effects, a binary mixture of granular materials, in which one species was magnetisable, was used. As outlined in previous chapters, the magnetic field induces a magnetic dipole attraction between the iron particles. At low field, the dipole nature of the attraction can be safely ignored as the particles can rotate freely. At high fields however, directional effects start to dominate and the particles begin to form chains which align with the field. With these caveats in mind, we consider the effect of increasing the field to be the same as increasing inter-particle force.

6.2 Experimental

Our experiment uses two, 35cm × 21cm × 1cm, Perspex plates. These are kept apart by spacers on the bottom and sides. The spacing of the plates was not found to affect the qualitative behaviour of either the segregation or the stratification processes. However, the width of the stratification layers was influenced by the spacing. For all of the following experiments, the spacing was held constant at 4mm. A mixture of non-magnetic particles (for example bronze) and iron particles is poured into the gap between the plates by means of a funnel and rotating stopcock. The stopcock allowed the flow rate to be controlled. The granular mixture was

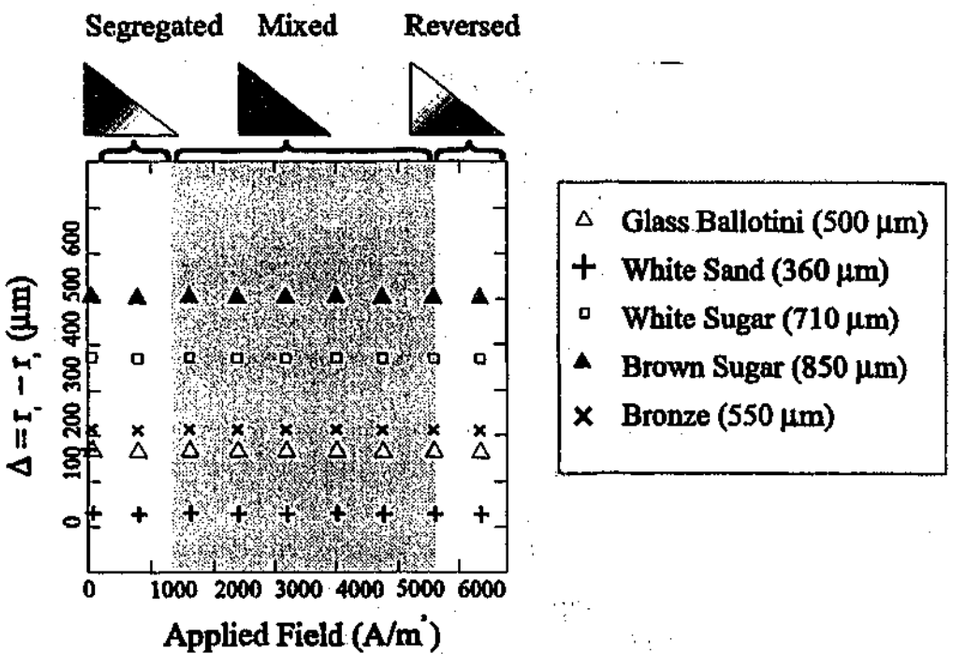

Figure 6.3: Phase diagram for segregation. In the grey region, segregation was observed to weaken and then reverse as the field was increased.

stirred prior to pouring to ensure homogeneity. To show that segregation does not occur during the pouring process, the mixture was pouring onto a flat surface. The material remained homogeneously mixed.

The experiments were performed using a variety of non-magnetic materials mixed with 350 μm iron particles. The particles were sieved into fractions differing by approximately $\pm$ 5% of the mean particle diameter. When sieving the particles, care was taken to ensure that the layer of material covering the sieve was only one particle deep. This allowed any small particles present to pass through the sieve. The material was also fluidised to remove light impurities and dust which may have become mixed in with the material.

6.3 Results and Discussion

6.3.1 Segregation

Images of the segregation and stratification were captured using a digital CCD camera[1]. Using binary mixtures of iron particles and non-magnetised particles allows the investigation of the effects of inter-particle forces upon the segregation

[1] see Appendix A for equipment details.

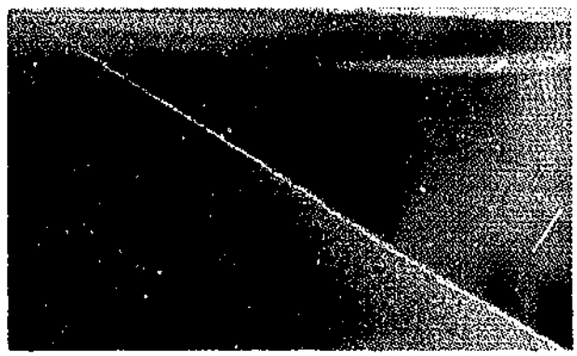

Figure 6.4: Segregation at low field.

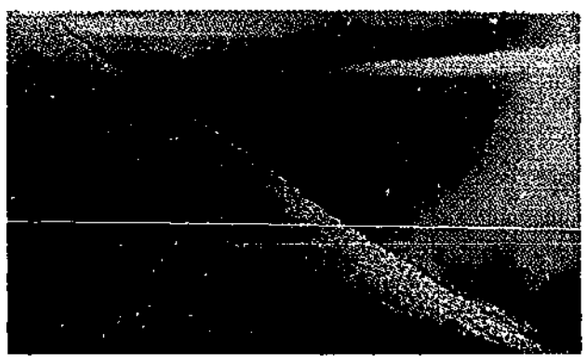

Figure 6.5: Segregation at high field.

and stratification processes. Koeppe et al. (Koeppe et al., 1997) have noted that the strength of segregation is unaffected by flow rate until a critical flow rate, f_c, is reached at which point stratification abruptly disappears. Above f_c the flow is too fast for kinks in the grain profile to form and propagate up the slope and so, continuous flow across the free surface is observed. Koeppe et al. found that the value of f_c depends upon the plate separation. In order to investigate the effect of inter-particle forces on segregation, experiments were carried out with flow rates above f_c.

Segregation was observed to occur in mixtures of sand and iron particles[2]. As the magnetic field was increased, the segregation effect was eliminated and then reversed. The experiments were repeated with other materials and similar results were found. The results of these experiments are summarised in the phase diagram (Figure 6.3). The effect of applying a magnetic field to the mixture is to reverse the segregation as can be seen in Figures 6.4 and 6.5. At low fields, the smaller

[2]The results of these experiments have been presented in (Hutton et al., 2000a) and (Hutton et al., 2000b)

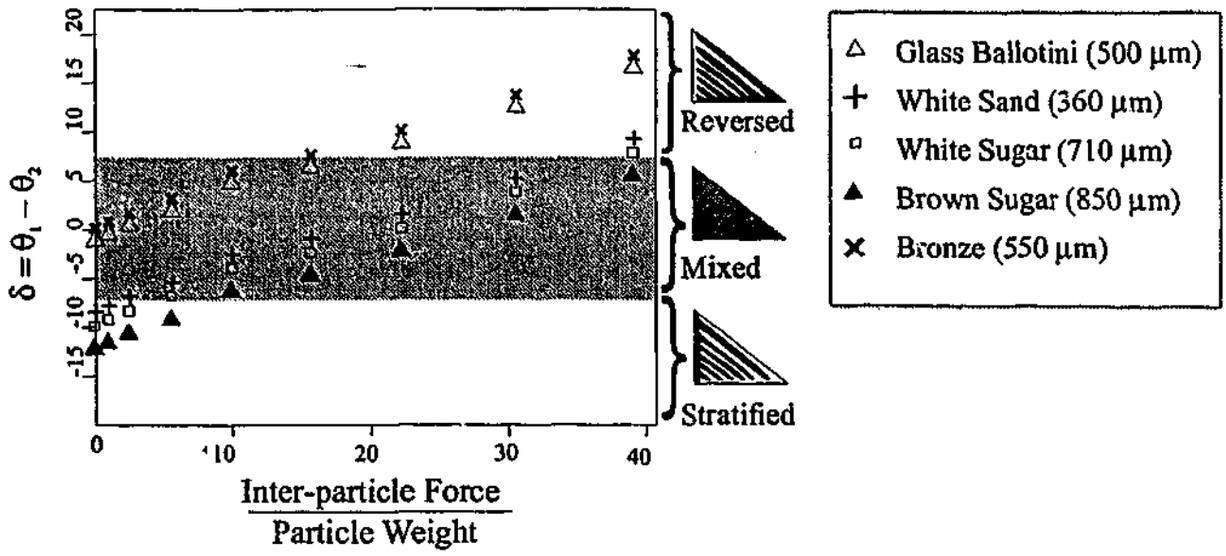

Figure 6.6: Phase diagram for stratification. In the grey region, stratification was observed to weaken and then reverse as the field was increased.

iron shot was found mostly at the top of the slope. For high fields, however, the iron was found to segregate to the bottom of the slope. For very high fields, the avalanche flow is slowed sufficiently for some stratification to occur.

6.3.2 Stratification

A second series of experiments were carried out to investigate the stratification process. Experiments were carried out using a mixture of sand and iron shot. The flow rate in these experiments was kept constant and below f_c.

Without an applied field, the sand has a larger angle of repose ($\theta = 35°$) than the iron particles ($\theta = 30°$) and so stratification occurs spontaneously during avalanching. When a magnetic field was applied, it was found that as the field increased the stratification was observed to weaken, disappear and then reverse. As the field was increased, the width of the stratified layers decreased until the material appeared well mixed. As the field increased further the width of the layers increased again (Figure 6.7, 6.8 and 6.9). However, at low field the layers consisted of sand over iron shot and at high field the iron layers formed above the sand layers. The experiments were repeated for a range of different coil voltages and materials. The results are summarised in the phase diagram (see Figure 6.6).

In our previous experiments, the angle of repose of the iron shot was observed to

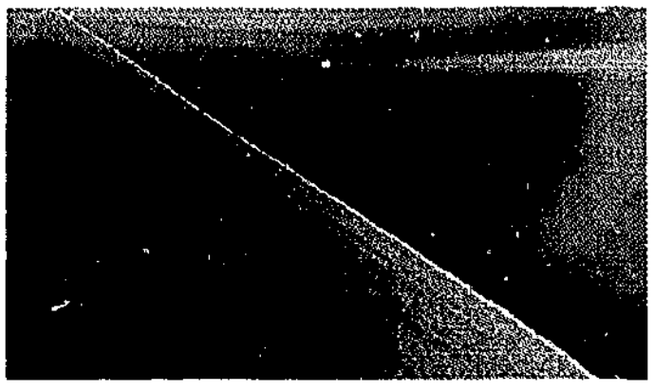

Figure 6.7: Stratification at low field (note: iron on bottom).

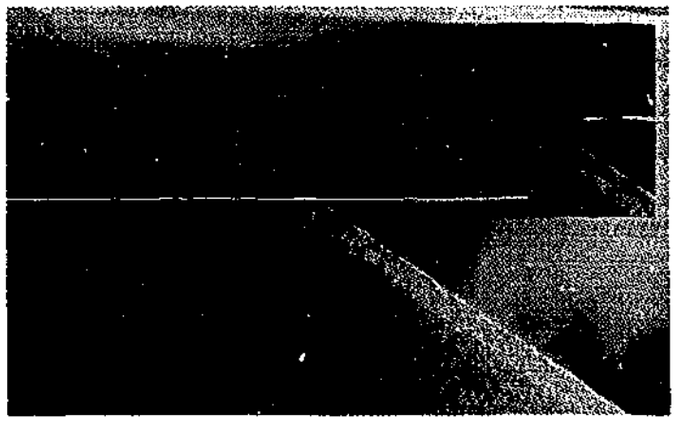

Figure 6.8: At intermediate field values mixing occurs. Inset shows magnified region of mixing.

increase with field strength. Only the sand and iron shot mixture was observed to undergo a full transition between the stratified, mixed and reversed stratified phases. It was noted that at high field the profile of grain piles become more irregular as long chains of particles form. This irregularity also translates into irregularities within the layers of grains. As material avalanches down the slope, at high field, the flow becomes more irregular. Groups of particles will often stick together impeding the flow of material from above. Eventually enough material accumulates above the jammed material for it to flow over the top. The result is that at high field the stripes become increasingly irregular.

6.3.3 Imaging

In order to obtain a better understanding of the mechanisms leading to the reversal of segregation and stratification, the process was filmed using a high-speed video camera. The frame rate used was 128 frames /second. When examining the

Figure 6.9: Reverse stratification at high field (note: iron on top).

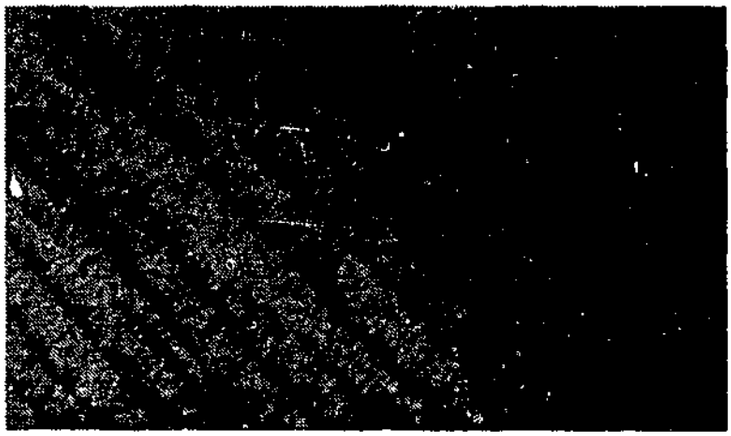

Figure 6.10: Stratification at high field - notice the irregularity in the stripes

avalanching at high field, the particles were observed to cluster together. They therefore acted like larger particles, explaining why the segregation is reversed at high field. This clustering becomes more obvious at high fields when the clusters grow to form large clumps that slide down the slope as a single mass. This can be seen in the sequence of images (see Figure 6.11).

The results from the experiments in chapter 2, where it was found that the angle of repose increased with inter-particle force, suggest a mechanism for the reversal of stratification. The stratification instability is caused by differences in the angle of repose. The angle of repose of the iron shot is initially lower than that of the sand, for example. As the field increases the differences in angle of repose is reduced as is the width of the stratification. When the angle of repose of the sand and iron are equal, no stratification is observed. When the angle of repose exceeds that of the sand, the stratification is reversed.

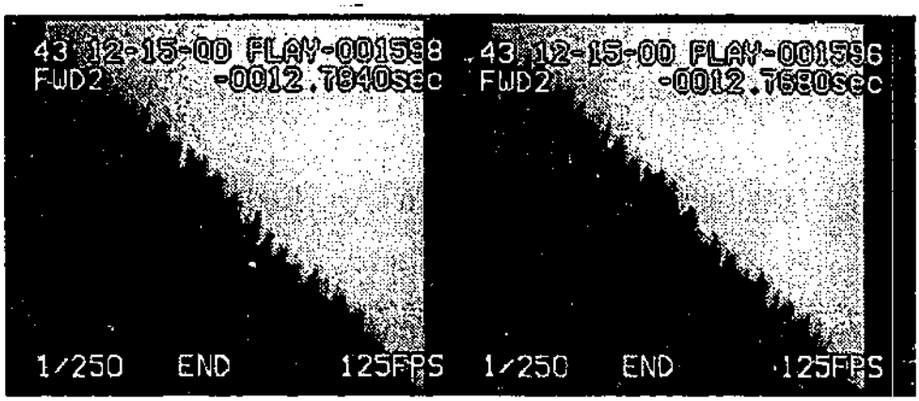

Figure 6.11: High speed sequence of avalanching at high field showing material sticking together.

While examining the segregation behaviour, it was noted that the region of material directly below the stopcock and funnel did not segregate. When material was initially poured between the plates a small pile of unsegregated material formed directly below the funnel. When the pile became large enough for shearing and continuous avalanching to occur on the free surface, segregation was observed. The shearing appears to be necessary for segregation to reverse. The reason for this may be that shearing brings the iron particles together allowing them to stick. Once they stick together, the particles act like larger particles and so segregate to the top surface of the flowing granular material. The situation is analogous to immiscible liquids. The binding of the particles appears to inhibit mixing and causes to avalanching material to "float" across the surface below.

The segregation and stratification can both be completely reversed by the presence or absence of inter-particle forces. These results have important implications for segregation and stratification in flowing powders, pastes and other materials where differences in inter-particle forces become important.

6.4 Cellular Automata Simulations

Makse et. al. (Makse et al., 1997) introduced a simple model of avalanche segregation and stratification that gives quite realistic results (see Figure 6.12). A modified version of this model was used to investigate the effect of increasing inter-particle

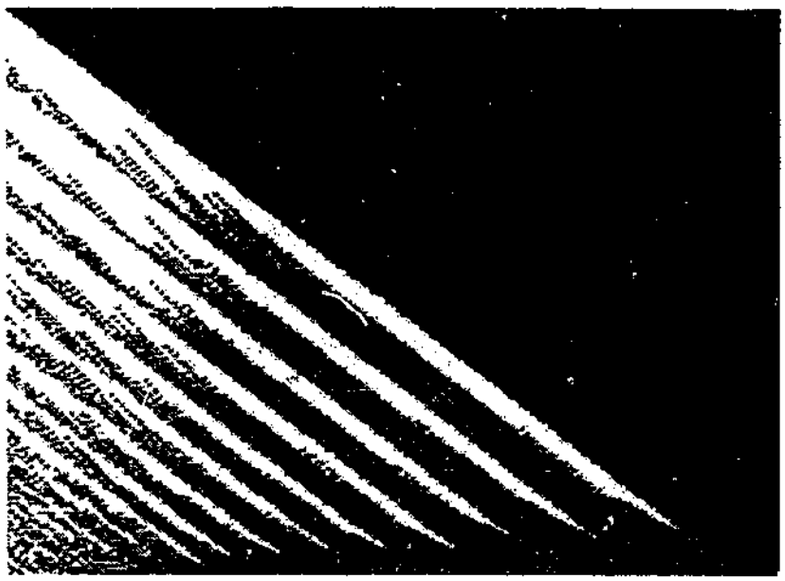

Figure 6.12: Cellular automata model of segregation and stratification. (From Makse et. al.)

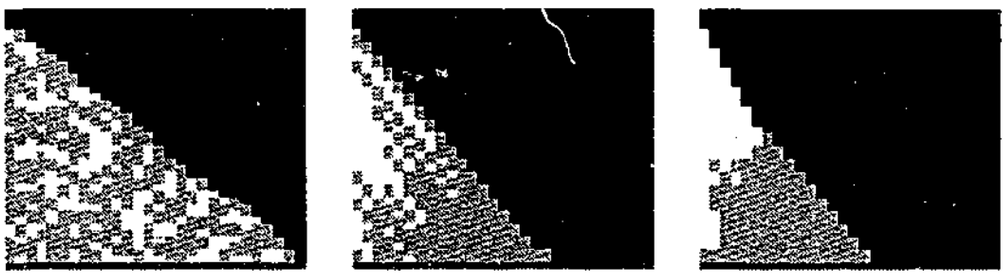

Figure 6.13: Cellular automata simulations by the author showing (from left to right) the effect of increasing inter-particle force.

force on the segregation of particles as the inter-particle force between one species of particle was altered. The results of the computer simulations, shown in Figure 6.13, agree with the experimental results[3].

6.5 Conclusion

In summary, we have found that inter-particle forces effect both stratification and segregation in avalanching granular mixtures. In view of this, the current theoretical models by Makse *et. al.* (Makse, 1997b) may need to be expanded to take into account inter-particle forces. Segregation and stratification are of particular interest to many industries, for example the manufacturing and pharmaceutical industries, where these effects are undesirable. It may be possible to alter the bulk properties of certain granular materials to prevent these effects. The main results of this investigation are the phase diagrams showing how the avalanching and segregation is effected. It was found that increasing inter-particle force could reduce and reverse both segregation and stratification in avalanching granular flows.

In the next chapter the effects of mixing and segregation in rotating drums is investigated and the influence of inter-particle forces on these processes examined.

[3] A Mathematica^{TM} notebook of the computer model is in the back of this thesis and a program listing is in Appendix C.

CHAPTER 7

Bands and Drums

Rotating drums are commonly used to mix materials. The most familiar example of this is the cement mixer. However, under certain circumstances granular mixtures can undergo spontaneous segregation when placed in a rotating drum. In this chapter, the role of inter-particle force plays in mixing and segregation in rotating drums is investigated. Segregation experiments involving three types of particles are presented. A model for axial segregation is advanced and discussed.

7.1 Overview: Segregation in Rotating Drums

A rotating drum is commonly used to turn sand and cement into an homogeneous mix, so it is surprising that the same process can lead to segregation when applied to other granular materials. As early as 1939, Oyama (Oyama, 1939) observed that a binary mixture of large and small grains spontaneously segregates into axial bands when placed in a cylindrical drum and rotated. The band patterns in segregation experiments are not, in general, stable features and over time tend to merge. In all these axial segregation experiments, the materials are also observed to segregate radially (Hill et al., 1997). For drums that are less than half full, a core of smaller, rougher particles is formed as the drum rotates (Dury et al., 1998). When a mixture of uncooked rice and split peas is placed in a cylindrical drum and rotated the mixture separates. Alternating bands of rice and peas appear along the axis of the drum from the initial homogeneous mix as the drum rotates. The width of the bands does not vary randomly, but there is a tendency for bands of a certain width to form. A distinct length scale appears to emerge throughout the system (Ball,

1999a).

The first regions of the cylinder to undergo axial segregation are at the ends of the drum. This is most probably a boundary effect, as the dynamical angle of repose in a rotating cylinder is steeper at the ends of the drum (Dury et al., 1998). Bands have been observed to move axially, merge and even occasionally divide. When two bands merge, they do not travel closer to one another. Instead, the area between bands tends to become more contaminated with particles from the surrounding bands and the region becomes more homogeneously mixed. The material between the bands then disappears and the bands merge. The merging events are relatively sudden compared with the length of time that the bands persist. This is suggestive of meta-stable progressions. The initial segregation bands are not stable in the long term and over time tend to merge until a single central band is formed in addition to the end bands.

7.1.1 Reversible Axial Segregation Patterns

In some experiments the segregation is found at high speeds and when the speed is lowered the segregation disappears (Hill and Kakalios, 1995), (Hill and Kaklois, 1994). Segregation reappears when the rotation is increased again. This reversible segregation is observed in systems where the difference in dynamical angle of repose between the mixed and segregated phases is zero for a finite rotation speed. This reversible segregation has been likened to first order phase transitions that occur in ferro-magnetic and paramagnetic systems (Hill et al., 1997).

Magnetic Resonance Imaging (or MRI) studies revealed that there are sometimes more axially segregated regions within the bulk than can be seen from the surface (see Figure 7.1). Many of these bands never reach the surface of the material as the rotation continues (Hill et al., 1997). In reversible axial segregation the segregated bands in the radial core remain. In other words, the reversible segregation only occurs at the surface and not through the bulk of the material. The fact that some axially segregated regions may exist in the bulk without ever extending to the surface implies axial segregation may not be driven exclusively by differences in angle of repose as has suggested in some models (Savage, 1992). The variation in dynamical angles of repose may even reflect variations in the bulk concentration

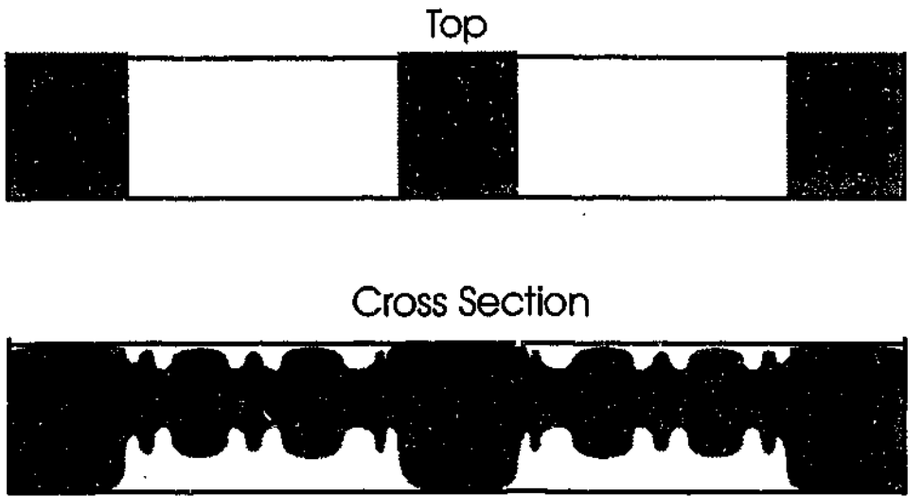

Figure 7.1: Cross section of a rotating drum with axial segregation. Magnetic resonance imaging experiments have revealed that there are often more axial bands hidden beneath the surface.

Figure 7.2: Materials with the same angle of repose but different sizes can segregate when placed in a rotating drum consisting of a series wide bellies and narrow necks. From (Ball, 1999a)

rather than cause the segregation (Hill et al., 1997).

Another aspect of axial segregation is observed in containers that are not cylindrical. Materials with the same angle of repose but different sizes can segregate when placed in a rotating drum consisting of a series of wide bellies and narrow necks as shown in Figure 7.2. If the container is less than half full small grains find their way into the necks whilst the large grains collect in the bellies. This occurs even if the angle of repose of the two materials is the same (Ball, 1999a).

In all these axial segregation experiments, the materials are also observed to segregate radially (Hill and Kakalios, 1995). For a mixture of different sized particles, the small particles form a radial core before axial segregation occurs.

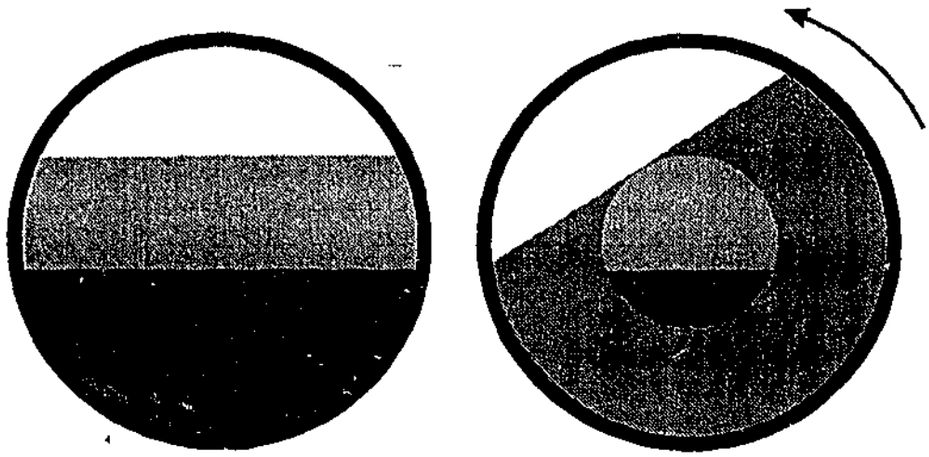

Figure 7.3: A central core of material will remain undisturbed during mixing if the drum is over half full

7.2 Experimental

Experiments were carried out to determine the effect of inter-particle force on radial and axial segregation. These experiments were conducted using the magnetic field arrangement outlined in chapter 2. For the radial segregation experiments a perspex drum of diameter 150 mm and width 10 mm was used. For axial segregation experiments a perspex drum of diameter 7 cm and length 40 cm was used. Both drums were filled with various mixtures of bronze and iron shot and placed on a pair of rollers, at the centre of the field. The roller assembly was constructed entirely out of non-magnetisable material and driven by an electric motor by means of a drive belt. This drive belt was long enough to enable the motor driving the drum to sit outside the field.

Three different binary mixtures were prepared from 600 μm diameter bronze particles and iron particles of diameters 350 μm, 600 μm and 850 μm. In each of the radial experiments, the drum was loaded with the iron particles at the bottom of the drum and bronze particles at the top. The level of loading was important in these experiments. For drums which are more than half full a central core of material will remain unmixed (see figure 7.3). For drums which are exactly half-full, little, if any, mixing will occur[1]. For this reason, the drum was filled less than halfway to allow the maximum amount of mixing to take place.

[1]Simulations demonstrating this can be found on Troy Shinbrots web page (http://sol.rutgers.edu/ shinbrot/Marwan/RollingApplet.html)

Figure 7.4: Reversal of radial segregation with increasing field

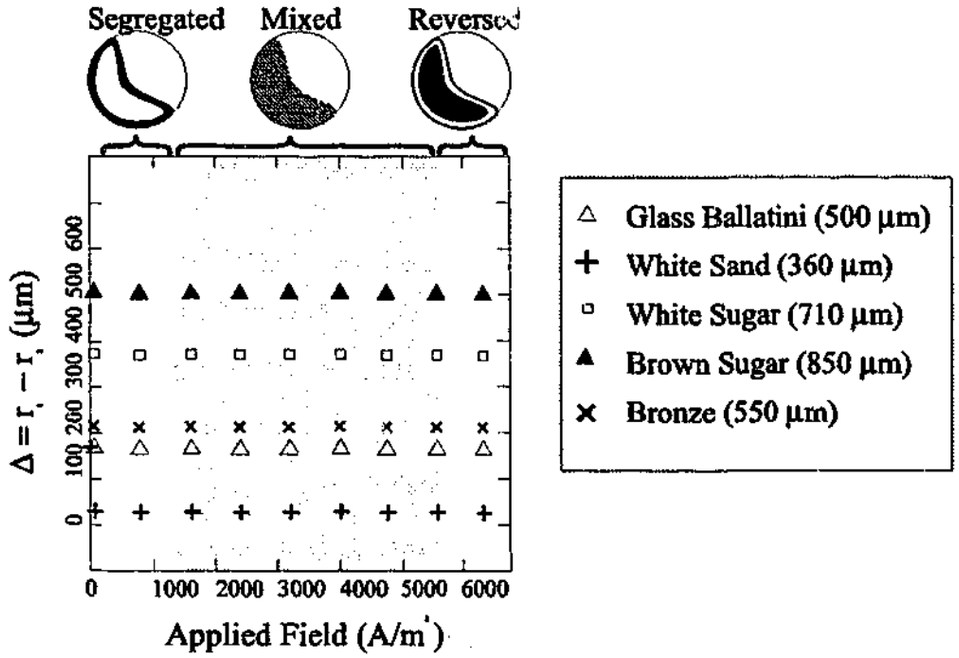

Figure 7.5: Phase diagram showing the reversal of radial segregation with increasing field. Iron shot (dark region in drum) initially segregates to the centre of the drum but, as the inter-particle force increases, slowly mixes and then segregates to the outside of the drum

7.3 Results and Discussion

7.3.1 Radial Segregation

In these experiments, the drum was rotated until radial segregation was observed[2]. The field was then increased in a stepwise manner and the effect on radial segregation observed. The results of the radial segregation experiments are summarised in the phase diagram (Figure 7.5). These results are very similar to the avalanche segregation results discussed in the previous chapter. For mixtures of 600 μm diameter bronze particles and 350 μm diameter iron particles, the iron was found to segregate to the centre. However, as the field increased the segregation was found

[2]The results of the authors experiments have been published in (Hutton et al., 2001)

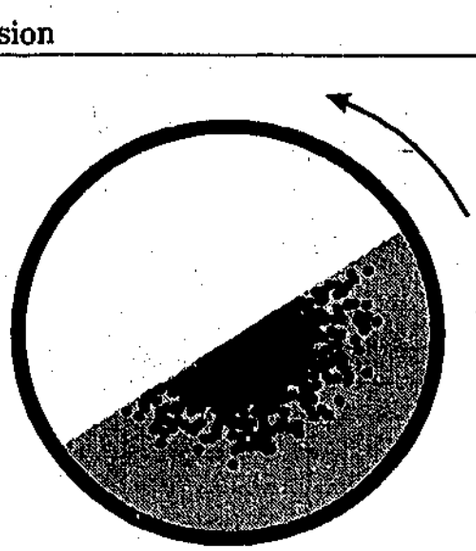

Figure 7.6: The growth of the central radially segregated region can be modelled as a diffusion limited aggregation process.

to disappear, then reverse.

The central core of the radial segregation is not sharply defined as the bands in axial segregation. It has been noted that the growth of a radial core can be considered a type of diffusion limited aggregation (Duran, 2000). Such a growth mechanism leads to a fractal like form (see Figure 7.6). Another way of looking at these results is to view the system as having two points towards which particles are attracted. One of these "attractors" is at the centre of the avalanching surface and the other at the base. As the inter-particle force is increased, the iron particles begin to stick to one another with increasing frequency and duration. The results of the segregation experiments suggest that, as the ratio of inter-particle force to weight is increased, the particles act as if they have a much larger effective particle size. Increasing the field has the effect of changing the attractor to which the iron particles are attracted. As the field is increased the iron particles wander further from the centre of the drum and the system becomes increasingly well mixed.

The field was increased still further and the mixing observed to decrease as the segregation was reversed. The results of the segregation experiments suggest that as the ratio of inter-particle force to weight is increased the particles act as if they have a much larger effective particle size. Given that altering inter-particle force or cohesion has such an effect on segregation and stratification, it seems natural to ask what effect they have on mixing.

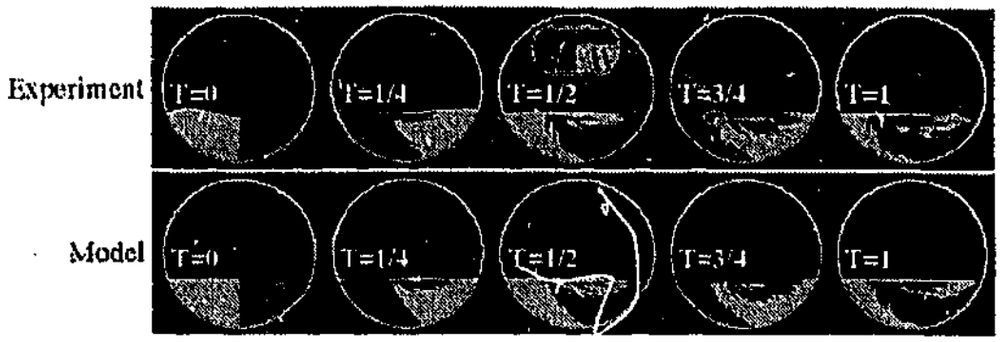

Figure 7.7: Chaotic mixing in rotating drums (from (Shinbrot et. al., 1999b)).

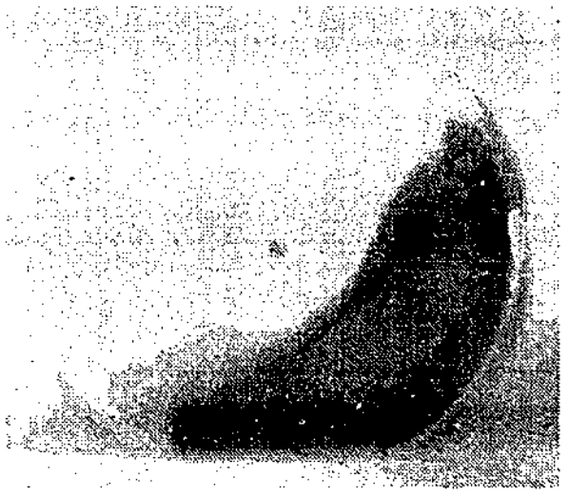

Figure 7.8: Reversal of segregation at high field.

7.3.2 Mixing

Consider a binary granular mixture composed of a fraction α of particle A and β of particle B (such that $\alpha + \beta = 1$). A mixture is defined as homogeneously mixed if on scale d if the volume d^3 is composed of the two ingredients in the correct proportions. Simulations carried out by Shinbrot *et al* (Shinbrot et al., 1999) and experiments carried out by Nasuno *et al* (Nasuno et al., 1998) have shown that increasing inter-particle forces can increase mixing by increasing slip-stick shearing in the free surface. In Shinbrot *et. al.*'s model the mixing process is described as follows. The layer of material in the upper end of free surface undergoes a slip once per slip cycle after which material continues to creep down. The lower boundary of this avalanching material is given by

$$z = f(x + A(t)f(x)) \tag{7.1}$$

where f is a function given by

$$y = f(x) = ax^2 - D \tag{7.2}$$

(the boundary between the flowing and solid body regions is therefore parabolic) and a is sawtooth function

$$A(t) = A_o \begin{cases} 1 - (2t/\epsilon) & \text{if } 0 < t|\tau| \leq \epsilon \\ (2(t-\epsilon)/(\tau-\epsilon)) - 1 & \text{if } \epsilon < |\tau| \end{cases}$$

This slip-stick flow leads to fractal striations in the mixing patterns (see Figure 7.7) and an increase in the rate of mixing. Experiments on mixing of glass particles by Nasuno *et. al.* have shown that as the size of the particles is decreased the mixing behaviour of the particles can change dramatically. Large, coarse particles are observed to undergo relatively smooth mixing, the rate of which increases linearly with time. For fine particles however the mixing becomes highly irregular with the appearance of fractal - like striations and an exponential rate of mixing. This mixing has been shown by Shinbrot to be chaotic.

The appearance of chaotic mixing is thought to be due to the appearance of cohesive forces between the grains. To test this idea, experiments were carried out using iron particles in a magnetic field. Two containers of 600 μm iron particles were painted. One group of particles was painted white and the other black. These particles were loaded into a rotating drum and mixing experiments were carried out both with and without the applied magnetic field. For low magnetic field values smooth linear mixing was observed. As the field was increased, however the surface flow became slip-stick and the mixing resembled the chaotic mixing in Shinbrots model (see Figure 7.7). Similar slip stick flows were observed in the radial segregation experiments when the inter-particle force was increased so that the material began to mix. The striations resulting from this slip stick flow can be seen in Figure 7.8.

7.3.3 Axial Segregation

The results of the axial segregation experiments are shown in Figure 7.9. The sequence shown is for 350 μ m iron particles and 600 μ m bronze particles. The

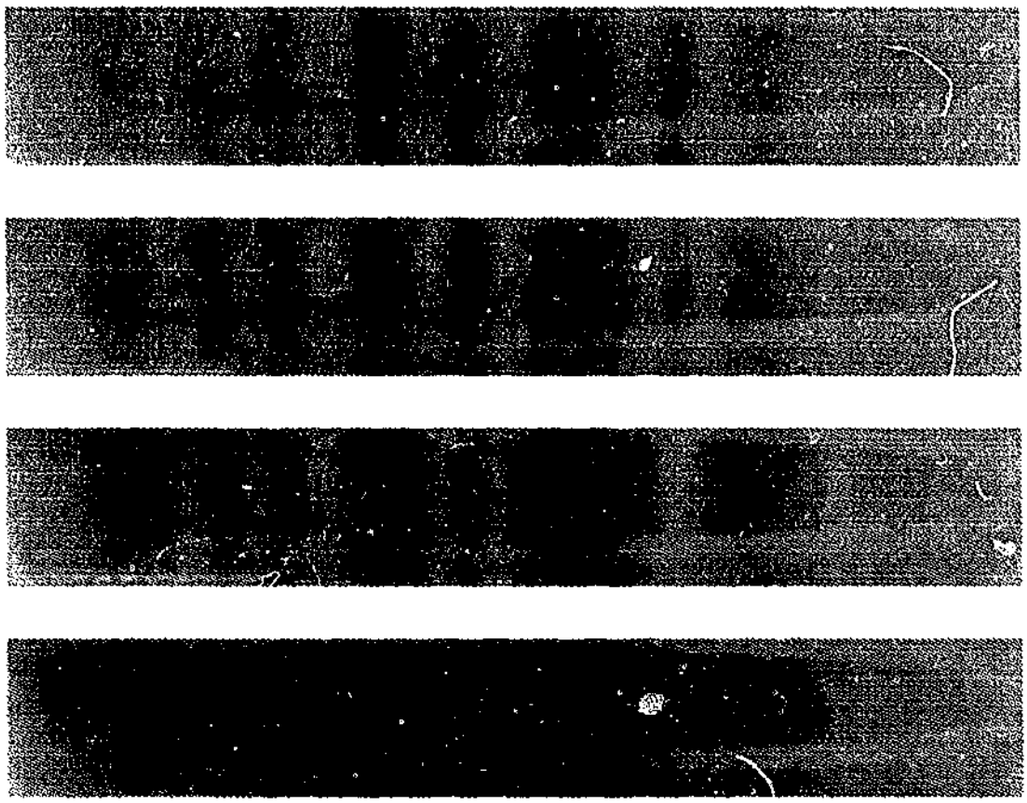

Figure 7.9: The segregation in a rotating drum for V=0, 2, 4, and 6V.

drum was rotated and the particles segregated in a matter of minutes. The magnetic field was then applied and slowly increased. The segregated bands were observed to broaden until they merged. When the field was switched off the segregated bands rapidly returned. Savage has proposed a model for axial segregation based on differences in kinetic angle between the materials in the mixture. In chapter 2, it was shown that the dynamic angle of repose increases with increasing field. It might be thought possible that for the right combination of materials a reversal of the axial segregation could be induced simply by increasing the applied field (just as avalanche segregation and stratification was reversed in the previous chapter). The situation, however is not quite that simple. Several experiments were carried out to reverse the axial segregation by changing the inter-particle force. Different mixtures of materials were tried including sand, white sugar, brown sugar and bronze. These materials were mixed with either iron shot or iron filings (which were rougher and had a higher angle of repose $\approx 38°$). In all experiments, the results were the

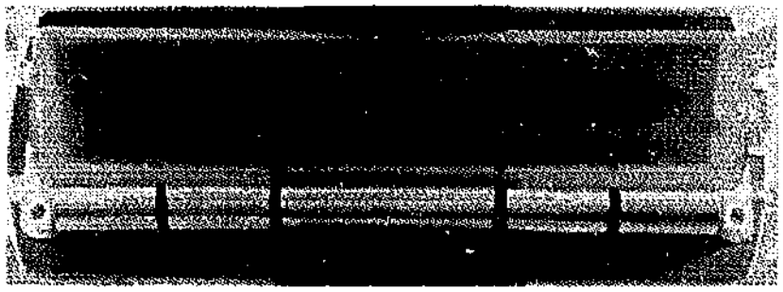

Figure 7.10: Axial segregation.

same. Axial segregation was initially observed, however, as the field increased the segregation disappeared.

7.4 An Alternative Model for Axial Segregation

Observations of test particles in the rotating drum suggest that that the larger particles are more mobile than the smaller particles. This seems reasonable since small particles will be trapped more frequently by other grains than large particles. Large particles will move more rapidly across small particles but will slow down when they collide with other large particles. The mixed state is therefore unstable. A region with a slight excess of large particles will therefore continue to accumulate large particles whereas a region with more small particles will lose large particles more rapidly as they are able to travel more quickly across it.

The critical feature of this model[3] is particle mobility. Granular materials have been observed to segregate by size, shape, surface roughness, friction and co-efficient of elastic restitution. All these properties influence mobility and so would be expected to result in segregation according to this model.

Consider the surface of the material in the drum during avalanching. The velocity of the avalanching material will decrease rapidly with depth. More mobile particles will roll over less mobile particles which will sink and so for the purposes of modelling can be ignored. The particles will move down the avalanching slope but will also move horizontally due to variations in the surface over which they roll. We can treat the fluidised surface layer as a granular gas and define a mean free path, l, and an average particle velocity, $\bar{v}$.

Let us now consider the lateral diffusion of particles across the surface. The

[3]At the time of writing, paper describing model is in preparation

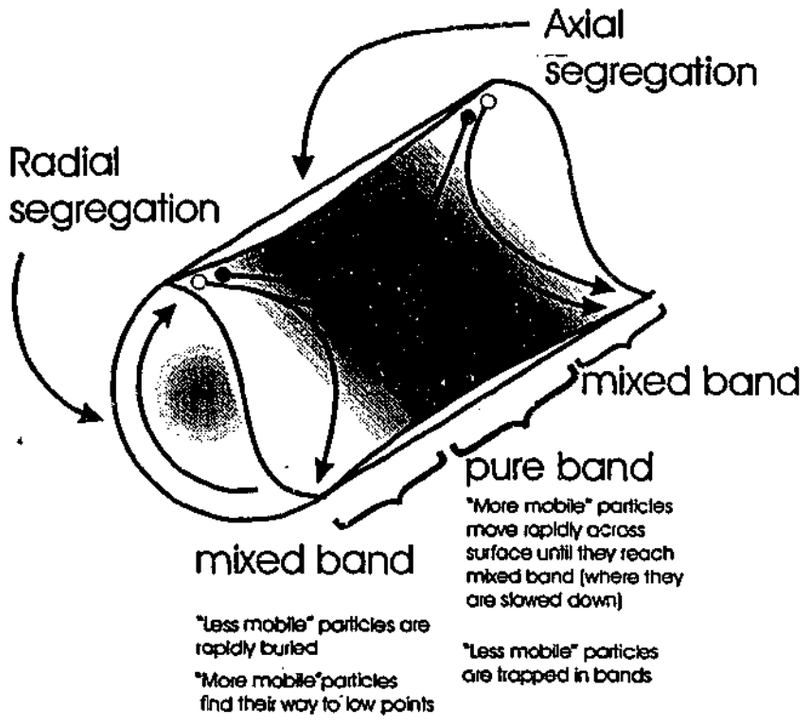

Figure 7.11: Segregation at the ends of the drum. The arrows represent the direction in which more mobile particles roll

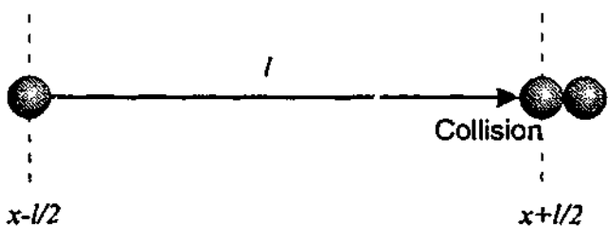

Figure 7.12: Diffusion with collisons

diffusion equation can be written in terms of the mean free path and average velocity as

$$\frac{1}{6}\frac{n_v A(\bar{v}\Delta t)}{A\Delta t} = \frac{1}{6}n_v\bar{v} \tag{7.3}$$

The flux of particles to the left $\overleftarrow{J}$ and right $\overrightarrow{J}$ are

$$\overrightarrow{J} = \frac{1}{6}(n_v - \frac{dn_v}{dx}l)\bar{v},\ \overleftarrow{J} = \frac{1}{6}(n_v + \frac{dn_v}{dx}l)\bar{v} \tag{7.4}$$

Therefore

$$J = \overrightarrow{J} - \overleftarrow{J} = -\frac{1}{3}l\bar{v}\frac{dn_v}{dx} = -D\frac{dn_v}{dx} \tag{7.5}$$

$$D = -\frac{1}{3}\bar{v}l \tag{7.6}$$

The mean free path can written as

$$l = \frac{\bar{v}\Delta t}{n\pi(2r)^2 v_{rel}\Delta t} \tag{7.7}$$

and so D becomes

$$D = -\frac{1}{3} \times \bar{v}\frac{\bar{v}\Delta t}{n\pi(2r)^2 v_{rel}\Delta t} = \frac{-\bar{v}^2}{3n\pi(2r)^2 v_{rel}} \tag{7.8}$$

The velocity will be influenced by the energy gained by avalanching across the surface under gravity and the energy lost through inelastic collisions. We can therefore write $\bar{v}$ as

$$\bar{v} = \sqrt{2gh - 2(\Delta K.E.)/m} \tag{7.9}$$

substituting for $\bar{v}^2$ we get

$$D = -\frac{1}{3}\frac{2gh}{n\pi(2r)^2 v_{rel}} + \frac{1}{3}\frac{2\Delta K.E.}{mn\pi(2r)^2 v_{rel}} = -D_1 + D_2 \tag{7.10}$$

D can therefore be seen as the sum of two competing processes D_1 and D_2. D_1 is diffusion driven by differences in surface height and acts in the direction of decreasing concentration. D_2 is due to dissipative collisions and acts in the direction of increasing concentration. It is the competition between these two processes which gives rise the axial bands. The rotating drum can be divided into two regions. The "solid phase", which is below the surface and undergoes rigid body rotation. The free surface undergoes more or less continuous flow and can be thought of as a "liquid phase". The liquid phase consists of a few layers at the free surface with the velocity of the particles decreasing very rapidly with depth. The avalanching surface can be thought of as consisting of several overlaid granular sheets. The upper layers of these sheets will form broad segregated stripes travelling at constant velocities. From this point of view, vertical (or radial) segregation between successive sheets occurs first, followed by axial segregation. Deeper layers will, however, be less mobile and undergo more collisions. D_2 therefore increase with depth and the wavelength of the bands of less mobile particles will be smaller (see Figure 7.1).

7.4.1 Three Particle Experiments

Experiments were carried out using three different particle types. Glass Ballotini of sizes $0.25\mu m$, $0.5\mu m$ and $0.7\mu m$ was loaded in layers into the drum (small on the bottom, medium in the middle and large on the top). The Ballotini was coloured with food dye. The drum was allowed to rotate so that continuous flow occurs at the surface. Initially stripes formed in no particular order, but as the system began to settle down the stripes began to align themselves so that the medium sized particles formed bands between the large and the small. Radial segregation was also observed to form in the same sequence. The rotational velocity did not have to be uniform for this segregation to occur. The results also did not appear to be dependent upon precise levelling of the container.

Observing the stripe development carefully, it was noticed that the shape surface changed as the axial segregation developed. This is consistent with diffusion-collision model. The bands with three particle sizes present, were observed to have higher angles of repose than the bands with two or one particle size present (This can be seen in Figures 7.13 and 7.14).

7.5 Conclusions

These experiments outlined in this chapter and the previous chapter, demonstrate that inter-particle forces can cause significant changes in the segregation and stratification behaviour of granular mixtures. In the experiments outlined in this chapter, it was found that radial segregation undergoes increasing mixing and then reversal of segregation. This parallels the avalanche segregation results found in the previous chapter. Axial segregation might have been expected to reverse since altering the inter-particle force alters the dynamical angle of repose (as was found in chapter 2). This, however, was not observed in these experiments. After consideration of these results, a new model of axial segregation has been proposed. In this model, the alteration of the angle of repose of the surface arises from differences in grain mobility. The model explains the bands that have been observed to exist beneath the avalanching surface in magnetic resonance imaging experiments. It should be possible to make predictions from the model that can be tested by experiment.

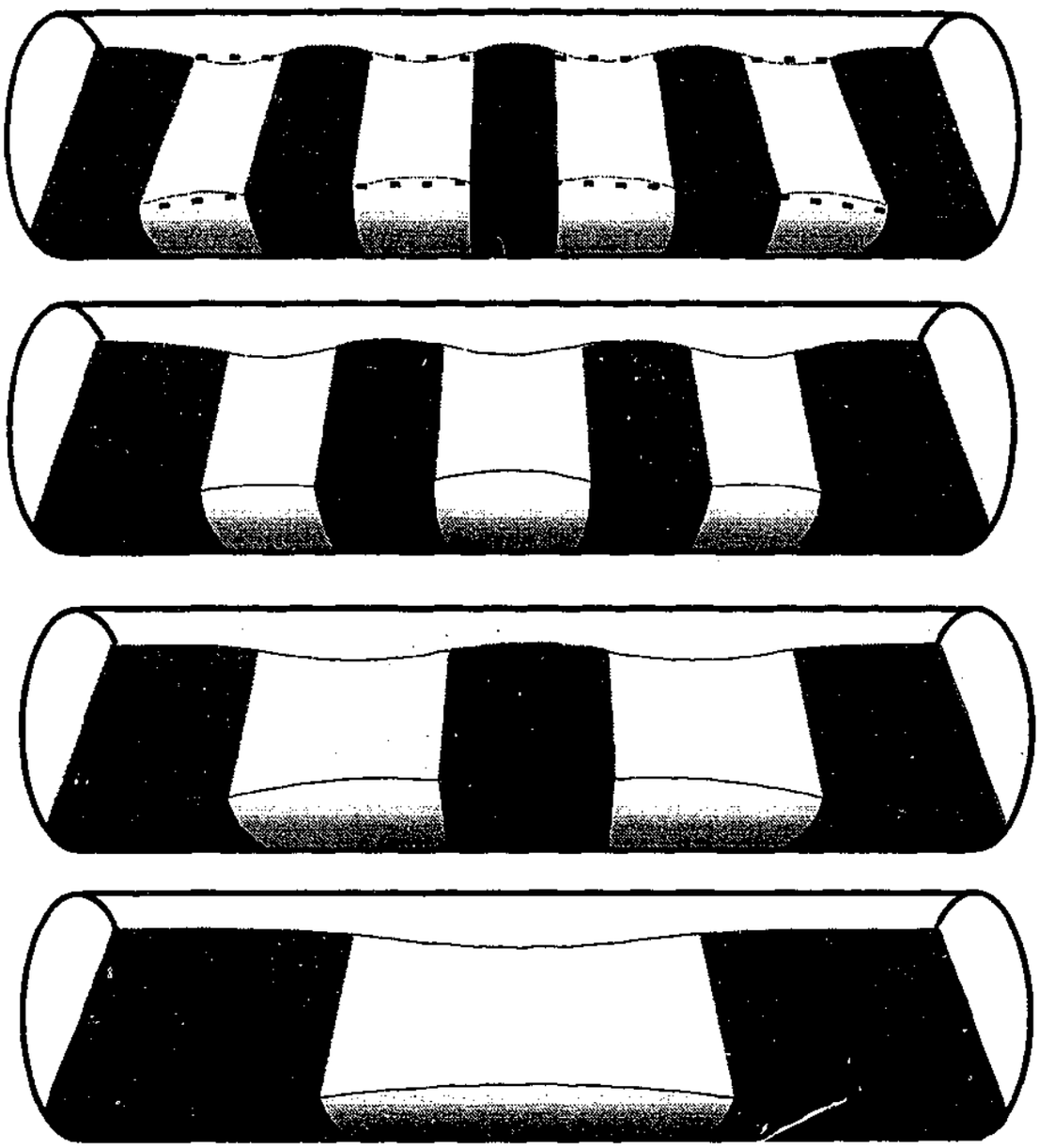

Figure 7.13: Axial segregation for two particle experiments showing how the kinetic angle differs with the bands. The more mobile particles (grey) will segregate to the ends.

Figure 7.14: End on view of three particle segregation experiments

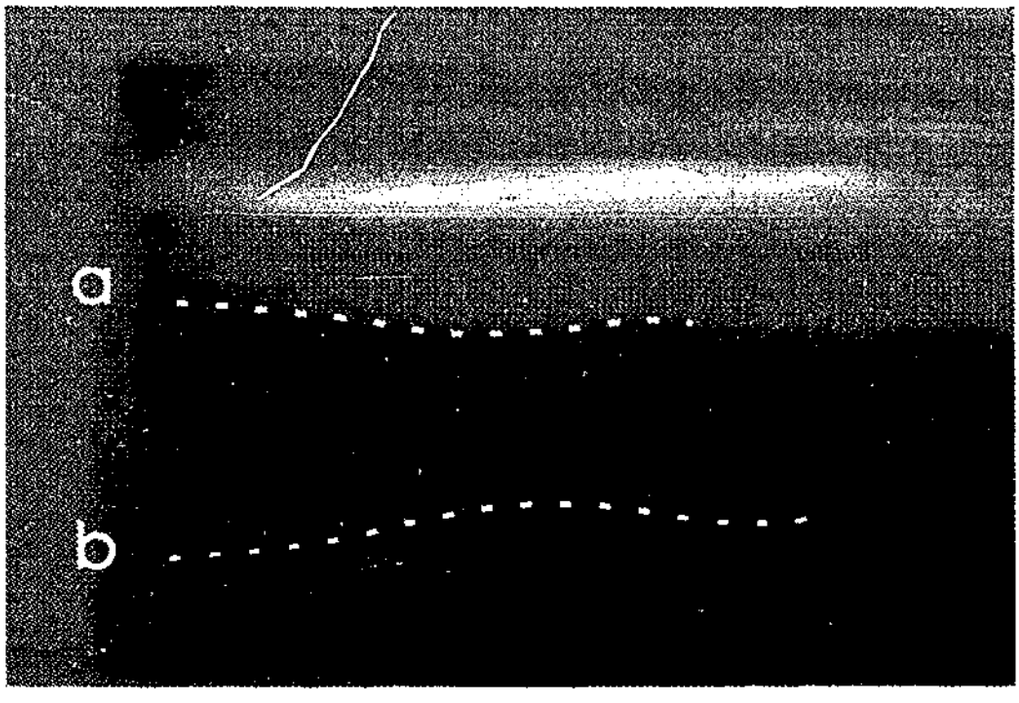

Figure 7.15: Three particle experiments showing the curving toward the ends of the drum

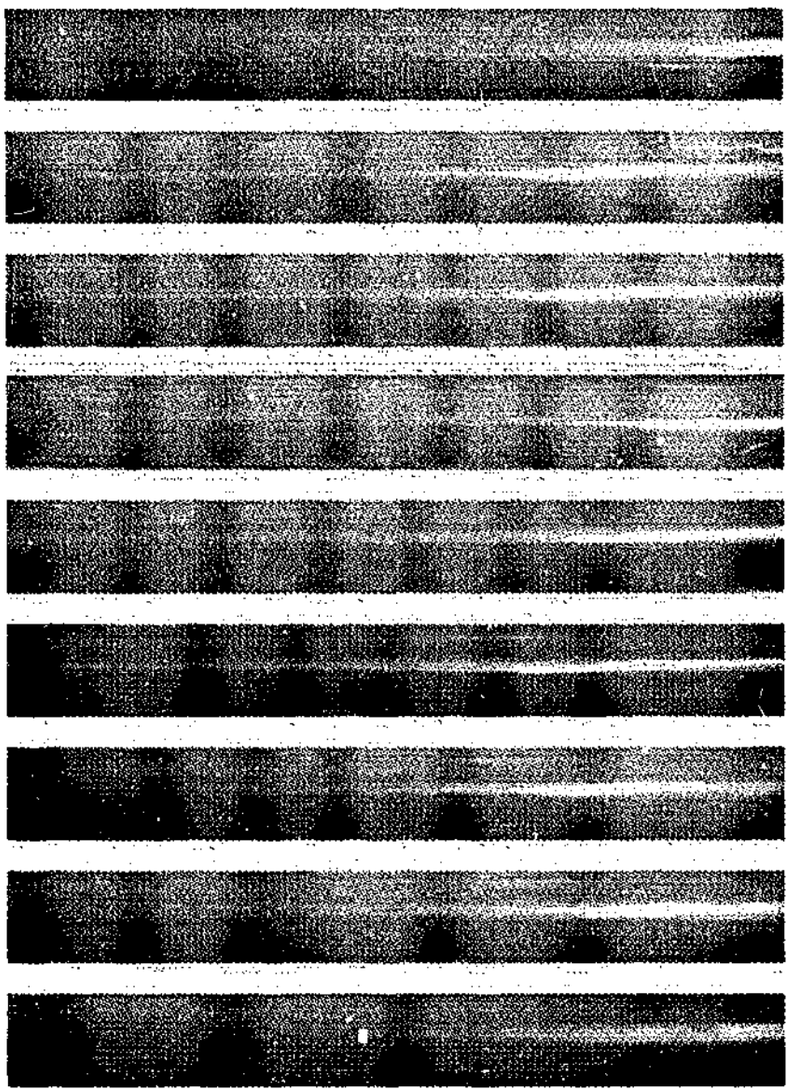

Figure 7.16: A time series for three particle axial segregation experiments. The images were taken at half-hour intervals.

Chapter 8

Conclusion

During these investigations, various aspects of self-organisation in granular materials, have been observed and analysed. A novel means of studying the effect of altering inter-particle forces in granular media has been introduced. By considering the behaviour of both magnetic and mixtures of magnetic and non-magnetic materials in a magnetic field, it has been possible to investigate how inter-particle force influences the behaviour of granular materials. These experiments give new insights into the powders and pastes and other particulate materials where inter-particle forces play an important role in the materials dynamics.

8.1 What Has Been Learned

The method of investigating the effects of inter-particle force on particulate materials introduced in this research allows the effect of inter-particle force to be investigated in isolation from other factors. This method was used to study the effects of inter-particle force on the angle of repose. The poured static angle of repose was found to increase linearly with inter-particle force. This was accompanied by an alteration of the geometry of the granular profile. The fractal dimension of the profile was found to increase with applied field. This raises questions as to how robust the self-organised critical state described by Bak *et. al* (Bak et al., 1987) is. Experiments on the dynamic angle of repose also reveal a linear increase with increasing inter-particle force.

Experiments were also conducted to investigate how the void fraction is affected

by inter-particle forces. It was found that the void fraction increased with inter-particle force and that it depended *only* on the ratio of inter-particle force to particle weight, F_{ip}/mg. The indications are that this is a universal phenomenon and applies to other non-magnetic systems.

Hydrodynamic models have been put forward to attempt to explain the behaviour of fluidised granular matter. Such models have been mostly unsuccessful. The results of the experiments in chapter 4 demonstrate why this is so. Inter-particle forces are responsible for the suppression of the bubbling behaviour in fluid beds. They cannot be ignored when looking at the behaviour of fluidised granular matter. By altering the inter-particle force, a transition from Geldart powder group B to group A behaviour was observed.

Experiments were carried out on pattern formation on vertically vibrated granular layers. The effect of adding and altering inter-particle forces on the pattern formation process was examined. Inter-particle force was found to suppress pattern formation over a wide range of frequencies. For vibrational frequencies of between approximately 23 Hz and 30 Hz however, it was found that increasing the inter-particle force has a similar effect to altering the vibration amplitude.

The effect of inter-particle force on mixing and segregation was also examined. It was found that inter-particle force could significantly alter-the mixing and/or segregation behaviour. Inter-particle force has recently been shown to increase mixing. The experiments described in this thesis have demonstrated that, under certain circumstances, inter-particle force can also increase segregation. It has been demonstrated that segregation and stratification can be reduced and even reversed by changes in inter-particle force. This suggests that insights gained from mixing, segregation and stratification experiments carried out on large particles, cannot be applied to fine powders where van der Waals forces are likely to have a significant influence. Finally, a model of axial segregation in rotating drums of granular materials was presented which involves competition between dissipative collisions and diffusive behaviour.

8.2 Directions for Future Work

Like most preliminary investigations, this research has left many unanswered questions about the range and extent of the effects that inter-particle forces have on the behaviour of granular matter. Many important questions remain unanswered and there remain many promising avenues for future research. For example:

1. **Measurement methods and angle of repose.** It would be interesting to repeat the experiments outlined in chapter 2 using different methods for measuring the angle of repose. In particular it would be interesting to perform experiments using the draining crater method to measure the angle of repose rather than the method used in our experiments. This would eliminate problems associated with inertial effects in the creation of the slope.
2. **Avalanche statistics** It would be very interesting to look at how avalanching statistics vary with inter-particle force. Can self- organised criticality be observed? How is the critical state affected by altering inter-particle force? These are questions such experiments could answer[1]. Consider a vibrationally isolated plate on to which grains of iron shot are dropped one at a time (see Figure 8.1). The grains are dropped, one at a time, by means of a "lotto" machine[2] and avalanches recorded by means of a imaging system which calculated the size of the avalanches from changes in the piles profile. The fractal dimension of the profile could be examined as a function of inter-particle force and related to the avalanche statistics. This experiment could give insights into the nature of self-organised criticality, the formation of granular piles and the nature of avalanches and mudslides etc.
3. **Pattern experiments** Some improvements to our shaking experiments could improve the results obtained in our pattern forming experiments. Using a lever with one arm attached to the drive shaft of the shaker and the other

[1] These experiments were actually begun but, unfortunately in order to obtain reasonable statistics the experiments will need to be carried out for many months and probably years to capture sufficient statistics on rare large avalanches. Because of this, there has been insufficient time to complete these experiments and so they were not included in this research. A Matrox program designed to count the avalanches is provided in appendix B

[2] This was essentially a wheel with a hole in it that was large enough to take only a single particle. The wheel was rotated horizontally above a second hole in the base of a container of 1600 μm iron particles. When the two holes aligned (once per rotation) a single particle was allowed to fall.

arm attached to the motor, would allow us to increase the amplitude of the vibrations. This would make it possible to access more patterns. This may enable us to obtain the patterns predicted by Shinbrot (Shinbrot, 1997), but not yet seen by experiment. It would also be interesting to study, in a systematic way, the effect of inter-particle forces on individual oscillons[3].

4. **Axial segregation** Several experiments could be performed to further test the model for axial segregation. It would be interesting to carry out experiments where the end conditions of the drums were altered (see Figure 8.2). The ends of the drum could be designed so that they can rotate relative to the rest of the drum. Experiments could then be carried out to see the effect on segregation if the ends of the drum were to be rotated at different rates (and/or directions) to the drum itself. It would also be interesting to measure the velocities of the avalanching particles in the bands (either using high-speed video techniques or laser Doppler interferometry).
5. **Flow and fracture dynamics** Experiments carried out by Baxter et al. (Baxter et al., 1989) on density waves in flows through a hopper, have suggested that density waves only occur in flows of rough grains. They suggest that there is a transition between smooth flow and density waves for a critical value of surface roughness. This could be investigated using an applied magnetic field and magnetisable particles to simulate the surface friction. Also fracture mechanics [4] could be examined as a function of inter-particle force. A container packed with iron shot in a magnetic field could be imaged as the bottom of the container is removed and the material allowed to fall.
6. **The Brazil nut effect** The Brazil and Hex nut effects could be examined to see what effect inter-particle forces play in the phenomenon. The effect of friction and inter-particle forces between the grains, the objects being segregated and the container walls could all be studied.
7. **Mixing and stirring** Using the techniques outlined in chapters 5 and 6 it would be interesting to conduct mixing experiments involving mixing in

[3]Unfortunately the apparatus used in the authors experiments was not stable enough to study oscillon dynamics in detail.

[4]See Duran (Duran, 2000) chapter 4.

containers with different geometries. It would also be interesting to determine the effects of stirring on mixing and how inter-particle forces effect the rate of mixing.

8. **Stress experiments** The effect on stress patterns within granular materials on the inter-particle forces could be examined using bi-refringent[5] disks rimmed with iron or some other magnetic material. Experiments were carried out using iron shot and the stress measured using carbon paper. Unfortunately these experiments were not conclusive as the impressions on the carbon paper were either too faint to make out or too uniform to determine any structure. It is possible that experiments using larger particles and/or less dense materials coated in a magnetisable material would yield better results.
9. **Bubbling experiments** Much more research is needed into the role inter-particle forces play in fluidised beds. Experiments could be carried out on the other transitions[6]. Ideally, it would be useful to image 3D bubbling using x-rays or some other means. Wake fraction measurements could then be taken to see what the major influencing factors are.
10. **Relaxation and inter-particle force** It would be interesting to look at the relaxation processes and inter-particle forces. Experiments could be carried out on vibrated collections of particles to see how increasing inter-particle forces alters the relaxation time and final packing densities of the particles.

8.3 Conclusion

Our experiments have demonstrated that granular matter exhibits many of the features of a complex system. These include emergent behaviour such as the appearance of a well-defined angle of repose (chapter 2) and bubbling (chapter 4). Self-organisation such as the appearance of stratification in avalanches (chapter 6) and axial segregation in rotating drums (chapter7). Pattern formation (chapter 5) and the appearance of universal behaviours (chapter 3).

Viewing granular materials as an example of complex system suggests new avenues

[5]For similar experiments (not involving inter-particle forces) see (da Silva and Rajchenbach, 2000).

[6]Such experiments are already under way in the Chemical Engineering department at Monash University.

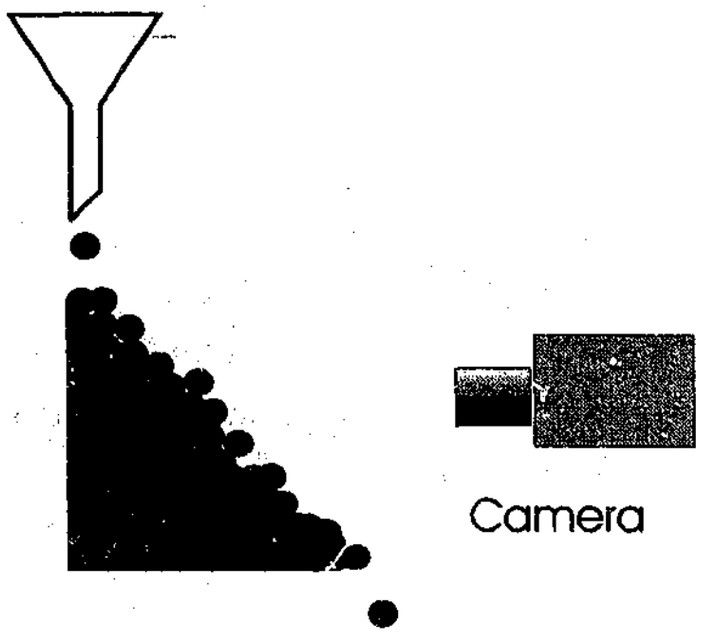

Figure 8.1: Avalanche experiment: By measuring changes in the granular profile the size of the avalanches can be determined.

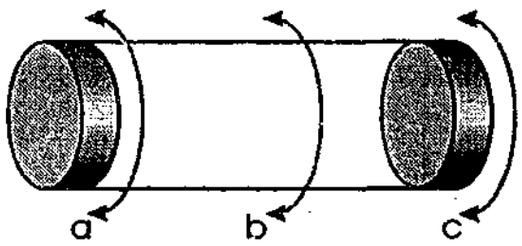

Figure 8.2: The ends of the rotating drum could be made to rotate independently of the barrel of the drum.

of investigation both for granular materials and for complex systems in general. For example, here are a few interesting questions to consider.

1. What features of a granular system are independent of the history of the system?
2. How do the macroscopic features of granular dynamics "emerge" from the microscopic physics
3. Under what conditions are granular dynamics dependent on the history of the system?
4. What are the attractor states and on what variables do they depend?

5. Is it the random nature of the impacts in vibrated granular layers which leads to the pattern formation or is it the homogeneous nature of the spreading of the particles?
6. the flow of granular materials across a surface or down a slope is strongly dependent on depth. This is similar to the definition of viscosity in liquids. To what extent can flowing granular materials be likened to viscous fluids?
7. can the observation of travelling waves and reversible axial segregation be explained in terms of the model in chapter 7?

Ultimately answers to these and other questions may give a better understanding of other complex self-organising systems for which granular materials have been used as a metaphor.

Appendix A

Equipment and Materials

Material	Sizes	Supplier
Brass Shot	550-600 μm 600-710 μm	Sintec Australia Pty Ltd Spherical bronze
Iron Shot	350-425 μm 800-900 μm 1.6-1.8 mm	Sintec Australia Pty Ltd
Iron Filing	0.5 -0.71 mm	"Technical" brand batch 15007/2 apparent density 4.9 g/cm mesh 5-12
White Sugar	710 μm	CSR Sugar Ground Floor 18 Little Cribb Street Milton QLD 4064 Australia PO Box 2059 Milton QLD 4064 Australia
Brown Sugar	850 μm	CSR Sugar(see above)
Sand	360 μm	From squeaky beach Wilsons Promitory Victoria (So named because it squeaks)

Table A.1: Materials Used and Suppliers

Equipment	Supplier
Signal generator	Wavetek 20 MHz pulse/function Generator model 191 San Diago CA
Power supply (for Helmholtz coils)	Power supply ± 35V DC (70 V_{pp}) total
Shaker amplifier	AEM6506 Power Amplifier Published Jan 1987 - Australian Electronics Monthly
Still photographs	Olympus *CAMEDIA* 1.4 million pixel progressive CCD camera model no. C1400L
Image recognition and analysis	Matrox image analysis system
High speed video	Kodak Motion Corder Analyzer (SR series) 500 frames/second 8 bit full NTSC or PAL grey scale 256 level
Sieves	Endecotts Pty Ltd London England Frame material: Brass Mesh material: Bronze
Subsonic Actuator (Shaker motor)	Jacar Electronics Catalogue number XC-1008 Aura Shaker Motor Assembly Max force: 0.5 foot pounds per watt Rated power:18 watts continuous RMS Size 120(W) × 40(H)mm weights 1.5 kgs

Table A.2: Equipment Used and Suppliers

Appendix B

Matrox Programs

B.1 Matrox Programs

```
-------------------------------------------------
THIS PROGRAM TAKES TWO IMAGES, THRESHOLDS THEM
AND LOOKS AT THE DIFFERENCES BETWEEN THEM.  IT
IS USED TO DETERMINE THE SCALE OF AVALANCHES
IN GRANULAR MATERIALS
-------------------------------------------------
FIRST WE CLEAR THE FRAME BUFFERS
-------------------------------------------------
clear 4 0
clear 5 0
-------------------------------------------------
GRAB AND THRESHOLD IMAGE 1 AND STORE
-------------------------------------------------
opmode 2 4
outpath 0 -1 0 0
inmode 1
chan 0
sync 1 0
video 1 1
snap 0
pause
-------------------------------------------------
```

```
 GRAB AND THRESHOLD IMAGE 2 AND STORE
 ------------------------------------------------

snap 1

outpath 1 -1 0 0

 ------------------------------------------------

 MOD SUBTRACT IMAGE2 FROM IMA   1

 ------------------------------------------------

interimage 0 1 2 1

absolute 2 2

pause

 ------------------------------------------------

 STORE RESULTS (AS A NUMBER) IN OUTPUT FILE

 ------------------------------------------------

histsample 1000 25 2 1

opmode 0 2

todisk data.out

 ------------------------------------------------

 RETURN UNTIL KEYPRESSED

 ------------------------------------------------

repeat 1 10
```

APPENDIX C

Mathematica Programs

The programs that appear here also appear on the accompanying disk.

C.1 Christmas Tree Effect

C.1.1 Stratification Program

This program was written by the author to model the effects of segregation and stratification as a function of increasing inter-particle force. It is based on the model by Makse et. al. (Makse et al., 1997) but has been modified to take into account the effects of inter-particle force. Inter-particle force can be altered in this model by altering the value of "field" which can take on a value of 1, 2 or 3. The model demonstrates the increase in mixing as the field is increased. Stratification can be observed by beginning with the field at 3 and "relaxing" (ie reducing the field to 1) the pile every time a grain reaches the bottom of the pile[1].

```
HPP[n_,t_]:=Module[{grain,RND,MvonN,initConf},
    field := 2;
    RND := field-(field+1)*Random[Integer,{0,1}];
    full:=-1|-2|f|1|2|3;
    grain[_,_,_,_,_,_,_,_,_,_,_,_,_]:=0;
    grain[x,_,_,_,_,_,_,_,_,_,_,_,_]:=x;
    grain[0,x,_,0,_,_,_,_,_,0,_,_,_]:=RND;
    grain[f,_,_,_,_,_,_,_,_,_,_,_,_]:=f;
    grain[0,-1,_,_,_,_,_,_,_,_,_,_,_]:=-1;
    grain[0,_,_,0,-1,_,_,full,_,_,_,_,_]:=-1;
```

[1] see Makse et. al. (Makse et al., 1997) for details

```
grain[-1,_,_,full,_,_,full,_,_,_,_,_]:=-1;
grain[0,_,-1,0,_,_,_,full,_,0,_,_]:=-1;
grain[-1,_,_,0,_,_,_,_,_,_,_,_]:=-2;
grain[-2,-1,_,0,_,_,_,_,_,_,_,_]:=-1;
grain[-2,_,_,-1,_,_,_,_,_,full,_,_]:=-2;

grain[0,1,_,_,_,_,_,_,_,_,_,_]:=1;
grain[0,_,_,0,1,_,_,full,_,_,_,_]:=1;
grain[1,_,_,full,_,_,full,_,_,_,_,_]:=1;

grain[0,2,_,_,_,_,_,_,_,_,_,_]:=2;
grain[0,0,_,0,full,_,_,_,2,_,_,_]:=2;
grain[2,_,full,full,_,_,full,_,_,_,full,_]:=2;
grain[2,_,full,full,_,_,full,_,_,_,0,_]:=2;
grain[2,_,full,full,_,_,0,_,_,_,full,_]:=2;
grain[2,_,0,full,_,_,full,_,_,_,full,_]:=2;
grain[2,_,full,full,_,_,0,_,_,_,0,_]:=2;
grain[2,_,0,full,_,_,full,_,_,_,0,_]:=2;
grain[2,_,0,full,_,_,0,_,_,_,full,_]:=2;

grain[0,3,_,_,_,_,_,_,_,_,_,_]:=3;
grain[0,0,_,0,full,_,_,_,3,0,_,_]:=3;

grain[3,_,full,full,_,_,full,_,_,_,full,_]:=3;
grain[3,_,full,full,_,_,full,_,_,_,0,_]:=3;
grain[3,_,full,full,_,_,0,_,_,_,full,_]:=3;
grain[3,_,0,full,_,_,full,_,_,_,full,_]:=3;
grain[3,_,full,full,_,_,0,_,_,_,0,_]:=3;
grain[3,_,0,full,_,_,full,_,_,_,0,_]:=3;
grain[3,_,0,full,_,_,0,_,_,_,full,_]:=3;
grain[3,_,0,full,_,_,0,_,_,_,_,full]:=3;
```

```
MvonN[func__,lat_]:=
      MapThread[
        func,(RotateRight[lat,#1]&)/@
{{0,0},{1,0},{0,-1},{-1,0},{0,1},{1,-1},
{-1,-1},{-1,1}, {1, 1},{-2,0},{-2,-1}, {-3,-1}},2];
initConf=Start;;
FixedPointList[MvonN[grain,#1]&,initConf,t]]

ShowHPP[list_,
    opts___]:=(
      Show[Graphics[
            RasterArray[
              Reverse[list\[LeftDoubleBracket]#1
        \[RightDoubleBracket]/.{
            0\[Rule]RGBColor[0,0,0],
        -1 |-2-> RGBColor[0.7,0.7, 0.7],
            f|x -> RGBColor[1,0, 0],
        1|2|3-> RGBColor[1,1, 1]}]]],
          opts]&)/@Range[Length[list]]

ShowHPP[HPP[40,3000]];
```

C.2 Per Bak's Avalanche Model of Self Organised Criticality

C.2.1 The Sandpile Model.

This model comes from Gaylord et. al. (Gaylord and Nishidate, 1996) with only minor modifications.

```
\!\(Sandpile[s_, m_] :=
    Module[{absorbBC, landscape,
    topHeavyNgbrs, update},
      absorbBC =
```

```
        Prepend[Append[\((Prepend
        [Append[#1, 0], 0]&)\)/@#1,
              Table[0, {Length[#1] + 2}]],
              Table[0, {Length[#1] + 2}]]&;
      landscape = absorbBC[Table
      [Random[Integer, {3, 4}], {s}, {s}]];
      While[Max[landscape] < 5,
        randx = Random[Integer, {2, s + 1}, {2, s + 1}];
        randy = Random[Integer, {2, s + 1}, {2, s + 1}];
        \(landscape\[LeftDoubleBracket]randx,
        randy\[RightDoubleBracket]++
         \)]; topHeavyNgbrs[mat_] :=
        Plus@@\(\((RotateRight[Floor[mat\/5.0], #1]&)
         \)/@{{\(-1\), 0}, {0, \(-1\)}, {0, 1}, {1, 0}}\);
      update[0, _] := 0; update[r_, t_] := r + t /; r < 5;
      update[r_, t_] := r - 4 + t;
      Attributes[update] = Listable;
      FixedPointList[update[#1,
      topHeavyNgbrs[#1]]&, landscape, m]]\)
Graphical Output
ShowCatastrophe2[list_,opts___]:=
  Scan[ListDensityPlot[
  list\[LeftDoubleBracket]#1\[RightDoubleBracket],opts,
        Axes->False, Frame -> False,
        Mesh -> False, ColorFunction ->Hue,
        Ticks -> Automatic]&,Range[Length[list]] ]
Experiments ShowCatastrophe2[Sandpile[20,35]]
ShowCatastrophe2[Sandpile[30,50]]
```

References

[Albert et al., 1997] Albert, R., Albert, I., Hornbaker, D., Schiffer, P., and Barabasi, A.-L. (1997). Maximum angle of stability in wet and dry spherical granular media. *Physical Review E*, 56(6):R6271–r6274.

[Alonso et al., 1998] Alonso, J. J., Hovi, J. P., and Herrmann, H. J. (1998). Model for the calculation of the angle of repose from the microscopic grain properties. *Phys. Rev. E*, 58(1):672.

[Anderson, 1996] Anderson, R. S. (1996). The attraction of sand dunes. *Nature*, 379:24.

[Bak, 1997] Bak, P. (1997). *How Nature Works: The Science of Self Organised Criticality*. Oxford University Press, London.

[Bak and Chen, 1989] Bak, P. and Chen, K. (1989). The physics of fractals. *Physica D*, 38:5–12.

[Bak et al., 1987] Bak, P., Tang, C., and Wiesenfeld, K. (1987). Self organised criticality: An explanation of 1/f noise. *Physical Review Letters*, 59(4).

[Bak et al., 1988] Bak, P., Tang, C., and Wiesenfeld, K. (1988). Self organised criticality. *Physical Review A*, 38(1).

[Ball, 1999a] Ball, P. (1999a). *The Self Made Tapestry: Pattern Formation in Nature*. Oxford University Press, Oxford.

[Ball, 1999b] Ball, P. (1999b). Transitions still to be made. *Nature*, 402:c73–c76. suppliment.

[Baxter and Behringer, 1990] Baxter, G. W. and Behringer, R. P. (1990). Cellular automata models of granular flow. *Physical Review A*, 42(2).

[Baxter et al., 1989] Baxter, G. W., Behringer, R. P., Fagert, T., and Johnson, A. (1989). Pattern formation in flowing sand. *Physical Review Letters*, 62(24).

[Boutreux and Degennes, 1997] Boutreux, T. and Degennes, P. G. (1997). Surface flows of granular mixtures: I. general principles and minimal model. *J. Phys, I France*, 6(10):1295–1304.

[Brown and Richards, 1970] Brown, R. L. and Richards, J. C. (1970). *Principles of Powder Mechanics*. Pergamon, Oxford.

[Chown, 1997] Chown, M. (1997). A pattern emerges. *NewScientist*, page 34.

[Clift, 1993] Clift, R. (1993). An occamists review of fluidized bed modelling. *Fluid Particle Processes*, 89(296):1–17.

[Coveney and Highfield, 1993] Coveney, P. and Highfield, R. (1993). *Frontiers of Complexity: The Search for Order in a Chaotic World*. Ballentine Books, New York.

[Cumberland and Crawford, 1987] Cumberland, R. J. and Crawford, R. J. (1987). *Packing of Particles*. Elsevier Science, Amsterdam.

[da Silva and Rajchenbach, 2000] da Silva, M. and Rajchenbach, J. (2000). Stress transmission through a model system of cohesionless elastic grains. *Nature*, 406(1):708.

[Daerr and Douady, 1999] Daerr, A. and Douady, S. (1999). Two types of avalanche behavior in granular media. *Nature*, 399.

[Ding and Gidaspow, 1990] Ding, J. and Gidaspow, D. (1990). A bubbling fluidization model using kinetic theory of granular flow. *AIChE*, 36(4).

[Duran, 2000] Duran, J. (2000). *Sands, Powders and Grains: An Introduction to the Physics of Granular Materials*. Partially Ordered Systems. Springer-Verlag, New York.

[Dury et al., 1998] Dury, C. M., Ristow, G. H., Moss, J. L., and Nakagawa, M. (1998). Boundary effects on angle of repose in rotating cylinders. *Physical Review E*, 57(4):4491.

[Eggers, 1999] Eggers, J. (1999). Sand as maxwell's demon. *Phys. Rev. Lett.*, 83(25):5322.

[Ennis et al., 1994] Ennis, B., Green, J., and Davies, R. (1994). The legacy of neglect in the U.S. *Chem. Eng. Prog.*, 90(4):32–43.

[Falcon et al., 1999] Falcon, E., Kumar, K., Bajaj, K. M. S., and Bhattacharjee, J. K. (1999). Heap corrugation and hexagon formation of powder under vertical vibrations. *Physical Reveiw E*, 59(5):5716–5720.

[Faraday, 1831] Faraday, M. (1831). On a peculiar class of acoustical figures: And on certain forms by groups of particles on vibrating elastic surfaces. *Philosophical Transactions of the Royal Society of London*, 52:299.

[Feng and Yu, 1998] Feng, C. L. and Yu, A. B. (1998). Effect of liquid addition on the packing of mono-sized coarse spheres. *Powder Technology*, 99:22–28.

[Fineburg, 1997] Fineburg, J. (1997). From cinderella's dilemma to rock slides. *Nature*, 386.

[Finney, 1970] Finney, J. L. (1970). Random packings and the structure of simple liquids: I the geometry of random close packing. *Proceedings of the Royal Society of London*, 319:479. Ser A.

[Forsyth et al., 2000] Forsyth, A., Hutton, S., Rhodes, M., and C.F.Osborne (2000). Effect of applied inter-particle force on packing density and the angles of repose in mono-sized granular material. *presented at CHEMICA*. Perth.

[Forsyth et al., 2001a] Forsyth, A., Hutton, S., Rhodes, M., and C.F.Osborne (2001a). Effect of applied inter-particle force on the static and dynamic angles of repose of spherical granular material. *Physical Review E*, 63(3).

[Forsyth et al., 2001b] Forsyth, A., Hutton, S., Rhodes, M., and C.F.Osborne (2001b). Effect of inter-particle force on the packing of spherical granular material. *Physical Review Letters*, 87(24).

[Forsyth and Rhodes, 2000] Forsyth, A. and Rhodes, M. (2000). A simple model incorperating the effect of deformation asperties into the vander waals force for macroscopic spherical solid particles. *Journal of Colloid and interface Science*, 223:133–138.

[Forsyth et al., 2001c] Forsyth, A., Shen, F. W., Parker, I. H., Hutton, S., and Rhodes, M. (2001c). Effects of humidity on the flow characteristics of granular materials. *Powder Technology*.

[Frette et al., 1996] Frette, V., Christensen, K., Malthe-Sorenssen, A., Feder, J., Jossang, T., and Meakin, P. (1996). Avalanche dynamics in a pile of rice. *Nature*, 379.

[Fuller, 1975] Fuller, R. B. (1975). *Synergetics: Explorations in the Geometry of Thinking.* Macmillan Publishing Co. Inc, New York.

[Galileo, 1968] Galileo, G. (1968). *Dialogues Concerning Two New Sciences.* Northwest University Press. Translated by Henry and Alfonso de Silvio.

[Gaylord and Nishidate, 1996] Gaylord, R. and Nishidate, K. (1996). Modelling nature:Cellular automata simulations with mathematica. *Springer-Verlag.*

[Geldart, 1973] Geldart, D. (1973). Types of gas fluidization. *Powder Technology*, 7:285–292.

[Geldart and Wong, 1984] Geldart, D. and Wong, A. C. Y. (1984). Fluidization of powders showing degrees of cohesiveness-i bed expansion. *Chemical Engineering Science*, 39:1481.

[Geldart and Wong, 1985] Geldart, D. and Wong, A. C. Y. (1985). Fluidization of powders showing degrees of cohesiveness-ii experiments on rates of de-aeration. *Chemical Engineering Science*, 40:653.

[Gennes, 1999] Gennes, P. G. (1999). Granular matter: a tentative view. *Reviews of Modern Physics*, 71(2). Centenary.

[Gollub and Langer, 1999] Gollub, J. P. and Langer, J. S. (1999). Pattern formation in nonequilibrium physics. *Reviews of Modern Physics*, 71(2).

[Gonzalez and Wintz, 1987] Gonzalez, R. C. and Wintz, P. (1987). *Digital Image Processing.* Addison Wesley, Reading MA, 2nd edition.

[Goodwin, 1994] Goodwin, B. (1994). *How the Leopard Changed its Spots.* Weidenfeld and Nicolson, London.

[Grasselli and Herrmann, 1997] Grasselli, Y. and Herrmann, H. P. (1997). On the angles of dry granular heaps. *Physica A*, 246:301–312.

[Gupta and Sathiyamoorthy, 1999] Gupta, C. K. and Sathiyamoorthy, D. (1999). *Fluid Bed Technology in Materials Processing.* CRC Press, Florida.

[H. Kalman and Ben-Dor, 1993] H. Kalman, D. Goder, M. R. and Ben-Dor, G. (1993). The effect of particle surface friction on the angle of repose. *Bulk Solids Handling*, 13(1):123.

[Hamaker, 1937] Hamaker, H. C. (1937). The London-Van der Waals attraction between spherical particles. *Physica*, 4:1058.

[Held et al., 1990] Held, G. A., II, D. H. S., Keane, D. T., Haag, W. J., Horn, P. M., and Grinstein, G. (1990). Experimental study of critical mass fluctuations in an evolving sandpile. *Physical Review Letters*, 65(9).

[Heyman, 1998] Heyman, J. (1998). *Coulombs Memoir on Statics: An Essay in the History of Civil Engineering*. Imperial College Press.

[Hill et al., 1997] Hill, K. M., Caprihan, A., and Kakalios, J. (1997). Bulk segegation in rotated granular material measured by magnetic resonance imaging. *Physical Review Letters*, 78(1):50.

[Hill and Kakalios, 1995] Hill, K. M. and Kakalios, J. (1995). Reversible axial segregation of rotating granular media. *Physical Review E*, 52(4).

[Hill and Kaklois, 1994] Hill, K. M. and Kaklois, J. (1994). Reversible axial segregation in binary mixtures of granular material. *Physical Review E*, 49(5).

[Hoomans et al., 1996] Hoomans, B. P. B., Kuipers, J. A. M., Briels, W. J., and van Swaaij, W. P. M. (1996). Discrete particle simulation of bubble and slug formation in a 2D gas fluidised bed: A hard sphere approach. *Chemical Engineering Science*, 31(1):99–118.

[Hornbaker et al., 1997] Hornbaker, D. J., Albert, I., Barabasi, A. I., and Schiffer, P. (1997). What keeps sandcastles standing? *Nature*, 387:765.

[Hutton et al., 2000a] Hutton, S., Forsyth, A., Rhodes, M., and C.F.Osborne (2000a). The role of inter-particle force in segregation of particulate materials. *presented at AIChE Annual Meeting, Los Angeles, California*. paper 12g.

[Hutton et al., 2000b] Hutton, S., Forsyth, A., Rhodes, M., and C.F.Osborne (2000b). Segregation of particulate materials: Inter-particle force effects. Technical Report paper 0084, First Asian Particle Technology Symposium, Bangkok, Thailand. session S-I(2)-5.

[Hutton et al., 2001] Hutton, S., Forsyth, A., Rhodes, M., and C.F.Osborne (2001). Effects of inter-particle force on segregation in a rotating drum. Technical report, World Engineering Congress.

[Israelachvili, 1992] Israelachvili, J. N. (1992). *Intermolecular and Surface Forces.* Academic, San Diego, 2nd edition.

[Jaeger and Nagel, 1992] Jaeger, H. M. and Nagel, S. R. (1992). Physics of the granular state. *Science*, 255:1523.

[Jaeger and Nagel, 1997] Jaeger, H. M. and Nagel, S. R. (1997). Dynamics of granular material. *American Scientist*, 85:540.

[Jaeger et al., 1996] Jaeger, H. M., Nagel, S. R., and Behringer, R. (1996). The physics of granular materials. *Physics Today*, page 32.

[John F. Lindsay and Criswell, 1976] John F. Lindsay, David R. Criswell, T. L. C. and Criswell, B. S. (1976). Sound producing dune and beach sands. *Geological Society of America Bulletin*, 87(463-473).

[Jones et al., 1989] Jones, T. B., Miller, R. D., Robinson, K. S., and Fowlkes, W. Y. (1989). Charge relaxation in partially filled vessels. *Journal of Electrostatics*, 22(231).

[Kadanoff, 1999] Kadanoff, L. P. (1999). Built upon sand: Theoretical ideas inspired by granular flows. *Reviews of Modern Physics*, 71(1).

[Kadanoff et al., 1989] Kadanoff, L. P., Nagel, S. R., Wu, L., and min Zhao, S. (1989). Scaling and universality in avalanches. *Physical Review A*, 19(12).

[Kauffman, 1993] Kauffman, S. A. (1993). *The Origins of Order: Self Organisation and Selection in Evolution.* Oxford University Press, Oxford.

[Kauffman, 1995] Kauffman, S. A. (1995). *At Home in the Universe: The Search for Laws of Complexity.* Oxford University Press, New York.

[Kepler, 1976] Kepler, J. (1976). *The 6 cornered snowflake (de Niv sexangula).* Oxford University Press, Oxford. edited by C. Hardie.

[Knowlton et al., 1994] Knowlton, T. M., Carson, J., Klinzing, G. E., and Yang, W. C. (1994). The importance of storage, transfer, and collection. *Chem. Eng. Prog.*, 90(4):44–54.

[Koeppe et al., 1997] Koeppe, J., Enz, M., and Kakalios (1997). Phase diagram for avalanche stratification of granular media. *Physical Review E*, 4(58):R4104.

[Kunii and Levenspeil, 1991] Kunii, D. and Levenspeil, O. (1991). *Fluidization Engineering*. Butterworth-Heinmann, Sydney, 2 edition.

[Lewin, 1993] Lewin, R. (1993). *Complexity:Life on the Edge of Chaos*. Phoenix, London.

[Lioubashevski et al., 1999] Lioubashevski, O., Hamiel, Y., Agnon, A., Reches, Z., and Fineberg, J. (1999). Oscillons and propagating solitary waves in a vertically vibrated colloidal suspension. *Physical Review Letters*, 83(16):3190–3193.

[Liu and Nagel, 1998] Liu, A. J. and Nagel, S. (1998). Jamming is not just cool anymore. *Nature*, 396:21.

[Luding and Herrmann, 1999] Luding, S. and Herrmann, H. J. (1999). Cluster growth in freely cooling granular media. *Chaos*, 9(3):673–681.

[Makse, 1997a] Makse, H. (1997a). Stratification instability in granular flows. *Physical Review E*, 56(6).

[Makse, 1997b] Makse, H. A. (1997b). Stratification instability in granular flows. *Physical Review E*, 56:7008–7016.

[Makse, 2000] Makse, H. A. (2000). Grain segregation mechanism in aeloian sand ripples. *European Journal of Physics*.

[Makse et al., 1998] Makse, H. A., Ball, R. C., Stanley, H. E., and Warr, S. (1998). Dynamics of granular stratification. *Physical Review E*, 58:3357.

[Makse et al., 1997] Makse, H. A., Havlin, S., King, P. R., and Stanley, H. E. (1997). Spontaneous stratification in granular mixtures. *Nature*, 386:379.

[Malthe-Sorenssen et al., 1999] Malthe-Sorenssen, A., Feder, J., Christensen, K., Frette, V., and Jossang, T. (1999). Surface fluctuations and correlations in a pile of rice. *Physical Review Letters*, 83(4).

[Maslov et al., 1999] Maslov, S., Tang, C., and Zhang, Y.-C. (1999). $1/f$ noise in Bak-Tang-Wiesenfeld models on narrow stripes. *Physical Review Letters*, 83(12):2449–2452.

[McLaughlin and Rhodes, 2001] McLaughlin, L. J. and Rhodes, M. J. (2001). Prediction of fluidized bed behaviour in the presence of liquid bridges. *Powder Technology*, 114:213–223.

[Melo et al., 1995] Melo, F., Umbanhowar, P. B., and Swinney, H. L. (1995). Hexagons, kinks, and disorder in oscillated granular layers. *Physical Review Letters*, 75:3838–3841.

[Molerus, 1982] Molerus, O. (1982). Interpretation of Geldart type A, B, C and D powders by taking into account inter-particle cohesion forces. *Powder Technology*, 33:pp 81–87.

[Nasuno et al., 1998] Nasuno, S., Kudolli, A., Bak, A., and Gollub, J. P. (1998). Time resolved studies of stick-slip friction in sheared granular layers. *Physical Reveiw E*, 58(2):2161–2171.

[Oyama, 1939] Oyama, Y. (1939). *Bullitin of the Institute of Physical Chemistry Research*, 18(5):600. In Japanese.

[Pilpel1, 1958] Pilpel1, N. (1958). *The Flow of Powders and Granular Solids*, volume II, pages 699–702. British Chemical Engineering.

[Pouliquen et al., 1997] Pouliquen, G., Delour, J., and Savage, S. B. (1997). Fingering in granular flows. *Nature*, 386:816–817.

[Pouliquen and Vallance, 1999] Pouliquen, O. and Vallance, J. (1999). Segregation induced instabilities of granular fronts. *Chaos*, 9(3):621–630.

[Prigogine, 1980] Prigogine, I. (1980). *From Being to Becoming:Time and Complexity in the Physical Sciences*. W. H. Freeman and Company, New York.

[Prigogine and Stengers, 1984] Prigogine, I. and Stengers, I. (1984). *Order Out of Chaos: Man's Dialogue with Nature*. William Collins Sons and Co., Glasgow.

[Radjai et al., 1999] Radjai, F., Roux, S., and Moreau, J. J. (1999). Contact forces in granular packing. *Chaos*, 9(3):544–550.

[Reynolds, 1885] Reynolds, O. (1885). On the dilatency of media composed of rigid particles in contact: with experimental illustrations. *Philosophical Magazine*, 20(2):469–481.

[Rhodes et al., 2002] Rhodes, M. J., Hutton, S. R., Forsyth, A. J., and Osborne, C. F. (2002). Influence of inter-particle forces on the packing fraction of spheres.

AIChE Annual Meeting, Reno, Nevada, (paper 202e). paper appeared in proceedings but not presented due to travel restrictions.

[Rhodes and Wang, 2002] Rhodes, M. J. and Wang, X. S. (2002). Private communication.

[Rhodes et al., 2001] Rhodes, M. J., Wang, X. S., Forsyth, A. J., Gan, K. S., and Phadtajaphan, S. (2001). Use of a magnetic fluidised bed in studying Geldhart group B to A transition. *Chemical Engineering Science*, 56:1–8.

[Savage, 1992] Savage, S. B. (1992). *Disorder and Granular Media*, page p255. North-Holland, Amsterdam. edited by Bideau and A Hansen.

[Schroeder, 1990] Schroeder, M. (1990). *Fractals, Chaos and Power Laws: Minutes from an Infinite Paradise*. W. H. Freedman and Company, New York.

[Seibert and Burns, 1996] Seibert, K. D. and Burns, M. A. (1996). Simulation of fluidized beds and other fluid-particle systems using statistical mechanics. *Particle Technology and Fluidization*, 42(3):660. AichE Journal.

[Shinbrot, 1997] Shinbrot, T. (1997). Competition between randomizing impacts and inelastic collisions in granular pattern formation. *Nature*, 389:574.

[Shinbrot et al., 1999] Shinbrot, T., Alexander, A., Meakher, M., and Muzzio, F. J. (1999). Chaotic granular mixing. *Chaos*, 9(3):611–620.

[Shinbrot and Muzzio, 2001] Shinbrot, T. and Muzzio, F. (2001). Noise to order. *Nature*, 410(6825):251–258.

[Shinbrot and Muzzio, 2000] Shinbrot, T. and Muzzio, J. (2000). Nonequilibrium patterns in granular mixing and segregation. *Physics Today*.

[Sholtz et al., 1997a] Sholtz, P., Bretz, M., and Nori, F. (1997a). Booming and squeaking sands. *Scientific American*, page 84.

[Sholtz et al., 1997b] Sholtz, P., Bretz, M., and Nori, F. (1997b). Sound producing sand avalanches. *Contemporary Physics*, 38(5):329–342.

[Svarovsky, 1987] Svarovsky, L. (1987). *Powder Testing Guide*. Elsevier Science, New York.

[Tan and Jones, 1993] Tan, C. and Jones, T. B. (1993). Interparticle force measurements on ferromagnetic steel balls. *J. Appl. Phys.*, 73:3593–3598.

[Tegzes et al., 1999] Tegzes, P., Albert, R., Paskvan, M., Vicsek, T., and Schiffer, P. (1999). Liquid-induced transitions in granular media. *Physical Review E*, November(5):5823–5826.

[Umbanhowar, 1996] Umbanhowar, P. B. (1996). *Wave Patterns in Vibrated Granular Layers*. PhD thesis, Center for Nonlinear Dynamics: The University of Texas.

[van Wachem et al., 1997] van Wachem, B. G. M., Bakker, A. F., Schouten, J. C., Heemels, M. W., and de Leeuw, S. W. (1997). Simulations of fluidized beds with lattice gas cellular automata. *Journal of Computational Physics*, 135:1–7. Article# CP975719.

[Werner, 1995] Werner, B. T. (1995). Eolian dunes: Computer simulations and attractor interpretation. *Geology*, 23:1057.

[Wu et al., 1997] Wu, W. Y., Navada, A., and Saxena, S. C. (1997). Hydrodynamic characteristics of a magnetically stabilised air fluidised bed of an admixture of magnetic and non-magnetic particles. *Powder Technology*, 90:39–46.

Appendix D

Published Papers

List of published papers as of April 2002

Refereed Papers in Learned Journals

Forsyth, A.F., S. Hutton, M.J. Rhodes and C.F. Osborne, (2001) "Effects of interparticle force on the packing fraction of spherical granular material", Physical Review Letters, Vol. 87, 24, pp. 244301-1 to 244301-3.

Forsyth, A.F., S. Hutton, M.J. Rhodes and C.F. Osborne, (2001) "Effect of applied interparticle force on the static and dynamic angles of repose of spherical granular material", Physics Review E, *Vol. 63*, pp. 031302-1 to 031302-5.

Works in progress: *Forthcoming journal papers:*

Forsyth, A.F., W. Shen, I.H. Parker, S. Hutton and M.J. Rhodes, "Effect of humidity on the flow characteristics of granular material", Powder Technology, *in press*.

Refereed Papers Read at Conferences with Published Proceedings

Hutton, S. R., A. J. Forsyth, C. F. Osborne and M. J. Rhodes, "Effect of interparticle force on segregation in a rotating drum", Proceedings of the 6th World Congress of Chemical Engineering, Melbourne, Australia, 24 – 27 September 2001, Editor D. Shallcross, Session 2318.

Forsyth, A., M.J. Rhodes, S. Hutton and C. Osborne, (2000) "Effect of applied interparticle force on packing density and the angles of repose in mono-sized granular material", presented at CHEMECA 2000, Perth, 9 – 12 July.

Non-Refereed Papers Read at Conferences

Rhodes, M.J., S. R. Hutton, A. J. Forsyth, C. F. Osborne (2001), "Influence of interparticle forces on the packing fraction of spheres", paper 202e, AIChE Annual Meeting, Reno, Nevada, 5-9 Nov. 2001, (paper included in proceedings but not presented due to travel prohibition).

S. R. Hutton, A. J. Forsyth, C. F. Osborne and M. J. Rhodes (2000) "Segregation of particulate materials: interparticle force effects", presented at the First Asian Particle Technology Symposium, Bangkok, Thailand, 13 – 15 December 2000, session S-I(2)-5, paper #0084.

Forsyth, A.J., S. R. Hutton, C.F. Osborne and M.J. Rhodes, (2000), "The role of interparticle force in segregation of particulate materials", paper 12g, presented at the AIChE Annual Meeting, Los Angeles, California, 12-17 Nov. 2000.

Effects of Interparticle Force on the Packing of Spherical Granular Material

A. J. Forsyth,[1] S. R. Hutton,[2] C. F. Osborne,[2] and M. J. Rhodes[1]

[1]*Department of Chemical Engineering, Monash University, Victoria 3800, Australia*

[2]*Department of Physics, Monash University, Victoria 3800, Australia*

(Received 7 September 2000; revised manuscript received 1 October 2001; published 26 November 2001)

We present a study of the influence of interparticle cohesive forces on the packing of spheres. This is achieved by changing the external magnetic field on iron spheres in the millimeter size range. The force of cohesion between two spheres is measured by opposing magnetic and gravitational force. The void fraction of the bed resulting from many spheres being poured into a container at a given magnetic field is measured. The void fraction of the packed spheres as a function of interparticle force is thus established. We find that the void fraction is determined only by the ratio of interparticle force to particle weight, regardless of particle size. This is shown to be a universal effect, not limited to magnetic systems.

DOI: 10.1103/PhysRevLett.87.244301 PACS numbers: 45.70.Cc

While there has been a recent upsurge in interest in granular materials among physicists (for example [1–3]), the study of granular packing has a long history dating back as far as Kepler [4]. In addition to its theoretical interest, understanding how particle properties affect packing arrangements in powders is of great practical importance. Examples range from the formation of tablets from complex particulate mixtures in the pharmaceutical industry through manufacture of sintered metal products from metal powders to the apparently simple task of ensuring that 25 kg of a powder product will fit into a 25 kg bag for distribution and sale. The void fraction (ratio of the volume occupied by voids to the volume occupied by voids plus particles) in packed particulate materials is affected by particle size distribution, particle shape and interparticle forces F_{ip}. In general, for random packing arrangements, void fraction decreases with increasing width of size distribution, increased particle sphericity, and decreasing interparticle cohesive forces. This paper focuses on the role of interparticle cohesive forces in influencing the void fraction of packed particulate materials. Industrially relevant interparticle cohesive forces may appear as van der Waals forces in dry powders or liquid bridges forces in damp powders.

In the absence of interparticle forces a powder will attain a void fraction somewhere between the loose random packing limit ($\cong$0.42) and the dense random packing limit ($\cong$0.37) [5]. Interparticle forces allow "vaulting" to occur, leading to large (on the scale of the particles) voids within the powder, and hence a greater void fraction.

It is well known that for dry powders the range of possible packing densities under normal gravity increases with decreasing particle size [6,7]. For dry powders the dominant interparticle force is van der Waals, which increases linearly with particle diameter [8], while inertial forces increase with the cube of the particle diameter. Consequently, with dry powders the interparticle cohesive forces become more dominant with decreasing particle size. Hence the void fraction for dry powders increases with decreasing particle size. This effect is demonstrated in the data presented by Feng and Yu [7].

Several groups [2,9,10] have added liquids of varying surface tension and viscosities to dry powders to observe the effect of the resulting increase in interparticle force. Work has also been done on examining the effect of liquid on packing of monosized coarse spheres [7]. The limitation of this method is that the addition of more and more liquid increases the interparticle force in a stepwise manner. It is difficult to remove liquid in a controllable way. Adding liquids to dry powders not only increases the interparticle interaction, but also the interaction between the powder and the wall, further complicating the analysis. In addition, it is difficult to relate the quantity of liquid added to the interparticle force.

We have examined the packing of iron spheres within a magnetic field B. Varying B allowed us to continuously vary the resulting interparticle magnetic force. As the walls of the vessel used were plastic, the particle-wall interaction is unchanged. The magnetic field for this experiment is supplied by a pair of Helmholtz coils. These coils each have an inner diameter of 456 mm, an outer diameter of 568 mm, and a thickness of 76 mm. The former are constructed from nylon, and were wound with 1.1 km of 2.2 mm insulated copper wire. The coils are powered by a 16 A, 16 V stabilized dc power supply and have a total resistance of 2.2 Ω.

B was measured as a function of current by a Bell 2400 series Gaussmeter. The field was found to vary less than 10% throughout the volume between the coils, and by less than 5% within a sphere of diameter 140 mm centered on the axis of symmetry, midway between the coils. Previous interparticle force experiments [11] demonstrated that chains of two particles can be considered a basic building block for understanding the string interparticle interactions of more complex arrangements of particles. In the present work the measured force between two isolated particles is taken as being representative of the force between particles in a bed, although it is recognized that within the bed

the mean attractive force between particles may be somewhat different. To directly measure the interparticle force between two particles as a function of field strength, the following method was used. A sphere of iron of the approximate size (0.35 mm, 0.8 mm, 1.6 mm) was glued to a plastic spatula and positioned on the axis of symmetry at the point midway between the coils. With B at full strength (approximately 6400 A/m) a second particle of the same size was brought into contact with the fixed sphere. Because of the strong magnetic force between the two particles, the second particle became suspended from the first. The current in the coils, and hence B, was slowly decreased until the suspended particle fell from the fixed particle. At this point the interparticle force is equal to (or marginally less than) the weight of the particle. This measurement, as well as all subsequent measurements, was repeated several times. The weight of the particle was measured with a sensitive laboratory balance.

To obtain further points for the graph, small ($\cong$0.5 mm) bronze spheres were carefully glued to the bottom of the particle to be suspended. This served to increase the weight of the particle without significantly altering the interparticle force. This new "particle" was weighed, and the measurements repeated, making sure that none of the bronze particles became dislodged when the suspended particle fell. For all the particles used, Fig. 1 shows the interparticle force, scaled to the particle weight, versus the square of the field.

The standard method for the measurement of the poured packing fraction of dry particles [12] was used, with slight modifications described below. With B set at a particular level, iron spheres were poured into a cylindrical container approximately 4 cm in diameter and 10 cm high (volume 128 cm^3) through a funnel with a stopcock attached to regulate flow. The height of the stopcock was kept constant at a level of 5 cm above the top of the container. Once the container was full, excess particles were carefully leveled off and the sample was weighed. This was repeated for a number of particle sizes and field strengths. Using Fig. 1 as a calibration curve, we plot the void fraction against the ratio of interparticle force F_{ip} to particle weight mg (Fig. 2). We see that the data for the three different particle sizes fall on the same curve, demonstrating that the void fraction of the packed bed of spheres formed by pouring under normal gravity is a function only of F_{ip}/mg.

One might argue that perhaps this only holds for our magnetic system, so let us now consider dry powders. We shall assume that void fraction is only dependent F_{ip}/mg. We shall also assume that the relationship is universal—that is that the void fraction for dry powders varies in the same manner with F_{ip}/mg demonstrated for the magnetic system. From Fig. 2, it is apparent that the void fraction rises approximately linearly with increasing F_{ip}/mg. We shall assume that the void fraction increases according to

$$\varepsilon = \varepsilon_0 + k\left(\frac{F_{ip}}{mg}\right), \tag{1}$$

where ε is the void fraction, ε_0 is the void fraction at zero field, and k is the rate at which void fraction increases with increasing F_{ip}/mg. For dry, nonmagnetic powders the dominant interparticle force is the van der Waals force. Asperities play an important role in determining the van der Waals force, so we shall use an expression for the force between two particles developed previously by the present authors [13].

$$F_{ip}(d) = -\frac{2Ar^3}{3d^2(d+2r)^2} - \frac{2AR^3}{3(d+r)^2(d+r+2R)^2}, \tag{2}$$

where d is the particle separation, A is the Hamaker constant, r is the asperity radius (assumed to have a spherical profile), and R is the particle radius. Standard values for asperity size, Hamaker constant, and separation data are given in [14–16], with $d = 0.4$ nm and $r = 0.1$ μm. The Hamaker constant for glass is 1.6×10^{-19} J, and we take the density of glass to be 2950 kg m^{-3}. The values of k and ε_0 were calculated from Fig. 2, giving approximately

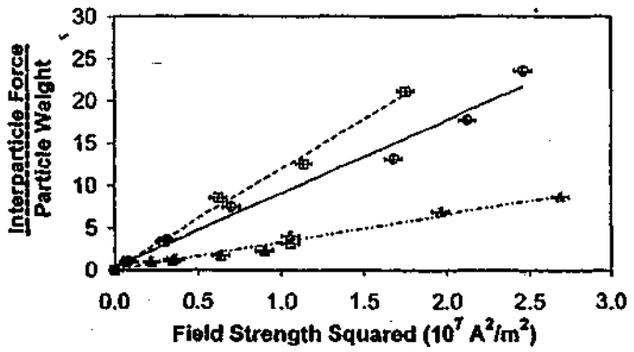

FIG. 1. Interparticle force (scaled to particle weight) versus magnetic field strength squared for 0.35 mm (squares), 0.8 mm (circles), and 1.6 mm (triangles) iron spheres.

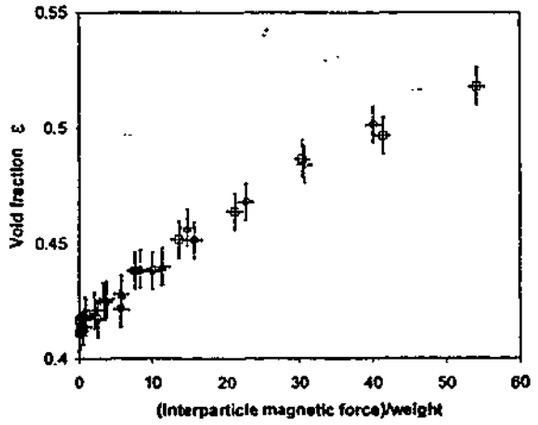

FIG. 2. Void fraction versus the ratio of interparticle force to weight for 0.35 mm (squares), 0.8 mm (circles), and 1.6 mm (triangles) iron spheres in a magnetic field.

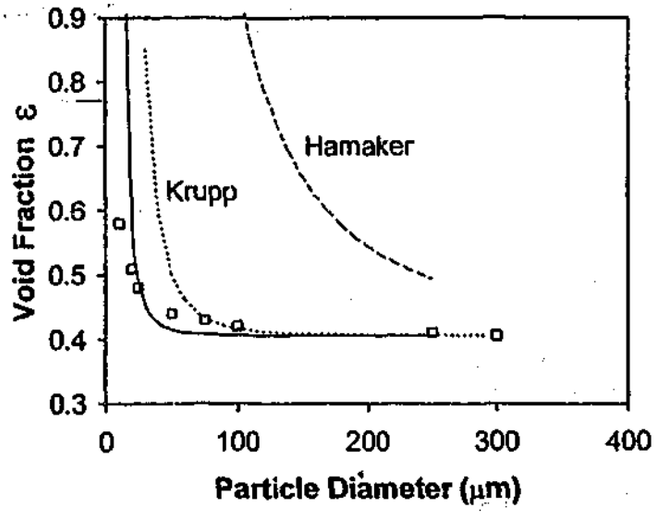

FIG. 3. Void fraction versus particle diameter for dry powders. The predicted values are based on the assumption that the void fraction should depend only on the ratio of interparticle force to particle weight. Models for the interparticle force are taken from Forsyth and Rhodes [13] (solid line), Hamaker [17] (dashed line), and Krupp [14] (dotted line). Data points are from Feng and Yu [7].

2×10^{-3} and 0.41, respectively. Using this data, we can now estimate how the void fraction for dry powders should vary with particle diameter. The prediction is shown in Fig. 3, compared with the experimental data of Feng and Yu [7]. Predicted curves using the models of Hamaker [17] and Krupp [14] to model the interparticle van der Waals force are also shown. Krupp's model considers only the asperity contributing to the interparticle force, and hence underestimates the force [13]. All parameters in Krupp's model were taken from Molerus [16].

The prediction of Forsyth and Rhodes [13] provides good agreement with experiment for particle diameters larger than about 25 μm. For particles smaller than 25 μm we overestimate the void fraction. This is due to the fact that we have assumed a linear dependence between void fraction and F_{ip}/mg. Obviously this approximation must break down at high values F_{ip}/mg. By definition, the void fraction can never exceed unity, and in practice void fractions never even approach this value. For a 20 μm particle F_{ip}/mg is approximately 137, which is far beyond the maximum ratio examined by our magnetic system (approximately 54). Hence, it is not surprising that the model breaks down for very small particles. At 25 μm F_{ip}/mg is down to 70. In fact, one can see the data in Fig. 2 rises more and more slowly as the interparticle force increases.

By choosing a relationship between void fraction ε and F_{ip}/mg that does not rise linearly, we could more closely model the experimental data. Until we have a better theoretical understanding of the effect of interparticle force on void fraction, the form of the curve will be completely arbitrary, and will require the introduction of extra parameters. For instance, using a curve of the form

$$\varepsilon = \varepsilon_0 + (\varepsilon_{max} - \varepsilon_0) \exp\left[-k\left(\frac{F_{ip}}{mg}\right)\right], \qquad (3)$$

where ε_{max} is the maximum attainable void fraction can be made to fit the experimental data more closely than the linear model in Eq. (1). This problem will be addressed at a later date.

We have designed a novel system for studying the effect of interparticle force on the poured packing of spherical particles. We find that for magnetic particles the void fraction depends only on the ratio of interparticle cohesive force to particle weight. Using this result, we have demonstrated that the poured packing of dry spheres, where the dominant interparticle force is van der Waals, also depends only on the corresponding ratio of interparticle cohesive force to particle weight.

[1] H. M. Jaeger, S. R. Nagel, and R. P. Beringer, Phys. Today 49, 32 (1996).
[2] D. J. Hornbaker, I. Albert, A. L. Barabasi, and P. Schiffer, Nature (London) 387, 765 (1997).
[3] H. A. Makse, S. Halvin, P. R. King, and H. E. Stanley, Nature (London) 386, 379 (1997).
[4] J. Kepler, in *The Six-Cornered Snowflake (De Niv Sexangula)*, edited by C. Hardie (Oxford University Press, Oxford, 1976).
[5] D. J. Cumberland and R. J. Crawford, *Packing of Particles* (Elsevier Science, Amsterdam, 1987).
[6] D. Geldart and A. C. Y. Wong, Chem. Eng. Sci. 40, 1481 (1984).
[7] C. L. Feng and A. B. Yu, Powder Technol. 33, 22 (1999).
[8] J. N. Israelachvili, *Intermolecular and Surface Forces* (Academic Press, San Diego, 1992), 2nd ed.
[9] R. Albert *et al.*, Phys. Rev. E 56, R6271 (1997).
[10] L. J. McLaughlin and M. J. Rhodes, Powder Technol. 114, 213 (2001).
[11] C. Tan and T. B. Jones, J. Appl. Phys. 73, 3593 (1993).
[12] L. Svarovsky, *Powder Testing Guide* (Elsevier Science, New York, 1987).
[13] A. J. Forsyth and M. J. Rhodes, J. Colloid Interface Sci. 223, 133 (2000).
[14] H. Krupp, Adv. Colloid Interface Sci. 1, 111 (1967).
[15] H. Rumpf, *Particle Technology* (Carl Hanser Verlag, Munich, 1975).
[16] O. Molerus, Powder Technol. 33, 81 (1982).
[17] H. C. Hamaker, Physica (Amsterdam) 4, 1058 (1937).

Effect of applied interparticle force on the static and dynamic angles of repose of spherical granular material

A. I. Forsyth,[1] S. R. Hutton,[2] M. J. Rhodes,[1] and C. F. Osborne[2]
[1]*Department of Chemical Engineering, Monash University, Victoria 3800, Australia*
[2]*Department of Physics, Monash University, Victoria 3800, Australia*
(Received 25 June 2000; published 15 February 2001)

The static angle of repose for iron spheres in a narrow box, and the dynamic angle of repose for iron spheres in a narrow, half-filled rotating drum is investigated. A feature of this paper is the use of a homogenous magnetic field to induce an attractive interparticle force, allowing a wide range of angles of repose to be investigated and characterized as a function of interparticle force. The static and dynamic angles of repose were found to increase approximately linearly with increasing interparticle force.

DOI: 10.1103/PhysRevE.63.031302 PACS number(s): 45.70.Cc, 45.70.Ht

I. INTRODUCTION

A sandcastle is a particle technology laboratory. Ideally, we would like our structure to last until we decide to jump on it, or until the incoming tide washes it away. Experience quickly teaches us that damp sand is a much better building material than dry sand or very wet sand, especially if the castle is to have steeply sloped (or vertical) sides.

If one attempts to use dry sand, the sandcastle will have gently sloping sides, usually less than 25°. Gravity is attempting to flatten the pile, and the only force resisting this is the weak interparticle friction. Adding water to the sand provides an interparticle force in the form of liquid bridges. It is this interparticle force that allows the sand to form structures with steep sides. This paper examines the effect of interparticle force on the angle of repose. We shall examine both the static and dynamic angles of repose, described in detail below.

When a powder is poured onto a flat plate, it forms a cone. Once the powder has reached an equilibrium state, the angle the sides of the cone make with the plate is called the static angle of repose. The angle of repose depends on such factors as size, density, surface roughness, and level of moisture of the powder, and the surface roughness of the plate. The static angle of repose can be measured in other ways, though not all methods will give the same angle of repose. For instance, a flat bottomed box can be filled, and the powder allowed to flow out through a hole in the bottom of the box. The angle that the remaining powder forms with the horizontal, once flow has ceased, is the static angle of repose. Other methods also exist, but this paper concentrates on the first method described here, the so-called "poured" angle of repose.

In addition, we shall consider the dynamic angle of repose, obtained as follows. A thin cylinder is half-filled with powder and placed on a pair of rollers. While stationary, the powder forms a flat surface inside the drum. As slow rotation begins, the material is carried along with the motion of the drum until the maximum angle of stability (the highest angle at which the surface of the powder is still in equilibrium) is exceeded. An avalanche ensues and the powder slumps to a new, lower angle of repose.

As the rotational speed increases, the avalanches increase in frequency until the surface of the powder is in constant motion, with a well-defined angle of repose. This will be referred to as the dynamic angle of repose. If one continues to increase the rotational speed, the surface of the powder takes on the characteristic *S* shape seen in Fig. 1.

The cohesive properties of powders depend on factors such as size, density, surface roughness, presence of liquid, and degree of compaction. Rather than examine each of these variables in isolation, we shall use the widely suggested idea that competition between the interparticle forces and the inertial forces determines granular behavior. As the ratio of interparticle force to inertial forces increases, the powder becomes more cohesive and the angle of repose increases accordingly.

For smooth dry powders, the dominant interparticle force is the van der Waals interaction. This increases linearly with particle size, while inertial forces increase as the cube of the particle size. Hence, the effect of the van der Waals force is best seen for small particles. For instance, coarse dry beach sand is free flowing, and forms piles with a very low angle of repose. On the other hand, fine powders such as corn flour and icing sugar are typically cohesive, and piles of these

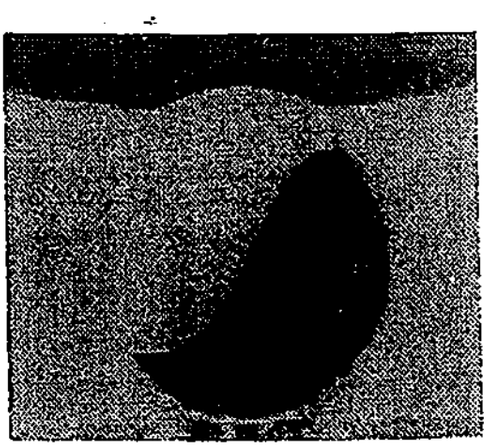

FIG. 1. Typical "Ying-Yang" shaped interface for a powder in a rotating drum at high rotational velocities. A threshold function was used to clearly delineate the powder surface. The aluminium rollers can be seen at the bottom of the picture. The dark bands at the top and bottom of the picture are the coils.

materials can support more steeply sloped sides.

Compaction will also have the effect of making a powder more cohesive. The van der Waals interaction for macroscopic particles falls off as the square of the interparticle separation [1]. Compaction decreases the average interparticle distance and hence increases the van der Waals force. In addition, compacting the powder increases the "coordination number" of the particles within the powders. For example in a loosely packed powder each particle may on average be in close contact with only 6 other particles, whereas in a closely packed state, they may be in contact with 8 to 12 particles, 12 representing the (in practice unattainable) hexagonal close-packed state.

The addition of liquid to dry powders will cause a transition in behavior. Experience shows that damp sand is better for making sandcastles than dry sand, due to its cohesive properties. The interparticle force in this case is caused by the formation of liquid bridges. Several groups [2,3] have added liquids of varying surface tensions and viscosities to dry powders to observe the transition from noncohesive to cohesive behavior.

To examine in detail this transition from noncohesive to cohesive behavior, a method for varying the ratio of interparticle force to inertial forces is needed. We shall discuss briefly methods used previously and note the disadvantages associated with each.

As discussed above, one may change the ratio of interparticle force to inertial force by altering the particle size. This leads to several complications. For instance, particles might not be available in the size you desire. Commercial batches of say 250 and 500 μm may not have the same relative size distribution. Most importantly however, it is difficult to obtain the same initial experimental conditions with different particle sizes. It is well known [4] that while particles larger than approximately 250 μm pack under normal gravity with roughly the same voidage, for particles smaller than this the voidage increases with decreasing particle size.

Liquid bridges can be used to increase the interparticle force. Several groups [2,3,5] have added liquids of varying surface tensions and viscosities to dry powders to observe the increase in interparticle force. Work has also been done on examining the effect of liquid on packing of monosized coarse spheres [4]. The limitation of this method is that the addition of more and more liquid increases the interparticle force in a stepwise manner. It is difficult to remove liquid in a controllable way. Adding liquids to dry powders not only increases the interparticle interaction, but also the interaction between the powder and the wall, further complicating the analysis. It is well known that the walls of a container can support a large fraction of the weight of the powder inside. For angle of repose experiments such as those performed here, this will increase the angle of repose, as part of the weight is supported by the walls, rather than by the pile of powder. Perhaps most importantly, it is difficult to relate the quantity of liquid added to the interparticle force.

To avoid these complications, we have examined the packing of iron spheres within a magnetic field. Varying the strength of the field allowed us to continuously vary the resulting interparticle magnetic force. As the walls of the vessel are nonmagnetic perspex, the particle-wall interaction is unchanged. As the same particles under the same packing conditions are used for all of the experiments, it is ensured that the initial conditions are as uniform as possible.

If it is assumed that the particles are magnetically linear, it follows that the interparticle force between two particles F_{mag} will vary in proportion to the square of the applied magnetic field ($F_{mag} \sim B_0^2$) [6]. Rather than rely on a calculation of the field from theory, we measure the ratio of interparticle force to buoyant weight directly, as described below. A plot of measured force against field strength squared was approximately linear, and we were confident in preparing a linear calibration curve to allow us to determine the interparticle force to buoyant weight ratio for any given field strength.

II. EXPERIMENTAL APPARATUS

To measure the static angle of repose, a narrow rectangular box of width 4 mm, length 300 mm, and height 150 mm was filled with iron spheres of mean diameter 800 μm from a funnel with a stopcock attached. The stopcock was used to control the flow rate.

To measure the dynamic angle of repose, a narrow perspex drum of diameter 150 mm and thickness 10 mm was placed horizontally on a set of aluminum roller supports and driven by an electric motor. Due to the presence of the magnetic field, only nonmagnetic materials were used in construction of the roller supports, and these were connected to the electric motor via a long belt. The drum was approximately half-filled with iron spheres.

The magnetic field for this experiment is supplied by a pair of Helmholtz coils. These coils have an inner diameter of 456 mm, an outer diameter of 568 mm, and a thickness of 76 mm. The formers are constructed from nylon, and were each wound with 1.1 km of 2.240 mm diam insulated copper wire. The coils are powered by a 16 A, 16 V stabilized dc power supply, and have a total resistance of 2.2 Ω. Thermal sensors on the inner wall of the coils provide information about temperature within the coils. If the temperature rises above a preset value, the power supply will automatically switch off. Additional cooling can be provided by a water jacket, but was not found to be necessary for these particular experiments. The magnetic-field axis was in the vertical direction.

The magnetic field was measured as a function of current by a Bell 2400 series Gaussmeter. The field was found to vary less than 10% throughout the volume between the coils, and by less than 5% within a sphere of diameter 140 mm centered on the axis of symmetry, midway between the coils. The variation in magnetic-field intensity with current is shown in Fig. 2.

To directly measure the interparticle force between two particles as a function of field strength, the following method was used. An iron sphere of the appropriate size was glued to a plastic spatula and positioned on the axis of symmetry at the point midway between the coils. With the field at full strength (approximately 6400 A/m) a second particle of the same size was brought into contact with the fixed sphere.

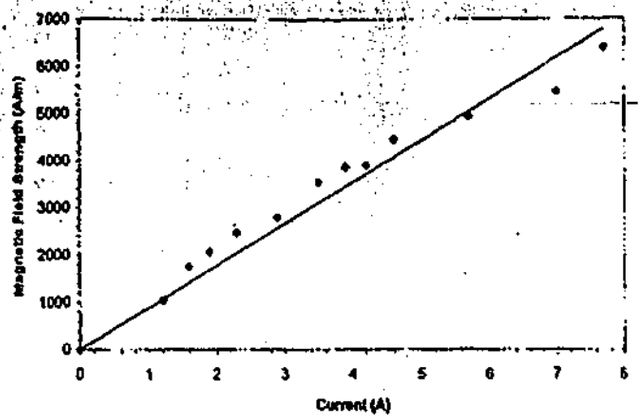

FIG. 2. Variation of magnetic-field intensity with current. The measurements were taken along the axis of symmetry, midway between the coils.

Due to the strong magnetic force between the two particles, the second particle became suspended from the first. The current in the coils, and hence the magnetic-field strength was slowly decreased until the suspended particle fell from the fixed particle. At this point the interparticle force is equal to the weight of the particle. This measurement (and all subsequent measurements) were repeated several times for accuracy. The weight of the particle was measured with a sensitive laboratory balance.

To obtain further points for the graph, small (500 μm) bronze spheres were carefully glued to the "bottom" of the particle to be suspended. This served to increase the weight of the particle without significantly altering the interparticle force. This new particle was weighed, and the measurements repeated, making sure that none of the bronze particles became dislodged when the suspended particle fell. The weight of the particle versus the square of the field at which it fell is shown in Fig. 3. By dividing through by the weight of each particle, we can obtain the ratio of interparticle force to weight, as shown on the right-hand axis of Fig. 3.

Ramping the field down slowly serves two purposes. First of all, it allows us to pinpoint the current and hence field at which the interparticle force and gravitational forces become equal. Secondly, it allows the magnetic field induced in the steel spheres to relax, so that the force is representative of the present field, rather than the higher field it was at moments ago.

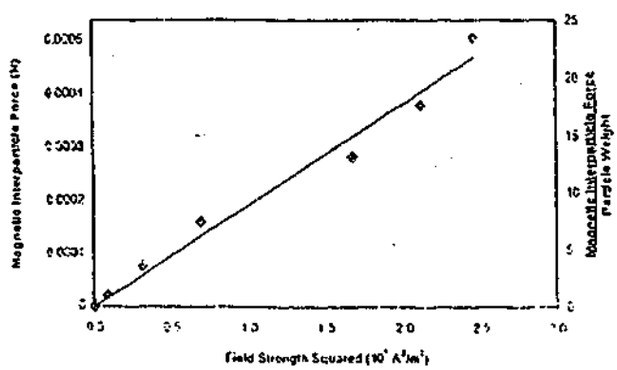

FIG. 3. Graph of interparticle force and interparticle force per unit weight vs magnetic-field strength squared for 800-μm steel spheres.

FIG. 4. Typical curves of the type analyzed in this paper. From left to right the figures represent a ratio of interparticle force to weight of 0, 0.62, 5.6, and 10, respectively.

An image recognition system consisting of a commercial digital camera attached to a Matrox card was used to capture the images and our own software used to analyze the results. Lighting was controlled by back lighting, using a diffuser to ensure uniformity of the lighting conditions. Preprocessing to remove noise and unwanted artifacts was applied to all images.

A set of experiments were conducted to measure the angle of repose for different values of interparticle force.

III. RESULTS

The increase in dynamic angle of repose with increasing interparticle force can be clearly seen in Fig. 4. The angle of repose was determined by first segmenting the image, and the angles were determined using a Hough transform. This approach is robust to noise and is preferred to other curve-fitting techniques [7].

The results of the experiments to measure the static and dynamic angles of repose are shown in Figs. 5 and 6. In both cases, the angle of repose increases approximately linearly with increasing interparticle force. Similar results for the static angle of repose have been demonstrated elsewhere [2,3,8] for liquid bridge forces, using the "draining crater" [2] method to measure the angle of repose.

This linear behavior corresponds to the *granular regime* of Tegzes *et al.* [8] for wet granular media, where surface flow is homogenous and involves only the top few layers of grains. This behavior manifests itself at low level of liquid addition. As the amount of liquid increases, two other regimes have been discovered. In the *correlated regime* surface flow becomes strongly correlated in that clumps of many attached grains fall in each avalanche, leading to a

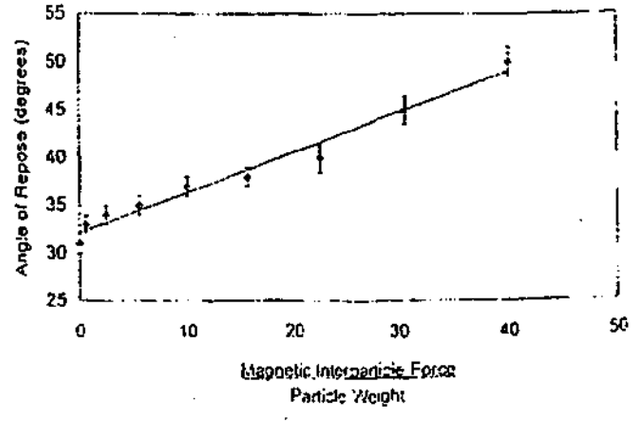

FIG. 5. Graph of static angle of repose vs ratio of interparticle force to weight for 800 μm steel spheres.

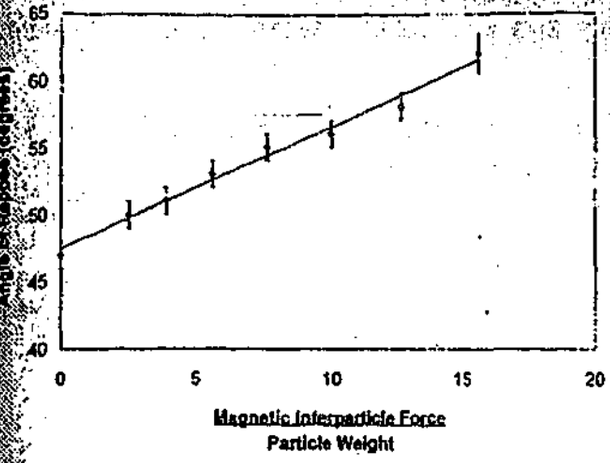

FIG. 6. Graph of dynamic angle of repose vs ratio of interparticle force to particle weight for 800-μm steel spheres.

cratered surface. In this regime the angle of repose rises more slowly than in the *granular regime*, though still in a somewhat linear manner. In the *plastic regime* surface flow is reminiscent of a viscous fluid in that the surface remains smooth, rather than taking on the cratered appearance that appears in the *correlated regime*. In the *plastic regime* the angle of repose stops increasing with additional liquid content, and indeed in some cases actually decreases.

It is unclear whether correlated and plastic regimes will show up at higher fields. Obviously the angle of repose cannot continue to increase linearly with increasing field, as the angle of repose cannot exceed 90°, and one doubts whether in practice this can even be approached closely. At high fields, the poured angle of repose becomes difficult to measure due to the cohesive nature of the iron spheres. The iron spheres begin to "clump," blocking the orifice in the funnel. Further experiments are planned using the "draining crater" method to search for these other regimes.

IV. DISCUSSION

Theoretical studies based on stability criteria [2] demonstrate that the maximum angle of stability should increase approximately linearly with increasing interparticle force from about 23° at zero interparticle force up to a little over 90° at a ratio of interparticle force to weight of 1. At ratios above 1 the graph tails off towards the maximum angle of repose at 90°. The work of Albert *et al.* [2] considered liquid bridge forces as the interparticle cohesive force. The theory is based on the maximum angle of stability for stationary particles, rather than the poured angle of repose measured here. In essence, this corresponds to taking a flat surface of particles and very slowly tilting it until flow begins. The particles in this experiment have been dropped from an average height of around 10 cm, and gain a velocity of the order of 1 ms^{-1} before impacting on the surface of the pile. This energy must be dissipated before the particle comes to rest, and obviously allows the particle to come to rest further down the slope than it would if it were placed gently at the top of the pile.

It is perhaps not surprising that the angles of repose measured here rise more slowly with increasing interparticle force than theory based on liquid bridge forces would suggest. One limitation of the system used here is that the force is a dipole interaction rather than an isotropic force such as the van der Waals force. Not only is the magnetic force anisotropic, but particles situated next to one another (in the same horizontal plane) will actually repel one another. If we assume the pile is packed in a cubic state, all particles on the surface of the pile will have a neighbor on the same plane up slope, but not necessarily corresponding neighbor down slope. This results in a net force F_{cub} attempting to push the particle further down the slope, lowering the angle of repose. If the packing was perfectly hexagonal close packed, the net horizontal force on a particle at the surface would be zero. In practice, the packing is random, and the net horizontal force on particles at the surface somewhere between zero and F_{cub}.

Additionally, we have quoted here only the maximum interparticle force F_{max}, obtained when the particles are touching and aligned with the field. It is easily demonstrated [1] that (at least for separations large compared to the dimensions of the dipole) that the interaction energy for particles aligned in the direction of the field is twice that of two dipole aligned parallel to each other at the same separation. When the line joining the centers of our particles is aligned with the field, our dipoles attract and repel when the line joining the centers of the particles is perpendicular to the field lines. The average force felt by the particles will overall be attractive, but less than F_{max}. Hence our ratio of interparticle force to particle weight is overestimated.

The liquid bridge force is also anisotropic. The liquid bridge force is always attractive, and acts along a line joining the centers of two particles. This results in a net horizontal force towards the slope, rather than away from the slope as in the magnetic case. One would therefore expect that the angle of repose for wet powders would increase more rapidly as a function of the ratio of interparticle force to particle weight than the magnetic case, and so perhaps better reflect the theory of Albert *et al.* [2]

It is difficult to quantitatively compare our data to those experiments done using liquid bridges to supply the interparticle force as there is at this stage no robust manner in which to calculate the interparticle force due to liquid bridges without resorting to fitted parameters. The work of Hornbaker *et al.* [3] plots a static angle of repose obtained by the draining-crater method [9] versus the average liquid layer thickness. The angle of repose rises approximately linearly with increasing liquid layer thickness. Albert *et al.* [2] demonstrate that for slightly rough particles, the liquid bridge force $F_{liq} \approx V^{1/3}$, where V is the volume of the liquid bridge. Hence, liquid bridge interparticle force is proportional to the thickness of the liquid layer. Qualitatively, this gives the same behavior seen using magnetic forces, that angle of repose increases linearly with increasing interparticle force.

Basic stability criteria [2] would predict an angle of repose at a zero field of approximately 23°. Our angle of repose is significantly higher ($\approx 31°$). The difference can possibly be attributed to the narrow box used for the experiments. It is well known that wall effects can add sev-

eral degrees to the angle of repose [10]. Repeating our experiments at zero field with boxes of width 6 mm and 8 mm gave angles of repose of 30° and 28°, respectively. Zero-field experiments were performed on iron spheres that had not previously been magnetized to ascertain whether residual magnetization was the cause. No effect due to residual magnetization was found.

The dynamic angle of repose at zero field (47°) is considerably higher than the static angle of repose at zero field (31° for the 800-μm particles). The motion of the drum carries the particles up the wall, leading to a higher angle of repose. As for the static case, the dynamic angle of repose rises linearly with increasing interparticle force, though more slowly than predicted by theory [2] due to the inertia of the particles.

V. CONCLUSIONS

We have designed a system for examining the effects of interparticle force on the behavior of powders. The static angle of repose for iron spheres in a box and the dynamic angle of repose for iron spheres in a rotating drum were measured as a function of interparticle force. Both the static and dynamic angles of repose were found to increase approximately linearly with interparticle force.

[1] J.N. Israelachvili, *Intermolecular and Surface Forces*, 2nd ed. (Academic, San Diego, 1992).
[2] R. Albert, A. Istvan, D. Hornbaker, P. Schiffer, and A.-L. Barabasi, Phys. Rev. E 56, R6271 (1997).
[3] D.J. Hornbaker, I. Albert, A.L. Barabasi, and P. Schiffer, Nature (London) 387, 765 (1997).
[4] C.L. Feng and A.B. Yu, Powder Technol. 99, 22 (1999).
[5] L.J. McLaughlin and M.J. Rhodes, Powder Technol. 114, 213 (2001).
[6] T.B. Jones, R.D. Miller, K.S. Robinson, and W.Y. Fowlkes, J. Electrost. 22, 231 (1989).
[7] R.C. Gonzalez and P. Wintz, *Digital Image Processing*, 2nd ed. (Addison-Wesley, Reading, MA, 1987).
[8] P. Tegzes, R. Albert, M. Paskvan, A.-L. Barabasi, T. Vicsek, and P. Schiffer, Phys. Rev. E 60, 5823 (1999).
[9] R.L. Brown and J.C. Richards, *Principles of Powder Mechanics* (Pergamon, Oxford, 1970).
[10] C.M. Dury, G.H. Ristow, J.L. Moss, and M. Nakagawa, Phys. Rev. E 57, 4491 (1998).

Segregation of particulate materials: interparticle force effects

Sean R. Hutton[1], Adam J. Forsyth[2], Charles F. Osborne[1] & Martin J. Rhodes[2*]

1. Department of Physics, Monash University, 3800, Victoria, Australia

2. Department of Chemical Engineering, Monash University, 3800, Victoria, Australia

Binary mixtures of particles are observed to stratify or segregate when poured into a heap. Previous studies have examined the effect of particle size, shape and surface roughness on this behaviour. In this paper we study the effects of interparticle force in avalanche segregation and stratification. Transitions were observed between mixed and segregated granular states as the interparticle force was increased. Inversion of the stratification patterns was also observed at higher interparticle forces. Phase diagrams of these behaviours are presented. It is shown that the behaviour is determined by the ratio of interparticle force to particle weight. In addition we demonstrate that the previously reported effects of particle size, shape and surface roughness can also be explained within this framework.

INTRODUCTION

Homogenous binary mixtures of particles are observed to stratify into layers according to particle size and/or shape when poured between two transparent vertical plates, held a small distance apart, and allowed to avalanche. Further to this, there is segregation between the large and small particles with more of the larger particles tending to collect at the bottom of the plates. Understanding these behaviours could have important implications for industrial processes requiring poured mixtures to remain homogeneous. They may also be important for understanding several geological processes. Makse *et. al.*[1,2] performed experiments on a mixture of sand and glass beads and found that the grains formed alternating layers of sand and glass. Working with Boutreaux *et al.*[3] they also proposed a model that describes quantitatively the segregation and stratification of particles due to particle size and/or shape. Koeppe *et. al.* [4] have extended this model to account for variations due to changes in the plate separation. The process of segregation appears to be due to the ability of the larger grains to travel faster than the smaller grains across the avalanching surface [4]. Since they have lower inertia, the smaller grains will be more susceptible to being stopped by small bumps and gaps in the underlying grain profile. Stratification, on the other hand, appears to rely upon differences in the angles of repose, of the two materials in the mixture [5]. This is why both grain size and shape are important to the process, since both influence angle of repose. If the larger particles have the smaller angle of repose they segregate out at the bottom of the slope forming a kink in the grain profile. As the avalanching grains

* Corresponding author E-mail: martin.rhodes@eng.monash.edu.au

hit the kink, they segregate and add more material to it. As material is added the kink propagates up the grain profile, forming a stripe of segregated material as it grows. Once the kink reaches the top of the pile materials spills down to the bottom of the profile again and the process repeats[5]. It has long been understood that interparticle forces play a role in fine granular materials or powders [6] and influence angle of repose. However, the above models do not take into account the of surface friction or other interparticle forces.

In this paper, we investigate the effect of altering interparticle force on segregation and stratification. To do this we placed iron particles in a magnetic field. The field induces a magnetic dipole attraction between the iron particles. The interparticle force decreases as $1/r^4$ and so can be considered to be essentially a contact force. In addition to this, there will be eddy currents in the iron particles, due to the horizontal component of the motion through the vertical magnetic field. These currents will tend to slow the particles and hence enhance the attractive effect of the interparticle force. At low field, the dipole nature of the attraction can be safely ignored as the particles can rotate freely. At high fields however, directional effects start to dominate and the particles begin to form chains which align with the field. With these caveats in mind we consider the effect of increasing the field to be the same as increasing interparticle force.

METHODS

Our experiment used two Perspex plates each, 35 cm × 21 cm × 1 cm. These are kept apart by spacers on the bottom and sides. A mixture of non-magnetic particles (such as sand or bronze) and iron particles was poured into the gap between the plates by means of a funnel and rotating stopcock. The stopcock allowed the flow rate to be controlled. The granular mixture was stirred prior to pouring to ensure homogeneity. The experiments were repeated using a variety of non-magnetic materials mixed with 350 μm iron particles. A pair of Helmholtz coils supplied the homogenous vertical magnetic field. The coils have an internal diameter of 458 mm and an external diameter of 568 mm. Each water-cooled coil is wrapped with approximately 1.1 km of copper wire and is powered by a 16 V, 16 A dc power supply. The homogeneity of the field was tested using an incremental Gaussmeter. At maximum voltage (16V) the field at the center of the coil was found to be 6.00 ± 0.25 Gauss and was found to not vary more than ± 0.5 Gauss throughout the volume of space between the coils. Images of the segregation and stratification were captured using a digital CCD camera. Using binary mixtures of iron particles and non-magnetized particles allows the investigation of the effects of interparticle forces upon the segregation and stratification processes. To show that segregation does not occur during the pouring process, a separate experiment was performed in which the mixtures were poured onto a flat surface. The material remained homogeneously mixed.

RESULTS

a). Segregation

Koeppe *et al.*[4] have noted that the degree of segregation is unaffected by flow rate until a critical

flow rate, f_c, is reached at which point segregation abruptly disappears. Above f_c the flow is too fast for kinks in the grain profile to form and propagate up the slope and so, continuous flow across the free surface is observed. Koeppe *et al* [4] found that the value of f_c depends upon the plate separation. In order to investigate the effect of interparticle forces on segregation, experiments were carried out with flow rates above f_c. Segregation was observed to occur in mixtures of sand and iron particles. Initially the mixture segregated with sand at the bottom and the iron shot at the top. As the magnetic field was increased, the segregation effect was eliminated and a well mixed state was found. At higher fields the segregation reversed, with the iron shot running to the bottom of the pile and the sand remaining at the top. The experiments were repeated with other materials and similar results were found. The results of these experiments are summarized in the phase diagram in Fig. 1.

b). Stratification

A second series of experiments were carried out to investigate the stratification process. Experiments were carried out using a mixture of sand and iron shot. The flow rate in these experiments was kept constant and below f_c. Without an applied field, the sand has a larger angle of repose ($\theta \approx 35°$) than the iron particles ($\theta \approx 30°$) and so stratification occurs spontaneously during avalanching. When a magnetic field was applied, it was found that as the field increased the stratification was observed to weaken, disappear and then reverse. As the field was increased the width of the stratified layers decreased until the material appeared well mixed.

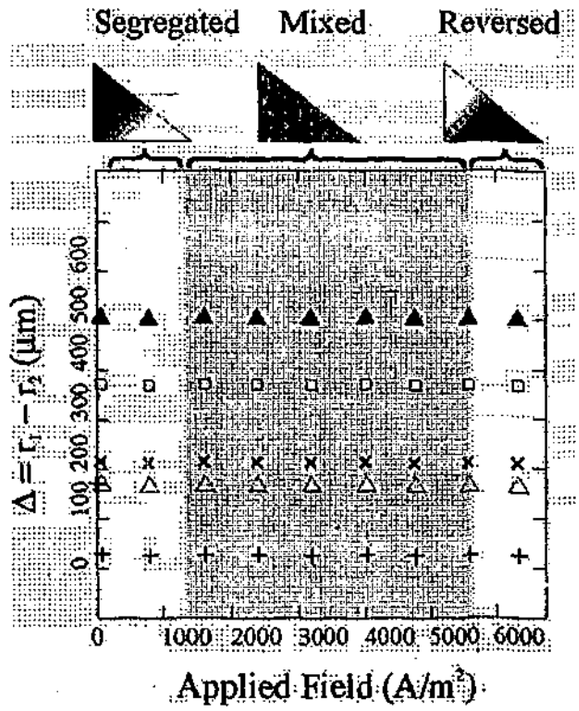

Fig. 1. Phase diagram for segregation. The grey area in the center represents the region where the mixture remains mixed and the materials does not undergo significant segregation. For low field, the iron was found to segregate to the top, but for high field, the iron segregated to the bottom. The binary mixtures used were iron spheres with: Δ Glass ballotini (500 μm), + white sand (360 μm), □ white sugar (710 μm), Δ brown sugar (850 μm) and × bronze spheres (550 μm).

As the field increased further the width of the layers increased again. However, at low field the layers consisted of sand over iron shot and at high field the iron layers formed above the sand layers. The experiments were repeated for a range of different coil voltages and materials. The results are summarized in the phase diagram in Fig. 2. In previous experiments [7], the angle of repose of the iron shot was observed to increase with field

strength. Only the sand and iron shot mixture was observed to undergo a full transition between the stratified, mixed and reversed stratified phases. It was noted that at high field the profile of grain piles become more irregular as long chains of particles formed. This irregularity is also apparent as irregularities within the layers of grains.

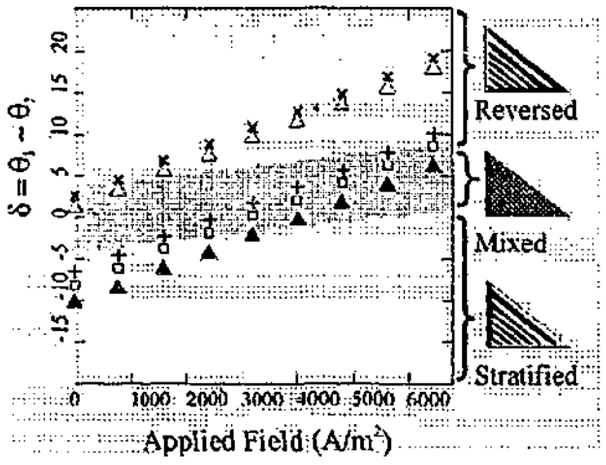

Fig. 2. Phase diagram for stratification. In the grey region, stratification was observed to weaken and then reverse as the field was increased. The binary mixtures used were iron spheres with: Δ Glass ballotini (500 μm), + white sand (360 μm), □ white sugar (710 μm), Δ brown sugar (850 μm) and × bronze spheres (550 μm).

DISCUSSION

As the iron particles move through the magnetic field they will experience eddy currents which will tend to slow its motion through the field. It might appear possible that these currents play a direct role in the segregation and or stratification processes. Using computer simulations, however, we can show that this is not the case. We created a cellular automata simulation of the avalanching sand in which the two types of particles behave identically in all respects except speed. Simply slowing the speed of one of the particles with respect to the other is not enough to induce either stratification or segregation, as seen in Fig. 3. While slow moving particles slow the avalanching process down they do not affect the final distribution of slow and fast moving particles. This is born out by our experimental results. If the segregation process were due to eddy currents then we would expect that the iron particles would segregate to the top in high fields rather than to the bottom as we observed.

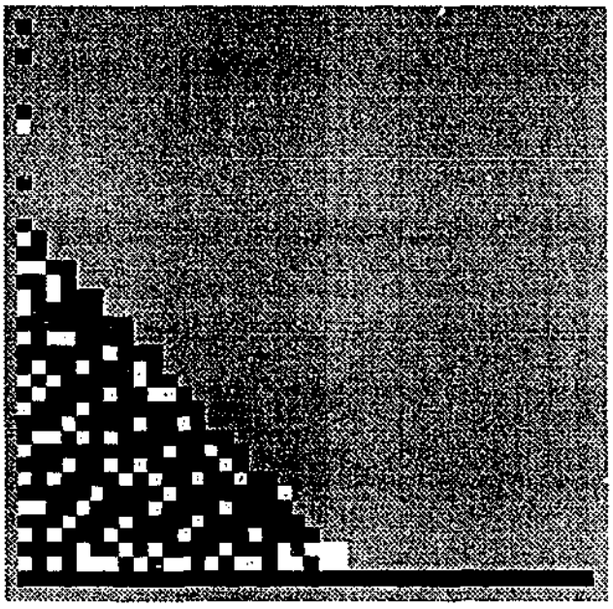

Fig. 3. Cellular automata simulation of the effect of eddy currents on segregation. The slowing of the iron particles by eddy currents cannot account for the segregation and stratification patterns shown above.

Makse *et al* [1] have already shown that if the angle of repose of one species of particle is changed, then both stratification and segregation spontaneously

occur. The mechanism for the reversal of the stratification is therefore most likely to be due to the changing of the angle of repose with field. The reversal of the segregation is probably due to small particles sticking together and acting much like larger particles. Both these processes should also occur in other granular materials where different interparticle forces (such as van der Waals forces in powders) play an important role.

CONCLUSION

In summary, we have found that interparticle forces effect both stratification and segregation in avalanching granular mixtures. In view of this, the current theoretical models by *Makse et.al.* [1,2] and Boutreaux *et. al.* [3] may need to be expanded to take into account interparticle forces. Our work may be relevant to understanding avalanches and flows in the real world situations where cohesive forces may play a role. Segregation and stratification are of particular interest to many industries, for example the manufacturing and pharmaceutical industries, where these effects are undesirable. It may be possible to alter the bulk properties of certain granular materials to prevent these effects.

The main results of this paper are the phase diagrams showing how the avalanching stratification and segregation is affected by interparticle force. Our experiments demonstrate that interparticle forces can cause significant changes in the segregation and stratification behaviour of granular mixtures.

REFERENCES

1. Makse H. A., *Phys. Rev. E* 56, 56 (1997).
2. Makse H. A., Havlin S., King P. R. and Stanley H. E., *Nature* 386, 379 (1997).
3. Boutreaux T. and Degennes P. G., *J. Phys.* 6, 1295 (1996).
4. Koeppe J., Enz M. and Kakalios J., *Phys. Rev. E* 58, R4104 (1997).
5. Ball P., *The Self Made Tapestry*, (Oxford University Press, Oxford, 1999).
6. Geldart D., *Powder Technol.* 7, 285 (1973).
7. Forsyth A. J., Hutton S. R., Rhodes M. J. and Osborne C. F., "Effect of applied interparticle force on the static and dynamic angles of repose of spherical granular material", *Phys Rev E*, in press (2000).

Paper No.

The Role of Interparticle Force on Segregation of Particulate Materials

Sean R. Hutton*, Adam J. Forsyth†, Martin J. Rhodes† & Charles F. Osborne*
*Department of Physics,
†Department of Chemical Engineering,
Monash University, 3800, Victoria, Australia

Prepared for presentation at the 2000 AIChE annual meeting, Los Angeles, California.

ABSTRACT

In this paper, we study the effects of inter-particle force on avalanche segregation and stratification. We observed transitions between mixed and segregated granular states as the inter-particle force is increased. We also observe an inversion of stratification in avalanching grains with increasing inter-particle force. Phase diagrams of these behaviors are presented.

INTRODUCTION

Homogeneous binary mixtures of particles are observed to stratify into layers according to particle size and/or shape when poured between two transparent vertical plates, held a small distance apart, and allowed to avalanche. Further to this, there is segregation between the large and small particles with more of the larger particles tending to collect at the bottom of the plates. Understanding these behaviors could have important implications for industrial processes requiring poured mixtures to remain homogeneous. They may also be important for understanding several geological processes[1]. Makse et. al.[2,3] performed experiments on a mixture of sand and glass beads and found that the grains formed alternating layers of sand and glass. Working with Boutreux et al. [3,4] they also proposed a model that describes quantitatively the segregation and stratification of particles due to particle size and/or shape. Koeppe et. al.[5] have extended this model to account for variations due to changes in the plate separation.

The process of segregation appears to be due to the ability of the larger grains to travel faster than the smaller grains across the avalanching surface[6]. Since they have lower inertia, the smaller grains will be more susceptible to being stopped by small bumps and gaps in the underlying grain profile. Stratification, on the other hand, appears to rely upon differences in the angles of repose, of the two materials in the mixture[6]. This is why both grain size and shape are important to the process, since both influence angle of repose. If the larger particles have the smaller angle of repose they segregate out at the bottom of the slope forming a kink in the grain profile. As the avalanching grains hit the kink, they segregate and add more material to it. As material is added the kink propagates up the grain profile, forming a stripe of segregated material as it grows. Once the kink reaches the top of the pile materials spills down to the bottom of the profile again and the process repeats.

It has long been understood that inter-particle forces play a role in fine granular materials or powders[7] and influence angle of repose. However, the above models do not take into account the effects of surface friction or other inter-particle forces. In this paper, we investigate the effect of altering inter-particle force on segregation and stratification.

To study this effect we placed iron particles in a magnetic field. The field induces a magnetic dipole attraction between the iron particles. The inter-particle force decreases as $1/r^4$ and so can be considered to be essentially a contact force. In addition to this, there will be eddy currents in the iron particles, due to the horizontal component of the motion through the vertical field. These

currents will tend to slow the particles and hence enhance the attractive effect of the inter-particle force. At low field, the dipole nature of the attraction can be safely ignored as the particles can rotate freely. At high fields however, directional effects start to dominate and the particles begin to form chains which align with the field. With these caveats in mind we consider the effect of increasing the field to be the same as increasing inter-particle force.

METHODS

Our experiment uses two, 35cm x 21cm x 1cm, Perspex plates. These are kept apart by spacers on the bottom and sides. A mixture of non-magnetic particles (such as sand or bronze) and iron particles is poured into the gap between the plates by means of a funnel and rotating stopcock. The stopcock allowed the flow rate to be controlled. The granular mixture was stirred prior to pouring to ensure homogeneity. To show that segregation does not occur during the pouring process, the mixture was pouring onto a flat surface. The material remained homogeneously mixed. The experiments were repeated using a variety of non-magnetic materials mixed with 350 μm iron particles.

A pair of Helmholtz coils supplied the homogenous vertical magnetic field. The coils have an internal diameter of 458mm and an external diameter of 568mm. Each water-cooled coil is wrapped with approximately 1.1 km of copper wire and is powered by a 16V, 16A dc power supply. The homogeneity of the field was tested using an incremental Gaussometer. At maximum voltage (16V) the field at the center of the coil was found to be 6.00±0.25 Gauss and was found to not vary more than ±0.5 Gauss throughout the volume of space between the coils. Images of the segregation and stratification were captured using a digital CCD camera.

Using binary mixtures of iron particles and non-magnetized particles allows the investigation of the effects of inter-particle forces upon the segregation and stratification processes.

Koeppe et al.[5] have noted that the strength of segregation is unaffected by flow rate until a critical flow rate, f_c, is reached at which point stratification abruptly disappears. Above f_c the flow is too fast for kinks in the grain profile to form and propagate up the slope and so, continuous flow across the free surface is observed. Koeppe et al. found that the value of f_c depends upon the plate separation. In order to investigate the effect of inter-particle forces on segregation, experiments were carried out with flow rates above f_c.

RESULTS

Segregation was observed to occur in mixtures of sand and iron particles. As the magnetic field was increased, the segregation effect was eliminated and then reversed. The experiments were repeated with other materials and similar results were found. The results of these experiments are summarized in the phase diagram (Figure 1). The effect of applying a magnetic field to the mixture is to reverse the segregation as can be seen in Figures 1 and 2. At low fields, the smaller iron shot was found mostly at the top of the slope. For high fields, however, the iron was found to segregate to the bottom of the slope. For higher fields, the avalanche flow is slowed sufficiently for some stratification to occur.

A second series of experiments were carried out to investigate the stratification process. Experiments were carried out using a mixture of sand and iron shot. The flow rate in these experiments was kept constant and below fc. Without an applied field, the sand has a larger angle of repose ($r = 35°$) than the iron particles ($r = 30°$) and so stratification occurs spontaneously during avalanching. When a magnetic field was applied, it was found that as the field increased the stratification was observed to weaken, disappear and then reverse. As the field was increased the width of the stratified layers decreased until the material appeared well mixed. As the field increased further the width of the layers increased again (Figure 4). However, at low field the layers consisted of sand over iron shot and at high field the iron layers formed above the sand layers. The experiments were repeated for a range of different coil voltages and materials. The

results are summarized in the phase diagram (Figure 3). In our experiments, the angle of repose of the iron shot was observed to increase with field strength. Only the sand and iron shot mixture was observed to undergo a full transition between the stratified, mixed and reversed stratified phases.

DISCUSSION AND CONCLUSION

In summary, we have found that inter-particle forces effect both stratification and segregation in avalanching granular mixtures. In view of this, the current theoretical models by Makse et. al.[3] and Boutreux et. al.[4] may need to be expanded to take into account inter-particle forces. Our work may be relevant to understanding avalanches and flows in the real world situations where cohesive forces may play a role. Segregation and stratification are of particular interest to many industries, for example the manufacturing and pharmaceutical industries, where these effects are undesirable. It may be possible to alter the bulk properties of certain granular materials to prevent these effects. The main results of this paper are the phase diagrams showing how the avalanching and segregation is effected. Our experiments demonstrate that inter-particle forces can cause significant changes in the segregation and stratification behavior of granular mixtures. In light of this, it may be worth investigating the effects of inter-particle force on other pattern forming granular systems[6].

REFERENCES

1. G. V. Middleton, *"Mechanics of Sediment Movement"*, (S.E.P.M. Providence, R.I. 1984); Geo. Assoc. of Canada, Special paper no. 7, 253 (1970).
2. H. A. Makse, S. Havlin, P. R. King and H. E. Stanley, *"Spontaneous stratification in Granular Mixtures"*, Nature 386, 379
3. Heman Makse, "*Stratification Instability in Granular Flows*", Phys. Rev. E. Volume 56, Number 6, December 1997.
4. Boutreux, T & Degennes, P. G., Surface Flows of Granular Mixtures: I. General Principles and Minimal Model, J. Phys, I France 6,1295-1304 (1996).
5. James Koeppe, Michael Enz and Kakalios "*Phase Diagram for Avalanche Stratification of Granular Media*", Phys. Rev. E 58 R4104 (1997).
6. Philip Ball "*The Self-Made Tapestry: Pattern Formation in Nature*", Oxford University Press 1999
7. Geldart, "*Types of Gas Fluidization*", Powder Technology 7, (1973) pp285-292.†

Figure 1. Phase diagram for segregation. The gray area in the center represents the region where the mixture remains mixed and the materials does not undergo significant segregation. For low field, the iron was found to segregate to the top, but for high field, the iron segregated to the bottom.

Figure 2. Segregation of particles for high field and low field.

□

Figure 3. Phase diagram for stratification. In the gray region, stratification was observed to weaken and then reverse as the field was increased.

It was noted that at high field the profile of grain piles become more irregular as long chains of particles form. This irregularity also translates into irregularities within the layers of grains.

a)□b)□c)□ EMBED Word.Picture.8 □□□Figure 4. Stratification at a) low, b) mediuth and c) high fields for a mixture of sand and iron shot.

Effect of interparticle force on segregation in a rotating drum

S. R. Hutton [#], A. J. Forsyth[*], C. F. Osborne[#] and M. J. Rhodes[*]
[#] Department of Physics
[*]Department of Chemical Engineering
Monash University
Victoria, 3800, Australia

Binary mixtures of particles with different physical characteristics such as size, shape or density are known to segregate in rotating drums. Little is known however about the effect of inter-particle forces on this segregation. In this paper, we look at the effects of inter-particle force on segregation in rotating drums. Binary mixtures of iron and (non magnetizable) brass spheres were placed in a rotating drum within a magnetic field. This set up allowed us to examine the effect of interparticle force on only one type of particle in the binary mixture, allowing the effects of interparticle force to be isolated from any other variable. The particles used were iron spheres of diameter 350 μm, 600 μm and 850 μm. The bronze spheres had a diameter of 600 μm. This allowed us to prepare samples that were "well mixed", or segregated such that band of bronze appeared in the iron. For binary mixtures that were initially "well mixed," it was found that segregation could be induced by increasing the magnetic field, and hence interparticle force between the iron particles. For mixtures that were initially segregated, increasing interparticle force was shown to result in a well mixed state. As the interparticle force was increased further, the initial segregation pattern was reversed.

INTRODUCTION

While cement mixers are used to turn separate granular materials into an homogeneous mix it is surprising that the same process can lead to segregation. As early as 1939, Oyama [1] observed that a binary mixture of large and small grains, spontaneously segregates into axial bands when placed in a cylindrical drum and rotated.

The band patterns in segregation experiments are not in general stable features and over time tend to merge. In all these axial segregation experiments the materials are also observed to segregate radially[2]. For drums that are less than half full, a core of smaller, rougher particles is formed as the drum rotates.

Axial segregation seems to require differences in the dynamic angle of repose for the two species. This has led to the proposal of models that treat the segregation as a reverse diffusion instability in which the initial concentration fluctuations are amplified [3,4]. MRI studies revealed that there are sometimes more axially segregated regions within the bulk of the drum than can be seen from the surface. Many of these bands never reach the surface of the material as the rotation continues. The fact that some axially segregated regions may exist in the bulk without ever extending to the surface implies axial segregation may not be driven exclusively by differences in angle of repose. The variation in dynamical angles of repose may even be a result of variations in the bulk concentration, rather than the cause of the segregation.

For many systems, such as powders for which van der Waals forces cannot be neglected, this segregation is complicated by the appearance of inter-particle forces. In this paper, the effect of inter-particle forces on both radial and axial segregation is examined.

Experimental

There are several methods currently used by researchers tc increase the inter-particle force and study its effect on granular behaviour. Several groups [5,6,7] have added liquids of varying surface tensions and viscosities to dry powders to observe the increase in inter-particle force. Work has also been done on examining the

in a controllable way and hence hysteretic effects cannot be examined. Adding liquids to dry powders not only increases the inter-particle interaction, but also the interaction between the powder and the wall, further complicating the analysis. It is well known that the walls of a container can support a large fraction of the weight of the powder inside. For experiments such as those performed here, this will affect the result by increasing the angle of repose, as part of the weight is supported by the walls, rather than by the pile of powder. Perhaps most importantly, it is difficult to relate the quantity of liquid added to the inter-particle force. With a different inter-particle force packing, and hence initial conditions, will be different.

To avoid these complications, we have examined the behaviour of iron spheres within a magnetic field. Varying the strength of the field allowed us to continuously vary the resulting inter-particle magnetic force. As the walls of the vessel are non-magnetic perspex, the particle-wall interaction is unchanged.

If it is assumed that the particles are magnetically linear, it follows that the inter-particle force between two particles F_{mag} will vary in proportion to the square of the applied magnetic field ($F_{mag} \propto B_o^2$ [9]). Rather than rely on a calculation of the field from theory, we measure the ratio of inter-particle force to buoyant weight directly, as described below. A plot of measured force against field strength squared was approximately linear, and we were confident in preparing a linear calibration curve to allow us to determine the inter-particle force to buoyant weight ratio for any given field strength.

In reality the interactions between particles in the magnetic field will be non-linear. Recent research, however, seems to suggest that the systems can be treated as linear in a wide variety of circumstances. Tan et. al. [10] have conducted experiments on the induced magnetic force between individual and/or regular configurations magnetically non-linear spherical particles. Whilst there was a slight tendency for particles to form chains and a tendency for layers of chains to repel, they concluded

"...we have not perceived a radical difference in results between the two particle and multiparticle arrangements. In light of our experimental results the two particle chain seems to warrant a role as the basic building block in modeling the strong particle interactions of more complex systems."

The magnetic field for this experiment is supplied by a pair of Helmholtz coils. These coils have an inner diameter of 456 mm, an outer diameter of 568 mm and a thickness of 76 mm. The formers are constructed from nylon, and were each wound with 1.1 km of 2.24 mm diameter insulated copper wire. The coils are powered by a 16 A, 16 V stabilized DC power supply, and have a total resistance of 2.2 Ω. Thermal sensors on the inner wall of the coils provide information about temperature within the coils. If the temperature rises above a preset value, the power supply will automatically switch off. The magnetic field axis was in the vertical direction. The magnetic field was measured as a function of current by a Bell 2400 series Gaussmeter. The field was found to vary less than 10 % throughout the volume between the coils, and by less than 5 % within a sphere of diameter 140 mm centered on the axis of symmetry, midway between the coils. The variation in magnetic field intensity with current is shown in Figure 2.

A perspex drum of length 40cm and diameter 7cm was placed on a pair of aluminium rollers and placed between the Helmholtz coils. The roller assembly was constructed entirely from non magnetisable materials. The rollers were driven by means of a drive belt. The belt was long enough to enable the motor driving the drum to sit outside the field.

To directly measure the inter-particle force between two particles as a function of field strength, the following method was used. An iron sphere of the appropriate size was glued to a plastic spatula and positioned on the axis of symmetry at the point midway between the coils. With the field at full strength (approximately 6400 A/m) a second particle of the same size was brought into contact with the fixed sphere (as shown in Figure 1). Due to the strong magnetic force between the two particles, the second particle became suspended from the first. The current in the coils, and hence the magnetic field strength, was slowly decreased until the suspended particle fell from the fixed particle. At this point, the inter-particle force is equal to the weight of the particle. This measurement and all subsequent measurements) were repeated several times for accuracy. The weight of the particle was measured with a sensitive laboratory balance. The results of these experiments are shown in Figure 2.

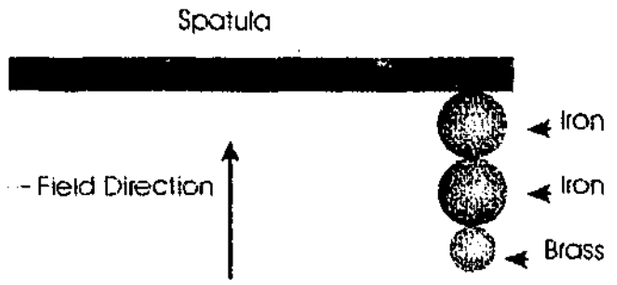

Figure 1: Method of measuring inter-particle force vs field.

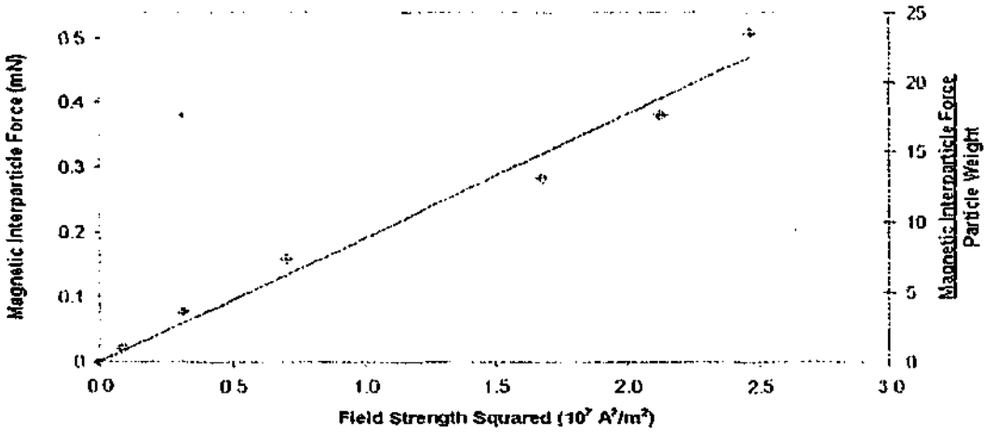

Figure 2: Interparticle force verses Field Strength

To obtain further points for the graph, small (500 μm) bronze spheres were carefully glued to the "bottom" of the particle to be suspended. This served to increase the weight of the particle without significantly altering the inter-particle force. This new particle was weighed, and the measurements repeated, making sure that none of the bronze particles became dislodged when the suspended particle fell. By dividing through by the weight of each particle, we can obtain the ratio of inter-particle force to weight, as shown on the right hand axis of Figure 2. Using this method, it was possible to observe the effect of increasing inter-particle force on radial segregation in the rotating drum.

Results and Discussion

The particles used were iron spheres of diameter 350 μm, 600 μm and 850 μm. The bronze spheres had a diameter of 600 μm. Binary mixtures were prepared using 600 μm bronze and 600 μm iron particles. These mixtures were initially "well mixed". It was found that segregation could be induced by increasing the inter-particle force between the iron particles. For mixtures consisting of the 350 μm iron shot and 600 μm bronze, as the inter-particle force was increased, the initial radial segregation pattern disappeared and then was reversed.

To examine this more carefully, experiments were carried out in a narrow perspex drum with diameter 150 mm and width 10 mm. The results of these experiments at high field and low field are summarized in the phase diagram (Figure 3).

One way at looking at these results is to view the system as having two points towards which particles are attracted. One of these "attractors" is at the center of the avalanching surface and the other at the base. As the inter-particle force is increased, the iron particles begin to stick to one another with increasing frequency and duration. The results of the segregation experiments suggest that as the ratio of interparticle force to bouyant weight is increased the particles act as if they have a much larger effective particle size. As the field is

[13] have shown that increasing inter-particle forces can increase mixing by increasing slip stick shearing in the free surface. Slip stick shearing was also observed in our experiments for low rotation velocities. As the applied field was increased the slip stick behaviour was observed to occur at higher velocities. Our results show that as the inter-particle forces increase, this mixing reaches a maximum, and then decreases as segregation reverses.

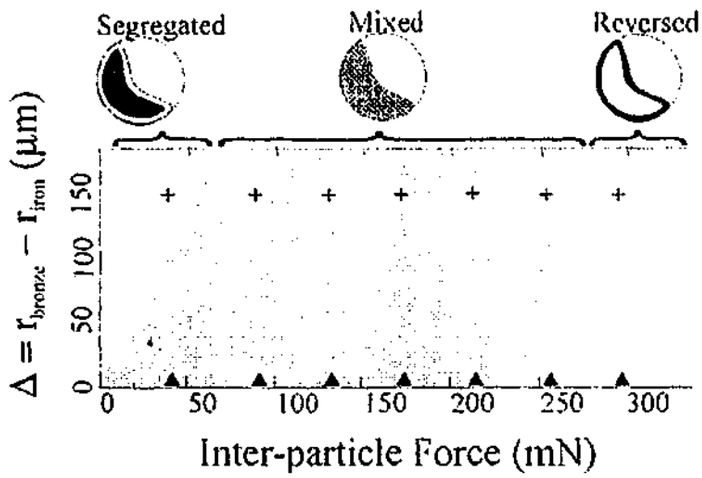

Figure 3: Phase diagram showing the reversal of radial segregation with increasing field. Iron shot (dark region in drum) intially segregates to the center of the drum but, as the inter-particle force increases, slowly mixes and then segregates to the outside of the drum

In other experiments it has been found that increasing inter-particle force, increases the dynamic angle of repose [14]. It might be expected therefore that increasing the inter-particle force would have an effect on the formation of axial bands. Experiments were carried out to investigate this. As the field was increased, the bands of iron particles were found to broaden, merge and then disappear altogether. The rotational velocity did not have to be uniform for this segregation to occur. The results also did not appear to be dependent upon precise leveling of the container.

The increased mixing in the axial segregation can be readily explained in terms of the radial mixing case. As inter-particle force increases, the drum becomes increasingly well mixed. As the radial segregation reverses, the axial bands disappear as the iron segregates to the outer surface of the drum.

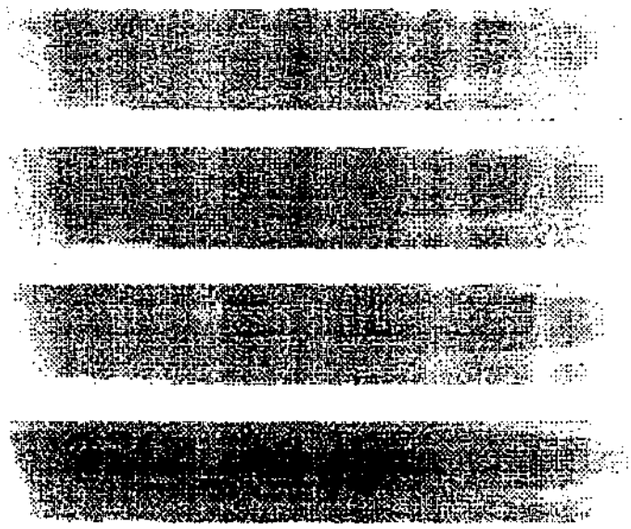

Figure 4: Mixing of granular materials with increasing inter-particle force. Axial bands broaden, merge and then dissappear

Conclusions

In conclusion, we have demonstrated a novel means of studying the effect of interparticle force on segregation and mixing rotating drums. These experiments demonstrate that inter-particle forces can cause significant changes in the segregation and stratification behavior of granular mixtures. We have found that increasing the inter-particle force in one-species of the material increases its ability to mix. For high values of interparticle force the segregation in the radial case was observed to reverse.

It would be interesting to compare and contrast these results with other means of altering inter-particle force, such as using fine powders or perhaps particles of different "wetability" in liquid. It may even be possible for a suitable choice of material to reverse the axial segregation effect by using particles which strongly segregate radially. If achievable such a result would suggest that the dynamical angle of repose does indeed play a role in the axial segregation.

References

1. Y. Oyama, Bull. Inst. Phys. Chem. Res. Tokyo, Rep 18, 1939, 6001.
2. K. M. Hill, A Caprlhan and J Kakalios,
   Bulk Segegation in Rotated Granular Material Measured by Magnetic Resonance Imaging, Phys. Rev. Lett. 1997, 78, 1, p50
3. O. Zik, D. Levine, S. G. Lipson, S. Shtrikman and J. Stavans. Phys. Rev. Lett. 73 644 1994
4. S. B. Savage "Disorder and Granular Media", D. Bideau and A. Hansen ed. North Holland Amsterdam, 1993 p255
5 R. Albert et al., Phys. Rev. E 56, R6271 (1997).
6. D. J. Hornbaker, I. Albert, A. L. Barabasi, and P. Schiffer, Nature 387, 765 (1997).
7. L. J. McLaughlin and M. J. Rhodes, Powder Technology, 114 (2001) 213-223.
8. C. L. Feng and A. B. Yu, Powder Technology 33, 22 (1999).
9. T. B. Jones, R. D. Miller, K. S. Robinson and W. Y. Fowlkes, Journal of Electrostatics, 1989, 22, 231
10. C. Tan, J. Appl. Phys. 73, (8), 1993.
11. Troy Shinbrot, and J. Muzzio, Nonequilibrium Patterns in Granular Mixing and Segregation, Physics Today, March, 2000
12. T. Shinbrot, A. Alexander, M. Meakher and F. J. Muzzio, Chaotic Granular Mixing, Chaos, September, 1999, 9, 3, 611-620,
13. S. Nasuno, A. Kudolli, A. Bak, and J. P. Gollub, Time resolved studies of stick-slip friction in sheared granular layers, Physical Reveiw E ,1998, 58, 2, 2161-2171
14 A.J Forsyth, S. Hutton, M.J. Rhodes, and C.F.Osborne, "Effect of applied inter-particle force on the static and dynamic angles of repose of spherical granular material", Physical Review E, 63, 2001 pp 031302/1-5.